ACOUSTIC RESPONSES FROM PRIMARY VESTIBULAR NEURONS

by

Michael Patrick McCue

B.S.E.E, Massachusetts Institute of Technology
(1981)

M.S.E.E., Massachusetts Institute of Technology
(1983)

M.D., Harvard Medical School
(1993)

SUBMITTED TO THE HARVARD/M.I.T. DIVISION
OF HEALTH SCIENCES & TECHNOLOGY

IN PARTIAL FULFILLMENT OF THE
REQUIREMENTS FOR THE DEGREE OF

DOCTOR OF SCIENCE

at the

MASSACHUSETTS INSTITUTE OF TECHNOLOGY

SEPTEMBER 1993

Signature of Author _____
Division of Health Sciences & Technology

Certified by _____
John J. Guinan, Jr.
Thesis Supervisor

Accepted by _____
Roger G. Mark
Co-Director
Division of Health Sciences & Technology

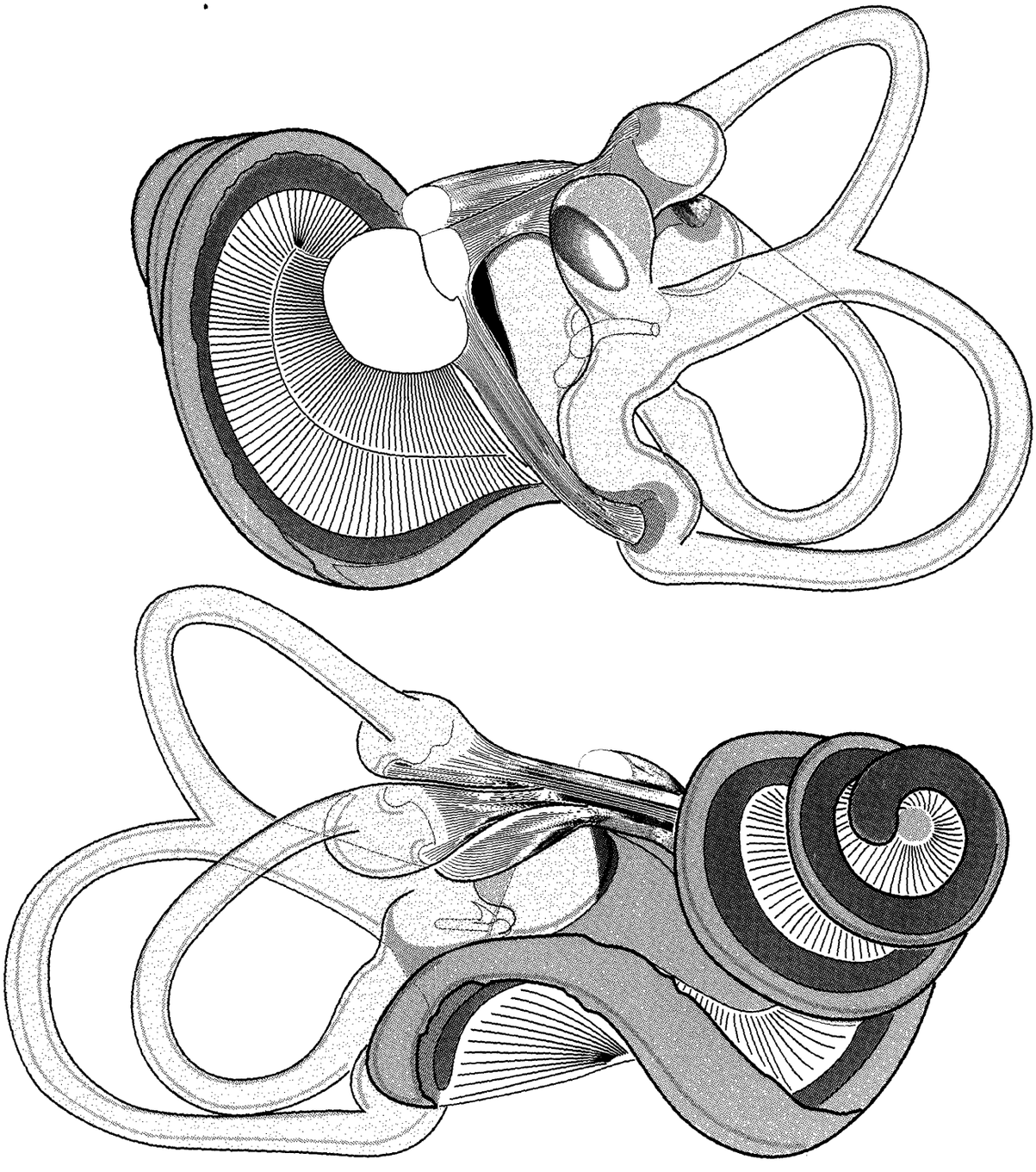

Frontispiece. The Membranous Labyrinth of the Cat (after Retzius, 1884).

ACOUSTIC RESPONSES FROM PRIMARY VESTIBULAR NEURONS

by

Michael Patrick McCue

Submitted to the Harvard/M.I.T. Division of Health Sciences & Technology
on June 23, 1993 in partial fulfillment of the requirements for the
Degree of Doctor Of Science

ABSTRACT

Mammals have evolved an inner ear with six different sense organs – a cochlea for detecting sound, three semi-circular canals for detecting rotation, and two otolith (*Gr.* ear rock) organs for detecting linear accelerations. The cochlea is a beautiful, coiled structure which imparts an esthetic, labyrinthine quality to the mammalian inner ear, but it is a relatively late evolutionary development. Fish lack cochleas and hear sounds adequately using one of their otolith organs, the saccule. Intermediate vertebrates, such as toads, also lack true cochleas and continue to rely on the saccule for some aspects of hearing.

In this thesis, I address the question of whether or not the vertebrate line completely abandoned the saccule as a hearing organ after the introduction of the mammalian cochlea. Afferent fibers in the cat's vestibular nerve were recorded from and found to be acoustically responsive. These neurons were labeled intracellulary and found to project to the saccule. Stimulation of the vestibular efferent system produced a complex excitation of these fibers and a concomitant amplification of their acoustic responses.

These experiments demonstrate that the mammalian saccule retains at least one class of neurons which continues to respond to sounds within the normal range of human hearing. I discuss some possible auditory roles which these neurons may continue to play. As a possible phylogenetic precursor of the cochlear hearing mechanism, the saccular auditory pathway may provide insights into remaining mysteries of cochlear function, particularly with regard to the brain's (efferent) control of the peripheral auditory apparatus.

Thesis Supervisor: Dr. John J. Guinan, Jr.
Title: Associate Professor of Otology & Laryngology, Harvard Medical School
Principal Research Scientist in Electrical Engineering & Computer Science, M.I.T.

This thesis is dedicated to my friend,
Robert Mayer Brown
(1927-1989)

He might not have read it,
but he would definitely have found out
whether or not
it was a
good job.

ACKNOWLEDGMENTS

Administrative Support
Susan Beckvold
Dianna Sands

Advice
Joe Adams
Alice Berglund
M. Christian Brown
M. Charles Liberman
Edmund A. Mroz
William F. Sewell

Engineering (Net Positive Input)
Robert M. Brown
Frank Cardarelli
Mark Curby
Debra Louisson
Michael Ravicz

Fiber Reconstruction
Barbara E. Norris

Financial Support
Fairchild Foundation
Fulbright Commission
Johnson & Johnson Co.
Kleberg Foundation
Metropolitan Life Insurance Co.
National Institutes of Health

Histology
Inge Knudson
Leslie Dodds Liberman
Barbara E. Norris

Indescribable Help
Robert M. Brown
Jennifer Lee Carrell
John J. Guinan, Jr.
Nelson Y.S. Kiang
Barbara E. Norris
Helen Peake
William T. Peake

Surgical Assistance
Monique Bourgeois
Kerstin Jacob
Inge Knudson
Leslie Dodds Liberman
Tracy Liu
Michelle Prince
Karen Whitley

Thesis Committe
David P. Corey
John J. Guinan, Jr.
William T. Peake

NOTE ON ORGANIZATION

This thesis was written as four independent manuscripts which have been unnaturally joined as "chapters" in the final document. Each paper was written in close collaboration with my thesis advisor, John J. Guinan, Jr., and hence reflects our joint thinking. Dr. Guinan is the implicit co-author when I make use of the first-person plural pronoun.

Note that figures in each "chapter" are sequentially numbered starting at 1 and appended to the end of the chapter. Figure references in the text to do not cross chapter boundaries.

TABLE OF CONTENTS

I. ACOUSTICALLY-RESPONSIVE NEURONS IN THE VESTIBULAR NERVE OF THE CAT

I. INTRODUCTION

The vertebrate inner ear contains several sense organs involved in the maintenance of equilibrium and the detection of vibration. The precise sensory role assumed by homologous organs varies among species. For example, the saccule is thought to act as a linear accelerometer in mammals (Fernández & Goldberg, 1976a-c) but is responsive to sound in certain amphibians (Moffat & Capranica, 1976; Lewis *et al.*, 1982), fishes (Popper & Fay, 1973; Saidel & Popper, 1983) and rays (Lowenstein & Roberts, 1951).

Whether or not any of the mammalian vestibular organs plays a role in normal hearing is an open question that hinges on two factors – acoustic sensitivity of the receptors and central processing of their outputs. The normal acoustic sensitivity of the vestibular receptors has been controversial. In a previous study in squirrel monkeys (Young *et al.*, 1977), primary vestibular afferents were found to synchronize to intense air-borne vibrations in the audio-frequency range, but increases in mean discharge rate were not observed in most units until the sound reached levels associated with rapid cochlear damage (>120 dB SPL). This study, which demonstrated acoustic responsiveness yet emphasized high thresholds, has been cited as evidence both for (Cazals *et al.*, 1980) and against (Kevetter & Perachio, 1989) a hearing role for the mammalian vestibular system.

Even if vestibular nerve fibers were to respond to sound, the signals they carried might be of no benefit (and potentially of some harm) if they were not processed centrally as auditory information. The possibility that the vestibular receptors are involved in auditory processing has thus been strengthened by recent demonstrations that primary vestibular afferents send projections into the auditory brain stem (cochlear nucleus) in mammals (Burian & Gstoettner, 1988; Kevetter & Perachio, 1989).

We have recently found a class of primary vestibular neurons in cats which could involve the vestibular receptors in normal hearing. We present here anatomical and physiological evidence thate indicates that these neurons originate in the saccule, are activated by normal hair-cell stimulation at moderately high sound levels, and are excited by acoustic stimuli that reach the inner ear via normal middle-ear transmission. In this report, we report unit reponses to clicks and tones. A preliminary report of this work has been presented (McCue & Guinan, 1993).

I. METHODS

Surgery. Treatment of experimental animals was in accordance with protocols approved by the Committees on Animal Care at the Massachusetts Institute of Technology and the Massachusetts Eye & Ear Infirmary. Adult cats were induced and maintained under anesthesia by intraperitoneal injection of diallylic barbiturate in urethane (Kiang *et al.*, 1965). A tracheostomy was performed. The ear canals were surgically exposed and the auditory bullae were opened. In some cats, the bony septum between the bulla and middle-ear was removed and the tendons of the middle-ear muscles (stapedius and tensor tympani) were cut. A posterior fossa craniectomy was performed, and the cerebellum was aspirated laterally to expose the dorsal surface of the temporal bone. After reflection of the periosteum, the roof of the internal auditory meatus was drilled away with a dental burr to expose the junction of the inferior and superior vestibular nerves (Liberman & Brown, 1986). Extreme care was taken to maintain the structural integrity of the bony labyrinth.

Monitoring. Animals were placed in an electrically shielded and sound-proofed chamber (Ver *et al.*, 1975). Rectal temperature was maintained between 36-39°C by adjustment of the chamber temperature. Pulse and respiration were continuously monitored and artificial ventilation was supplied when needed. Silver-wire electrodes were placed in contact with the cochlea near the round window and used to monitor cochlear thresholds. Cochlear threshold shifts were frequently noted after long periods of intense sound, but were not clearly associated with shifts in the acoustic response thresholds of vestibular neurons.

Sound Stimulation. Sound was delivered through metal acoustic assemblies sealed against each tympanic ring (Kiang *et al.*, 1965). The sound source (1-in. condenser earphone, Brüel & Kjaer) was rigidly fixed to the metal acoustic assembly. A condenser microphone (1/4-in., Brüel & Kjaer) was attached to a small metal probe tube ending near the tympanic membrane, and was used to determine sound levels as a function of frequency. The maximum sound pressure level was 115 dB *re:* 0.0002 dynes/cm^2 (sound pressure level or SPL).

Sound stimulation and neural recording were accomplished under computer control (Apple Macintosh Quadra 950) through two instrumentation buses (one GPIB, and one special-purpose bus connected via a high speed digital I/0 interface). Sound stimuli consisted of 800-Hz tone bursts (50 ms duration) or clicks. Tone burst voltage waveforms were generated by passing the output of a programmable oscillator (Hewlett-Packard 3325B) through an electronic switch (Wilsonics BSIT) with a shaped rise-fall time (2.5-ms cos^2 shaped). Click voltage waveforms consisted of rectangular 100-μs pulses. Voltage

waveforms were delivered to the acoustic system through programmable attenuators and controlled by a programmable timing system (Brown Advanced Timing).

Analog Recording. Cochlear response waveforms recorded near the round-window were amplified and digitized at a sampling rate of 10 kHz (National Instruments NB-A2000).

Neural Recording. Single-unit activity was obtained by impaling peripheral nerve fibers with glass micro-pipettes filled with 2M KCl (impedances 15-40 MΩ in saline). A remotely controlled micro-drive (Kopf 607W) was used to advance the micro-electrode in 3-μm steps. All recordings were made in the region of the inferior vestibular nerve near its junction with the superior vestibular nerve (Fig. 1). Action potentials were amplified, band-pass filtered, and transformed to discrete pulses by a Schmitt trigger. Arrival times of stimulus markers, positive-going zero crossings of voltage waveforms, and spike pulses were measured with microsecond accuracy by a special-purpose event timer and periodically downloaded to the computer for the construction of arbitrary histograms.

Measurement Protocol. Spike discharges were fed to a speaker for audio monitoring. Units were detected by a drop in the recorded DC potential or the onset of spontaneous activity. When a new unit was detected, it was tested with an 800 Hz tone burst at 110 dB SPL. Units which displayed audible increases in discharge rate to this stimulus were classified as acoustically responsive and studied further with a relatively standard measurement protocol. First, an iso-response measurement ("tuning curve') was taken for frequencies between 50 kHz and 100 Hz (Chapter II), followed by a 20-sec measurement of background activity. Condensation clicks were then delivered at a rate of 10 clicks/sec (n = 500) at the maximal amplitude of the acoustic system. These were followed by an identical sequence of rarefaction clicks. Tone bursts (50 ms duration) were then delivered at a rate of 3 bursts/sec (n = 64) with an amplitude of 80 dB SPL. The tone-burst amplitude was then incremented by 5 or 10 dB and the tone burst sequence repeated until the sound level reached 110 dB SPL. Collection of a complete data set (all sound levels tested) required 7-10 minutes.

Injury discharges. Not infrequently, units displayed abnormal discharges (e.g. sudden increases in background activity) consistent with neural injury. This phenomenon has been previously associated with proximity of the cell body and recording electrode (Walsh *et al.*, 1972). Injury discharges sometimes stopped spontaneously or after slight retraction of the electrode, thus allowing the unit to be studied further. In other cases, injury discharges led to bizarre waveforms or discharge patterns followed by loss of spike activity.

Occasionally, we obtained click responses during periods of minor injury discharge because we continued to find robust short-latency responses in the presence of elevated

background activity. No measurements were made of tone burst responses during injury discharge.

Intracellular labeling. In 8 experiments, one or more neurons with intracellular DC potentials below -30 mV were injected intracellularly with buffered solution of 2% biocytin (containing 0.05M Tris, 0.45 M KCl) as described for horseradish peroxidase (Liberman & Oliver, 1984). Injection current waveforms were square waves (100 ms period; 50% duty cycle) with an amplitude of 2-7 nA for periods ranging from 1-8 mins. After a minimum 24 hour survival time, cats were perfused with 4% paraformaldehyde, the brain was removed *en bloc* with attached cranial nerves VII and VIII. In one case, the saccule was separately micro-dissected from the bony labyrinth. All tissue was embedded in gelatin and 80 μm sections were cut in the horizontal plane. Tissue sections were incubated overnight in avidin-horseradish peroxidase complex and then reacted with diaminobenzidine (Horikawa & Armstrong, 1988).

Analysis. Mean spike rates were calculated from post-stimulus time (PST) histograms over the 50-ms duration of the tone-burst stimulus (e.g. Fig. 6A). To quantify the tendency of a unit to synchronize to individual tone cycles, we first computed a post-zero crossing (PZC) histogram relating spike occurrences to positive-going zero crossings of earphone voltage (e.g. Fig. 6C). A Fast-Fourier Transform was computed from the PZC histogram (e.g. Fig. 6C) and a synchronization index was defined as the magnitude of the first (fundamental) Fourier component divided by the total number of spikes in the PZC histogram. The response phase was defined as the phase of the first Fourier component. The synchronization index (Goldberg & Brown, 1969; Johnson, 1980; Gifford & Guinan, 1983) ranges from zero (no synchronization) to one (all spikes in one bin).

I. RESULTS

Unit Location, Definition and Prevalence

Single-unit recordings were made in the inferior division of the vestibular nerve (Fig. 1), which carries nerve fibers supplying the saccule and posterior semicircular canal. The recording site is in the caudal portion of Scarpa's ganglion, which contains the cell bodies of primary vestibular afferent neurons. The site also directly overlies the cochlear nerve (Fig. 1) and is in close proximity to the vestibulo-cochlear anatomosis (Bundle of Oort), which carries cochlear efferent fibers. Typically, vestibular nerve fibers and cell bodies were found to be intermingled with cochlear efferent fibers in the superficial 0.5-1.0 mm of each electrode penetration. Deeper electrode penetrations usually entered the cochlear nerve and

resulted in abrupt transition to cochlear units with characteristic Poisson-like spontaneous activity and low-threshold acoustic responses (Kiang *et al.*, 1965).

We defined a vestibular unit to be *acoustically responsive* if it increased its discharge rate in response to an 800 Hz tone burst at ≤115 dB SPL. Using this criterion, we have recorded 229 acoustically responsive units in the inferior vestibular nerves of 21 cats. Some of these observations were made in experiments focused on other issues, so that the total number of units does not adequately reflect their prevalence and the ease with which the units were found. We focus here on data from 57 units recorded in 3 ears in 3 cats.

Fig. 2 shows a record of all vestibular units recorded in one electrode puncture in which the electrode was advanced and retracted seven times. Two classes of vestibular afferent units can be distinguished based on the regularity of their spontaneous discharges (Walsh *et al.*, 1972). Units with regular discharges predominated at the recording site (n = 40), but were never found to be acoustically responsive. Of the eight irregular units recorded, 5 were "acoustically responsive" i.e. responded with a rate change at sound levels below 115 dB SPL.

Because the hallmarks of the vestibular units described here were Acoustic Responsiveness and Irregular Discharge, we refer to them as *ARID* units. The prevalence of ARID units was site-dependent; in some penetrations 100% of the irregular units were acoustically responsive. The prevalence represented in Fig. 2 is, however, fairly typical for our later experiments.

Responses to Clicks

Not all ARID units responded to acoustic clicks at the sound levels used here. Most (44 of 57) did, however, and these typically responded with minimum latencies of 0.7 ms, which contrasts sharply with the minimum latencies of 2.0 ms observed in cochlear afferents (Kiang *et al.*, 1965). Most ARID units fell into one of two classes based on their responses to condensation and rarefaction clicks (Fig. 3). As shown in Fig. 3, the classes were based on whether the shortest latency response was obtained with condensation clicks (*PUSH units;* Fig 3A) or rarefaction clicks (*PULL units;* Fig. 3D).

The shortest-latency (<1.0 ms) click responses were almost always followed by a period of reduced firing and then another period (>1.5 ms) of increased firing (Fig. 3A, D). In some cases, the second period of increased firing exceeded the first in amplitude (Fig. 3A). This cycle ("ringing") probably reflects an electro-mechanical oscillation at the level of the sensory epithelium (Chapter II).

Inversion of the click shifted the peaks of the click response in a predictable fashion such that a PUSH unit's response to a condensation click (Fig 3A) was similar to a PULL

unit's response to a rarefaction click (Fig. 3D). These mirrored responses are consistent with a simple hypothesis: *PUSH and PULL units are activated by "normal" hair-cell stimulation and arise from hair cells that are morphologically polarized* (Wersäll *et al.*, 1965)*in opposite directions.*

Responses to Tone Bursts

Frequency. Although responses were obtained at frequencies as low as 100 Hz and as high as 2.5 kHz, ARID units responded best to frequencies between 500 and 1000 Hz (Chapter II). For simplicity, we chose to study the units at one frequency (800 Hz), which was near the best frequency for all units.

Firing Rate. Fig. 4 shows one ARID unit's response to an 800 Hz tone burst as the sound level was increased in 5 dB steps from 80 dB SPL to 110 dB SPL. With few exceptions, ARID units exhibited no increases in discharge rate below 90 dB SPL (e.g. Fig. 4). As the sound level was increased above 90 dB SPL, discharge rates increased monotonically. No firing-rate plateau was observed at the highest sound levels in any unit examined. For the aggregate population of ARID units, firing rate increased from a mean background of 22 spikes/sec at 80 dB SPL to a mean of 127 spikes/sec at 110 dB SPL (Fig. 5). The maximum firing rate observed in any unit was 340 spikes/sec (at 110 dB SPL).

Synchronization. While the mean firing rate threshold was between 90 and 100 dB SPL (Fig. 5), spikes tended to synchronize to a preferred phase of the tone cycle ("phase lock") at levels 10 dB lower (Fig. 6). For example, the unit in Fig.6 showed a clear rate increase at 95 dB SPL (Fig.6A), but phase locked clearly at 85 dB SPL (Fig 6C).

Relationships between rate threshold and phase-locking threshold are shown for four units in Fig. 7. Monotonic increases in synchronization were observed beginning at levels at or near 80 dB SPL. The average synchronization index for these units was quite high (0.77 at 110 dB SPL; Fig. 8).

Fig. 9 shows synchronization and rate change plotted as a function of sound level for 25 ARID units. A dichotomy occurs in the synchronization indices at 90 and 100 dB SPL. Units with the lower synchronization at these sound levels (Fig. 9A, *dashed lines*) had higher rate thresholds and lower maximal rates (Fig. 9B, *dashed lines*). This phenomenon (bimodal synchronization) bears no clear relationship to the PUSH-PULL dichotomy presented above and discussed further below.

Phase. As sound level increased, ARID units began to respond at a preferred phase of the stimulus cycle (Fig. 6C). Fig. 10 shows polar plots of synchronization index (radial coordinate) vs. response phase (angular coordinate) for all units which achieved a synchronization index >0.3 (this criterion was chosen because response phase becomes more

reliable with increased synchronization and firing rate). At 90-110 dB SPL, phases clustered into two classes lying approximately 180° apart (Fig. 10). Almost all units showed a phase advancement of about 30° as the sound level increased from 100 to 110 dB SPL (e.g. Fig. 6).

At 110 dB SPL, ARID units that achieved the highest levels of synchronization (i.e. index > 0.75) fell into two classes 180° out of phase, but a few units with lower (though still marked) synchronization did not. These units tended to fire 90° out of phase from the majority of units (Fig. 10, top).

Relationship of Click and Tone Burst Responses

A strong relationship emerged between clusters of units with preferred phase and the nature of their click responses (Fig. 11). With few exceptions, units that responded with shorter latency to condensation clicks (PUSH units) had a phase near 90° while those units which responded with shorter latency to rarefaction clicks (PULL units) had a phase near 270° (Fig. 11).

Mechanism of Acoustic Conduction.

We wondered whether acoustic activation of these vestibular neurons was accomplished by ossicular transmission (i.e. through the middle ear) or through some non-ossicular mechanism (e.g. bone conduction). A serendipitous observation in one experiment provided strong evidence for ossicular transmission. The acoustic middle-ear muscle reflexes in the cat were usually suppressed by the anesthesia used in these experiments (Borg & Møller, 1975), so we sometimes left the muscles intact. In one cat, large doses of anesthesia were required to suppress the reflex long after the usual indicators (heart rate, respiration, withdrawal reflex) indicated deep anesthesia. We were alerted to the presence of the reflex by recording from ARID units and obtaining uncharacterisitic responses (Fig. 12B). The three ARID units recorded before inactivation of the reflex discharged normally at the onset of the 50-ms tone burst but then abruptly ceased firing within 15 ms. Attenuation of cochlear response at that time indicated a 20-dB reduction of ossicular transmission by the middle-ear muscles (Fig. 12B). After complete inactivation of the acoustic reflex by anesthesia, the cochlear reponse no longer showed attenuation of ossicular transmission (Fig. 12A). Fourteen ARID units were recorded subsequently and found to discharge continuously throughout the tone burst. We conclude that the acoustic input to ARID units enters the labyrinth principally via the middle ear.

Anatomical Identification

Seven ARID cell bodies were labeled intracellularly with biocytin and all were found to be bipolar ganglion cells located in the inferior division of Scarpa's ganglion near the exit of the saccular nerve. Labeling of central and peripheral projections often failed. We attributed this to transport failure caused by cellular injury due to the proximity of the injection site and soma.

In one ear, three ARID units were injected and two labeled cells were recovered. The peripheral processes of both cells extended to the sensory epithelium of the saccule. The central process of one cell was reconstructed and found to project to the vestibular nuclei (Fig. 13D-F). A marked arborization was also found with endings on cell bodies in a poorly defined region near the ventromedial edge of the cochlear nucleus (Fig. 13C). No terminals were observed within the cochlear nucleus.

I. DISCUSSION

Whether or not the mammalian vestibular system retains some role in hearing is the subject of a long debate ignited by the discovery of acoustic responsiveness in the saccule of lower vertebrates, notably rays (Lowenstein & Roberts, 1951), fish (Popper & Fay, 1973), and amphibians (Moffat & Capranica, 1976). The debate was fueled by ablation experiments which showed little or no deficit in equilibrium after destruction of the saccule in monkeys (Igarishi & Kato, 1975).

For the vestibular system in mammals to have a useful role in hearing, it must respond naturally to sounds at levels which are non-traumatic, and the signals it transmits centrally must be processed as auditory information i.e. interpreted as sensation or used to trigger behaviors. We summarize evidence that suggests that responses of saccular neurons may play a role in an organism's response to sound.

Saccular Acoustic Responses in the Cat

The available anatomical and physiological evidence suggests that most, if not all, of the ARID units reported here are of saccular origin. Grossly, the recording site is distal to the vestibular nerve bifurcation and the only afferents likely to be present are those supplying the saccule and posterior semicircular canal (Fig. 1). Our anatomical experiments have demonstrated projections to the saccule from a few well labeled ganglion cells (e.g. Fig. 13) and no evidence of labeling in the posterior canal nerve.

The PUSH-PULL dichotomy among ARID units in their responses to clicks (Figs. 3 & 11) and tones (Fig. 10-11) suggests that they arise mainly from two classes of hair cells

which are morphologically polarized in opposite directions. The saccular macula has two classes of hair cells which are oppositely polarized (Fig. 14). In contrast, the cristae of the semicircular canals each have hair cells with uniform morphological polarization (Lindeman, 1973).

The feline saccule is supplied by aproximately 1800 primary afferents (Gacek & Rasmussen, 1961) of which the majority have regular background activity (Walsh *et al.*, 1972). According to our criterion for acoustic responsiveness (rate change at levels ≤115 dB SPL), none of the regular afferents from the saccule was acoustically responsive. Some irregularly discharging afferents from the saccule may also be unresponsive, although we cannot rule out the possibility that insensitive irregular units (e.g. Fig. 2) arose from the posterior semicircular canal.

Irregular discharges have been associated with the large afferent fibers (Goldberg & Fernández, 1977) supplying chalice endings to the flask-shaped Type I hair cells more prevalent along the central part (striola) of the macula (Lindeman, 1973). The few ARID units we recorded which did not fall into the two polarized (PUSH and PULL) categories (Figs. 10-11) may have arisen from the curved head of the saccule (Fig. 14A) or from hair cells situated directly in the striola transition zone, in which intermediate morphological polarizations are commonly found (Lindeman, 1973).

Acoustic Response Latency. ARID units routinely respond to acoustic clicks with minimum latencies of 0.7 ms from the onset of voltage to the earphone. This short latency in comparison to cochlear neurons (minimun 2.0 ms) may be accounted for in part by shorter acoustic conduction times, a closer recording site, and larger axon diameters (Gacek & Rasmussen, 1961). Nonetheless, the synapses responsible for activation of these neurons must function in ≤0.7 ms and are therefore fast synapses (Guinan & Li, 1990). Previous speculations on the presence of electrical synapses have been made based on morphological specializations found in Type I vestibular hair cells (Spoendlin, 1966). Whatever their synaptic morphology, *ARID vestibular neurons represent the fastest known pathway for the conduction of acoustic information into the central nervous system*, and this property may turn out to be an important clue to their function as well as a useful feature in identifying their post-synaptic projections.

Acoustic Response Threshold. ARID units respond briskly within the upper range of normal hearing. The sound level at which they might make functional contributions to hearing depends, however, on the cues recognized by the central nervous system. If rate changes are necessary for the detection of vestibular nerve responses, then ARID units have minimum thresholds near 90 dB SPL (Fig. 7-8). If phase locking is detectable without an increase in mean firing rate, then acoustic thresholds are closer to 80 dB SPL (Fig. 7-8).

Acoustic Stimulation Mechanisms. The marked suppression of ARID-unit responses during contraction of the middle-ear muscles (Fig. 12) argues strongly for an ossicular conduction pathway. The possiblity that ARID units play some role in hearing is clearly strengthened by evidence that these units are activated through normal middle-ear sound transmission (Fig. 12).

Two aspects of the surgical procedure bear on the question of whether ARID responses occur in behaving animals. These include the opening of the posterior fossa, and the drilling of the superficial temporal bone. It is conceivable that opening the posterior fossa altered the mechanics of the vestibular system, which is in contiguity with the intracranial space through several pathways (but principally via the endolymphatic duct and sac). We note that the long, thin structure of the endolymphatic duct would favor acoustic transmission at very low frequencies.

The drilling of the temporal bone is of more concern, because fenestration of the labyrinth can produce dramatically lowered acoustic thresholds in the vestibular neurons of many animals (Tullio, 1938; Mikaelian, 1964; Wit *et al.*, 1984; Ribaric *et al.*, 1992). For this reason, we meticulously maintained the integrity of the bony labyrinth. In one instance, reported elsewhere (Chapter II), we attempted to record from acoustically responsive vestibular neurons near their brain-stem entry zone and were able to do so without drilling the temporal bone. We had more difficulty finding acoustically responsive neurons at this more proximal site, however, and attributed this difficulty to the presence of numerous afferents from unresponsive end organs.

Saccular Acoustic Responses in Species other than the Cat.

The extrapolation of our results to the awake and behaving mammal are supported by consistent findings in other mammalian preparations in which less extensive surgery was undertaken (Townsend & Cody, 1971; Young *et al.*, 1977; Cazals *et al.*, 1983; Colebatch & Halmagyi, 1992).

Guinea Pig. Sound-evoked potentials have been recorded from the guinea pig labyrinth after the chemical elimination of cochlear hair cells with aminoglycosides (Aran *et al.*, 1979; Cazals *et al.*, 1979; Cazals *et al.*, 1980; Cazals *et al.*, 1982), and some indirect evidence implicates the saccule as the generator for these potentials (Cazals *et al.*, 1983; Didier & Cazals, 1989). The applicability of these findings to normal mammals has previously been questionable in light of the unknown effects of chemical treatment on surviving hair cells.

Human. A number of human auditory phenomena have been attributed to the saccule. These include sound-evoked neck reflexes elicited through normal ears (Townsend & Cody, 1971; Colebatch & Halmagyi, 1992).

Squirrel Monkey. The most comparable study to the present work (Young *et al.*, 1977) examined the response sensitivity of vestibular afferent neurons to both sound and vibration in all five vestibular end organs of the squirrel monkey. The general conclusion of this study was that the mammalian vestibular apparatus was poorly sensitive to sound, and that the saccule was only slightly more acoustically sensitive than other vestibular end organs. Because of their broad approach, these investigators reported the acoustic response thresholds of only 7 saccular units and found a median threshold for rate change of >120 dB SPL. No division of units was made based on the regularity of their discharges. Separation of saccular units by synchronization phase to intense low-frequency tones was accomplished, however, and the phase was found to correlate strongly with morphological polarization as determined by responsiveness to head tilt (Young *et al.*, 1977). Interestingly, one unit in the study (from the saccule) showed a phase-locking threshold of 76 dB SPL, but this unit was not described in detail, possibly because it was not held long enough to be studied thoroughly (Young *et al.*, 1977). This low-threshold saccular unit from the squirrel monkey may be similar to the units studied here.

Central Projections of Saccular Afferent Neurons

The possibility that the saccule is involved in some sort of auditory processing has been strengthened by recent demonstrations that saccular afferents send projections into the auditory brain stem (cochlear nucleus) in mammals (Burian & Gstoettner, 1988; Kevetter & Perachio, 1989). In one study in the guinea pig, 40% of irregularly discharging saccular afferents had cochlear nucleus projections (Kevetter & Perachio, 1989). These demonstrations reinforce the anatomical link between cochlear and vestibular systems established by the observation that some cochlear efferent neurons collateralize within the vestibular nuclei (Rasmussen, 1960; Brown *et al.*, 1988).

We were unable to demonstrate cochlear nucleus projections from ARID neurons, although this negative result may be readily accounted for by the paucity of well-labeled ARID cells. We did, however, find an elaborate collateral that terminated on cell bodies in a nondescript region near the ventromedial border of the cochlear nucleus (Fig. 13C). This region is contiguous with the outflow fibers of the ventral acoustic stria (trapezoid body) and the properties of its constituent neurons remain unknown. It may represent a previously undefined region for the processing of auditory information.

With appropriate central connections, ARID units could serve a number of different auditory functions, the principal categories being sensation and the initiation of behaviors. Potential acoustic behaviors are plentiful. Saccular neurons are known to make oligosynaptic connections with numerous cranial and cervical motoneurons (Hwang & Poon, 1975; Wilson

et al., 1977). Furthermore, ARID units have acoustic thresholds associated with the rapid activation of motoneurons supplying the eye muscles (Galambos *et al.*, 1953), neck muscles (Townsend & Cody, 1971; Colebatch & Halmagyi, 1992), and middle-ear muscles (Guinan & McCue, 1987). The relationship between ARID units and middle-ear muscle (MEM) motoneurons is particularly intriguing, since both classes of neurons have best frequencies near 1000 Hz and thresholds >90 dB SPL (Guinan & McCue, 1987; Kobler *et al.*, 1992). The afferent neurons for the acoustic MEM reflexes have long been assumed to arise solely in the cochlea (Borg, 1973a), but the primary afferent neurons and interneurons remain unknown (Joseph *et al.*, 1985). All available anatomical evidence on the pathway of the acoustic MEM reflex is consistent with ARID contributions (Borg, 1973). However, we note that ARID units are unlikely to be solely responsible for acoustic MEM contraction owing to an additional high frequency response region exhibited by MEM motoneurons (Kobler *et al.*, 1992) and absent in ARID units (Chapter I).

The possibilities for ARID involvement in sensation are also numerous as ARID response thresholds are in the sound level range associated with transitions to discomfort (e.g. rock music) and pleasure (e.g. rock music). If this accessory auditory pathway is present in humans, it even holds the remote possibility of facilitating treatment for profound sensorineural deafness. An electronic hearing prosthesis interfaced with the saccule ("saccular implant") might produce an interpretable sensation, perhaps comparable to the single-channel cochlear prosthesis (Kiang & Moxon, 1972), for patients lacking cochlear neurons. Much of course depends upon the current usage and plasticity of central connections.

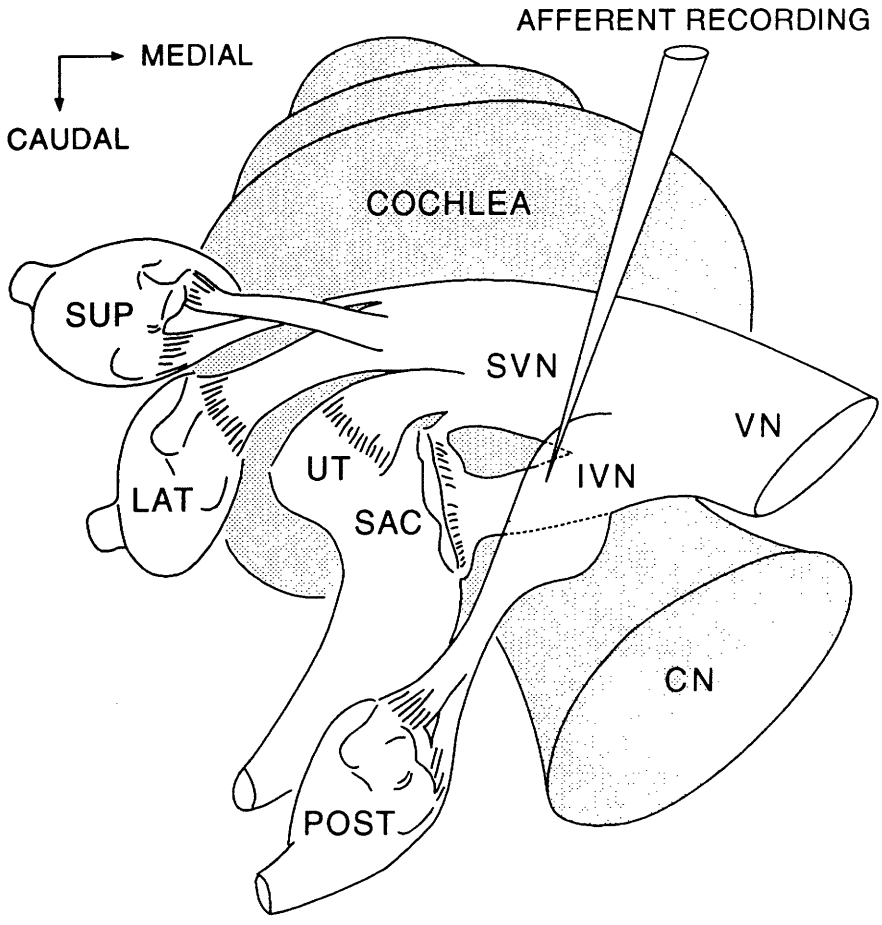

FIGURE I–1. Schematic showing the recording site in relation to the cat's cochlear and vestibular systems. The *shaded areas* represent the cochlea and cochlear nerve (*CN*). The *unshaded areas* represent the vestibular apparatus, which consists of two otolith organs (*SAC* = saccule and *UT* = utricle) and three semicircular canals (*SUP* = superior, *LAT* = lateral, *POST* = posterior). The vestibular nerve (*VN)* supplies the vestibular organs through its superior division (*SVN*) and inferior division (*IVN*). Acoustically-responsive vestibular neurons were recorded in the inferior division, which supplies the saccule and posterior semicircular canal.

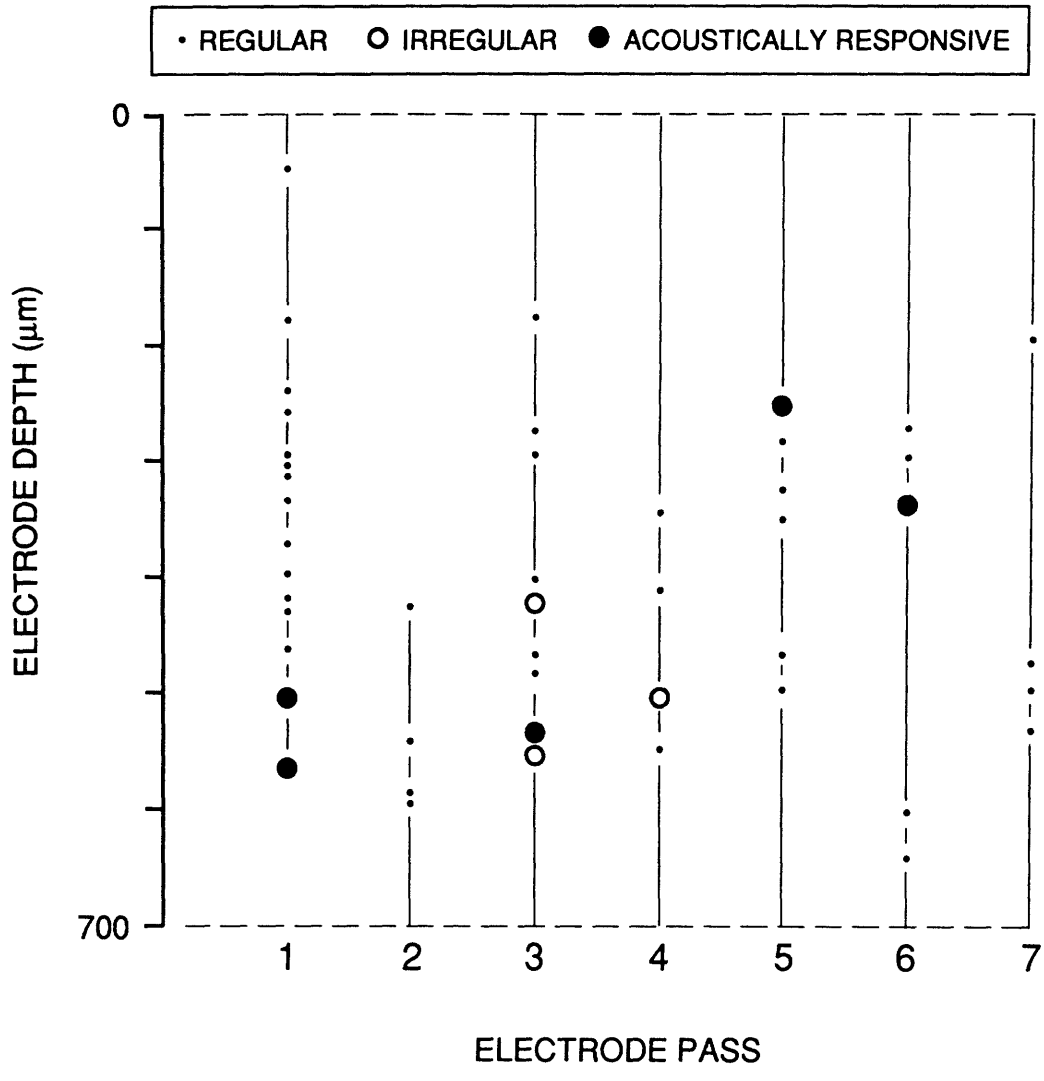

FIGURE I–2. Occurrences of acoustically responsive units encountered on one electrode puncture of the inferior vestibular nerve. Each *column* represents a separate pass (same location) in which the electrode was advanced slowly as each unit was encountered and noted. *Vertical lines* indicate the extent of each pass. Each encountered unit was classified according to the regularity of its spontaneous activity as judged by listening to amplified discharges played through a speaker. All units that displayed audible irregularity were tested for acoustic responsiveness. Of the 8 irregularly-discharging units encountered at this site, 5 showed an increased discharge rate in response to an 800-Hz tone burst at 110 dB SPL.

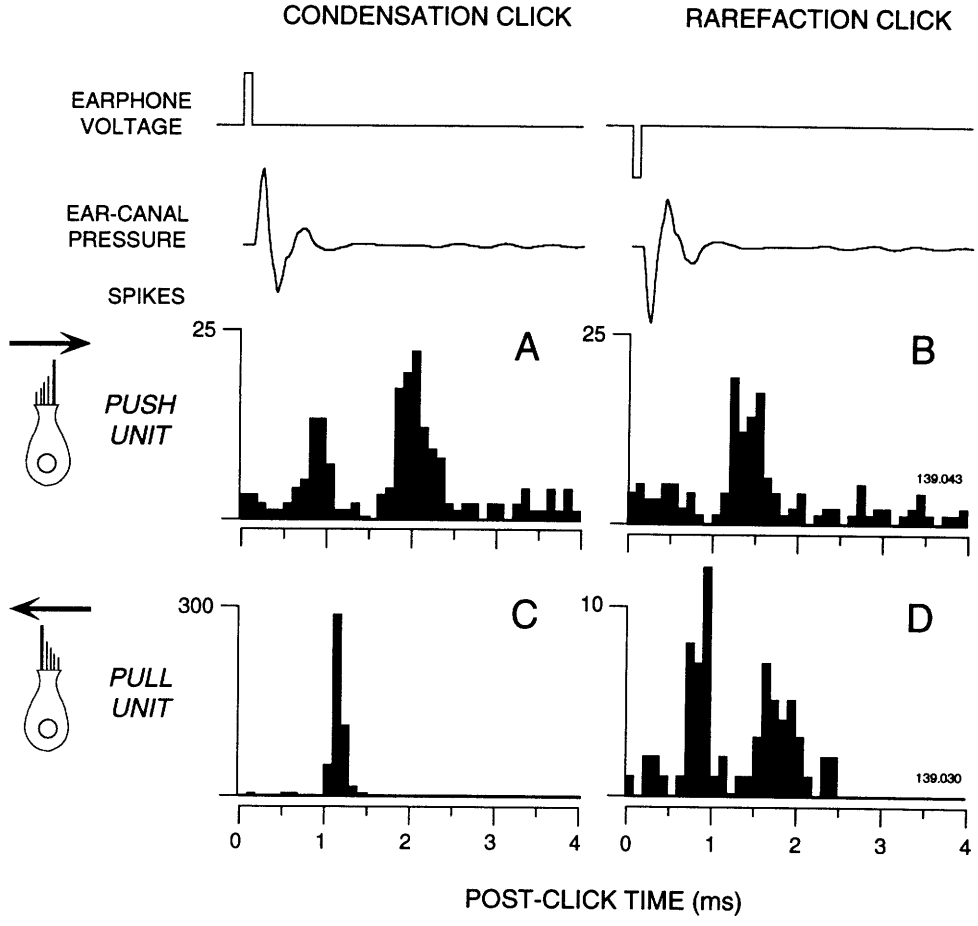

FIGURE I–3. Separation of acoustically responsive vestibular units into two classes (PUSH-PULL) based on responses to condensation and rarefaction clicks. The *first trace* shows the timing and polarity of the voltage waveform delivered to the earphone. The *second trace* shows the the pressure waveform recorded from the microphone near the tympanic membrane. The *lower panels* are PST histograms constructed from the spikes of two different units which are representative of their respective classes. PUSH units (*A-B*) responded with shortest latency to condensation clicks (*A*), while PULL units (*C-D*) responded with shortest latency to rarefaction clicks (*D*). *Cartoons* at left indicate a hypothetical hair cell orientation and *arrows* indicate the excitatory (depolarizing) direction. The bin width is 0.1 ms. The total number of spikes occurring in each bin are plotted for 500 repetitions of the click.

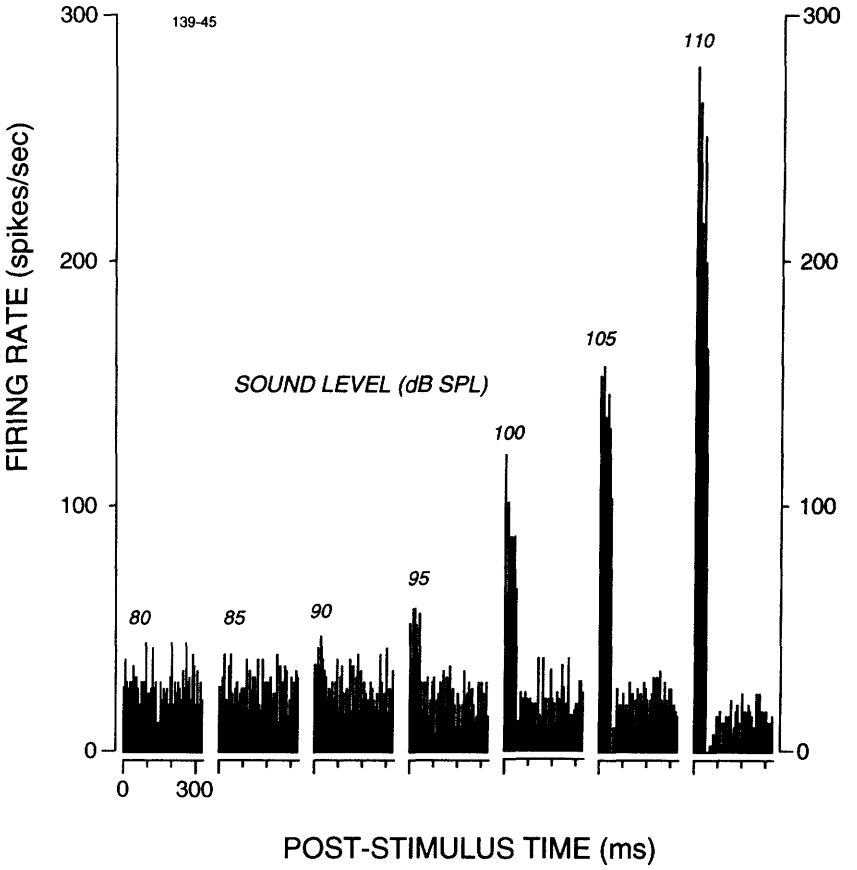

FIGURE I–4. PST histograms of an acoustically responsive vestibular unit to 800-Hz tone bursts of increasing amplitude. Each PST histogram represents responses to 64 tone bursts of 50 ms duration delivered at a rate of 3/sec. Tone burst onset is at t=0. Bin width is 6.7 ms.

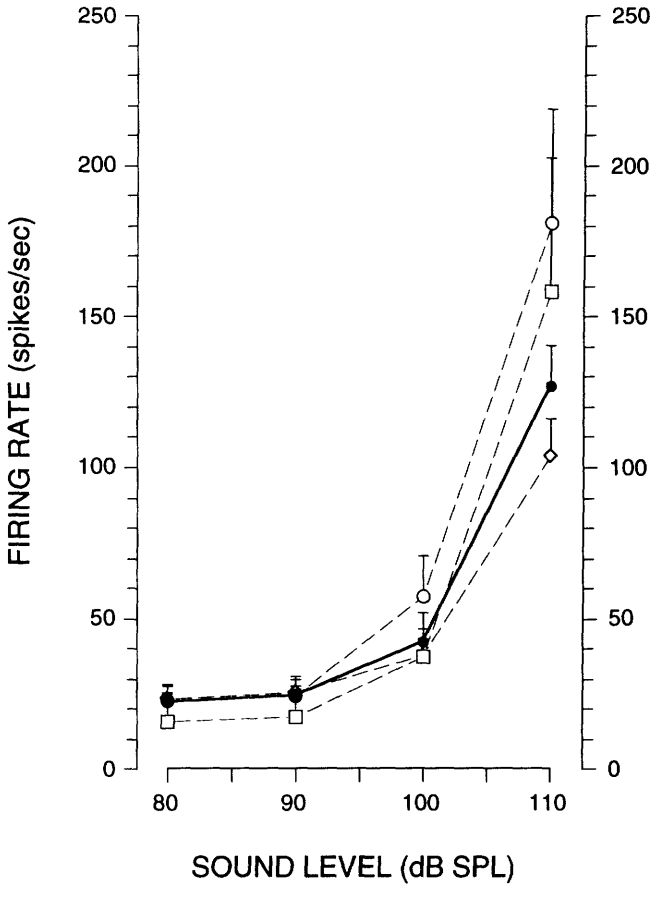

FIGURE I–5. Mean firing rates in acoustically responsive vestibular units at 4 sound levels. Units in which PST histograms were obtained at each level were included. The solid line represents the mean+SEM for all such units (n = 38). Each *dashed line* represents mean+SEM for units from one ear (circles, n = 8; squares, n= 5; diamonds, n = 25). Mean firing rate was calculated for each unit over the 50-ms stimulus interval of PST histograms similar to those shown in Fig. 4.

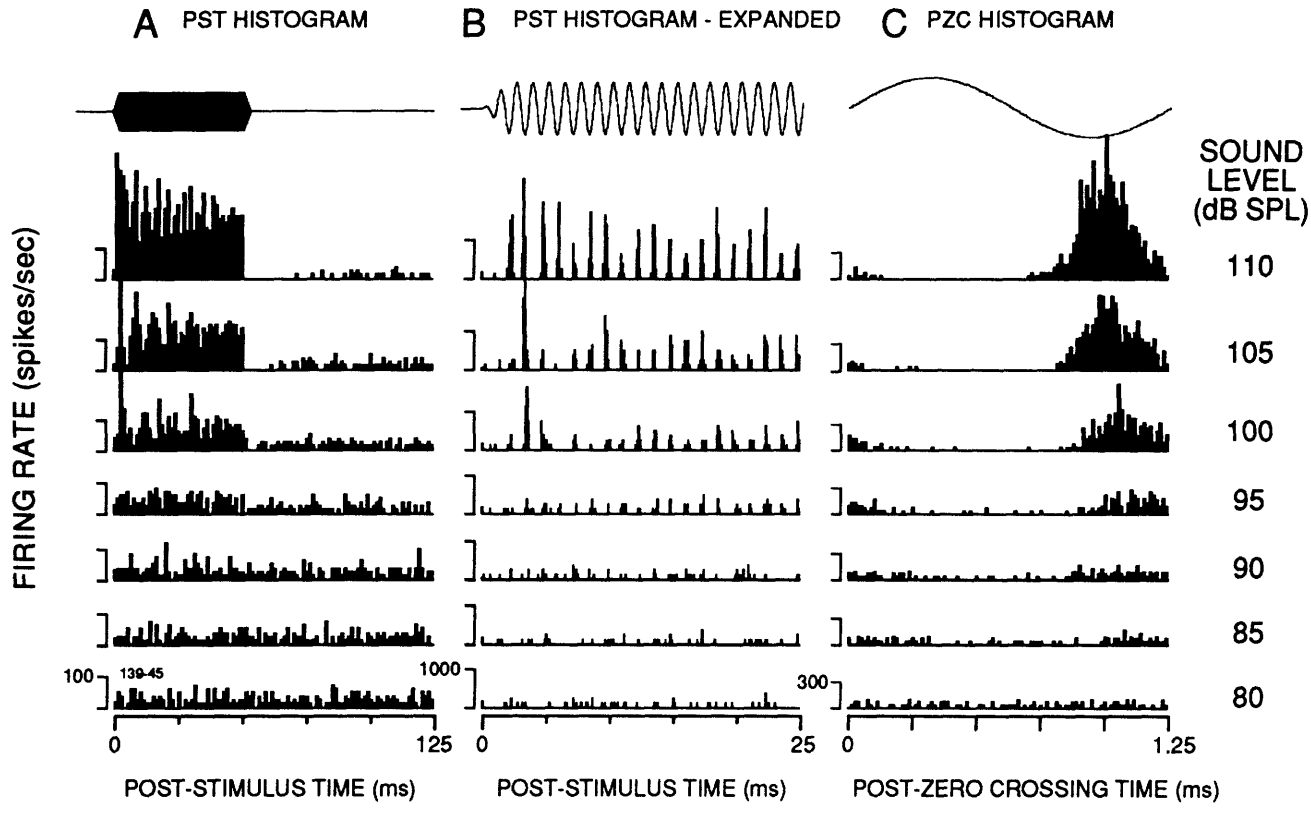

FIGURE I–6. Relationship of phase-locking and rate thresholds for an acoustically responsive vestibular unit. *Top traces* depict voltage waveforms at the earphone. *A*, PST histograms showing firing rate increases occurring at ≤ 95 dB SPL. *B*, Expanded PST histograms showing the tendency for discharges to occur at a preferred phase of the stimulus cycle. *C*, Post-zero crossing histograms showing tone synchronization occurring at levels ≤ 85 dB SPL. Note that the preferred phase in *C* advances noticeably with increasing sound level. The stimulus was an 800 Hz tone burst with a 50-ms duration and 2.5 ms rise-time. Same unit shown in Fig. 4.

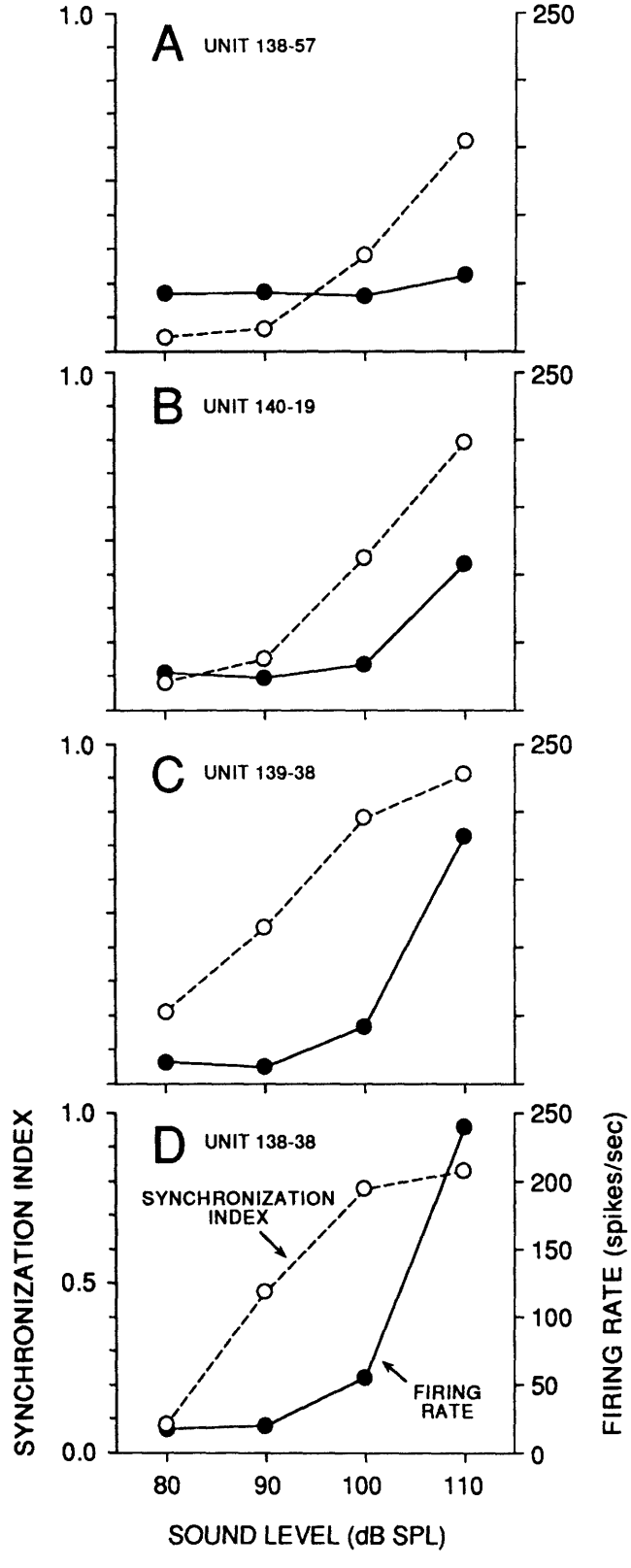

FIGURE I–7. Comparison of firing rate and synchronization in 4 units at 4 sound levels. *Dashed lines* show the synchronization index for each unit (*left scale*). *Solid lines* show the corresponding firing rate (*right scale*). Units were chosen to illustrate a range of maximal firing rates. In each unit, an increase in synchronization occurred at a level at least 10 dB below that which produced an increase in firing rate. Stimuli identical to Fig. 6. See Methods for calculation details.

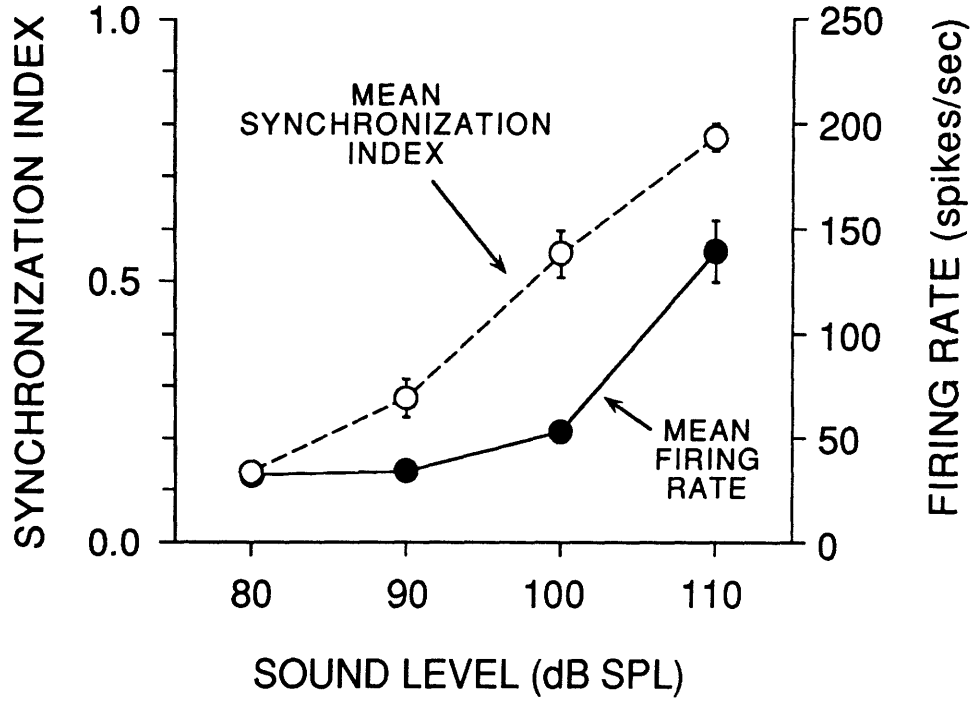

FIGURE I–8. Mean synchronization index and firing rate for all units studied at 4 sound levels. Units in which complete histograms were obtained at each level were included (n = 38). *Vertical bars* indicate ±SEM. Labeling conventions identical to Fig. 7.

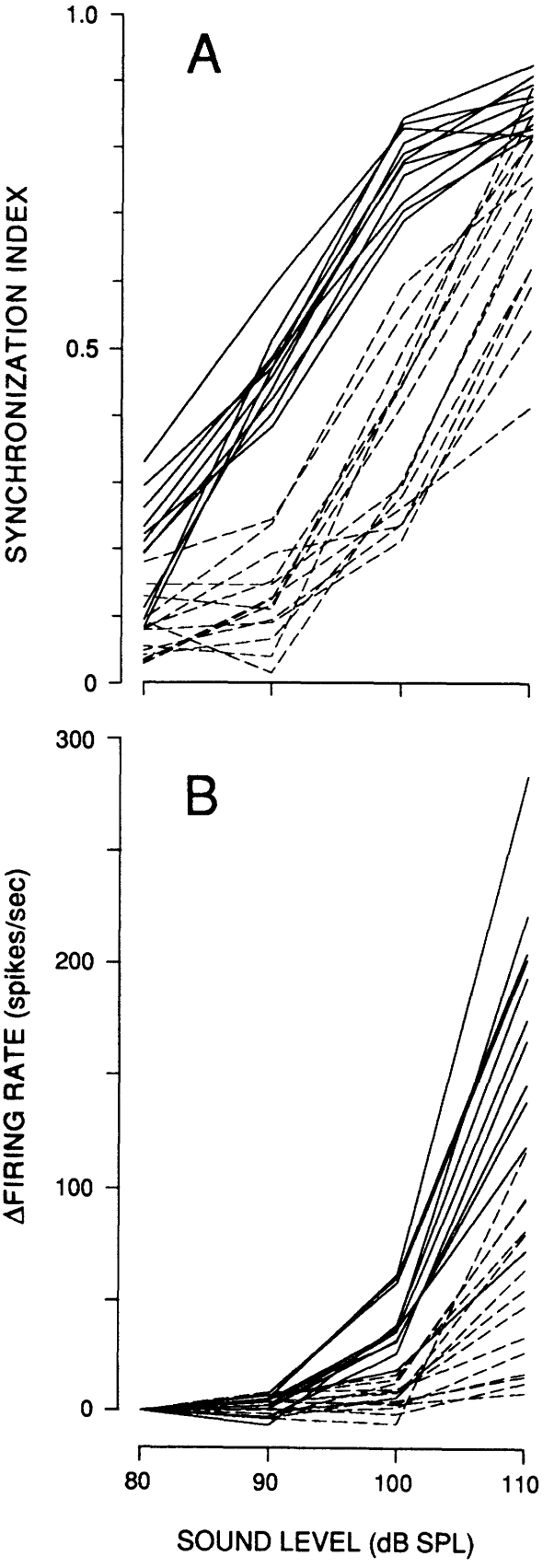

FIGURE I–9. Synchronization and firing rate changes for 25 units. *A*, Synchronization indices at four different sound levels. *B*, Evoked firing rate increase (change from background rate at 80 dB SPL) at four sound levels for the same units shown in *A*. To improve the accuracy of the synchronization index calculation, only units which had background firing rates ≥10 spikes/sec were plotted. *Dashed lines* indicate units which have synchronization indices <0.3 at 90 dB SPL and <0.65 at 100 dB SPL.

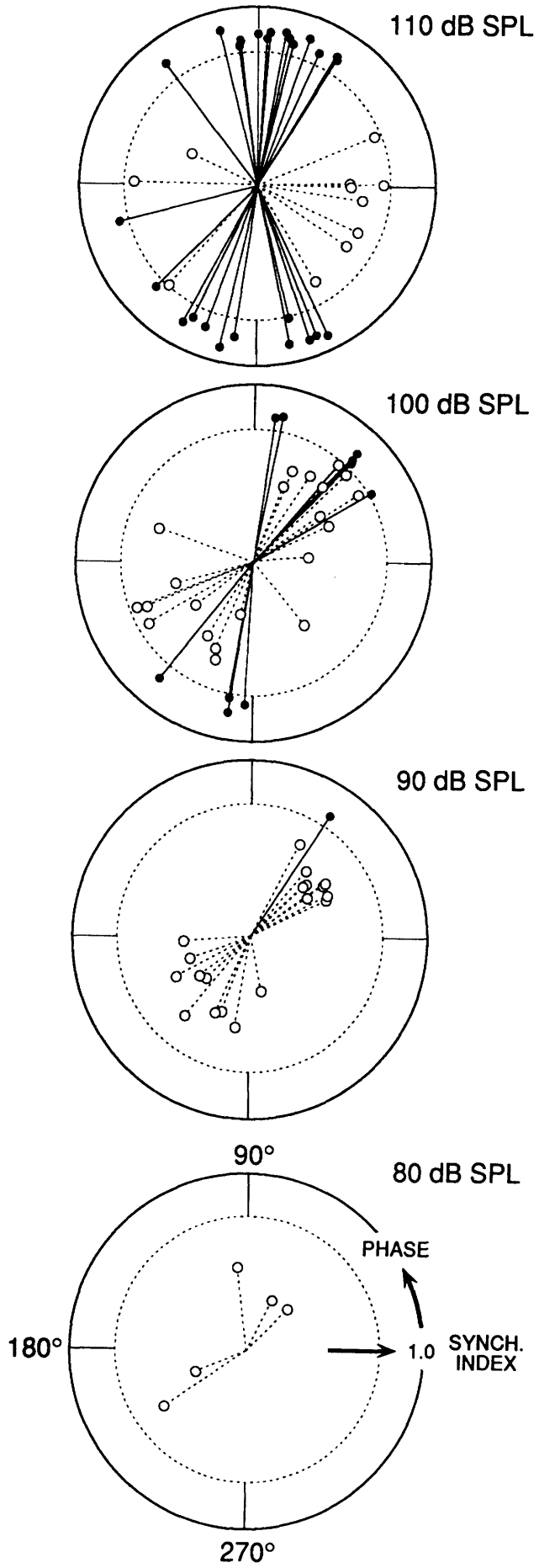

FIGURE I–10. Polarization of acoustically responsive vestibular units into two classes based on response phases to tonal stimuli. Each *panel* shows a polar plot of response phase vs. synchronization index (S.I.) for all units at one sound level. Representation scheme – S.I.>0.75 (*solid lines & filled circles*), 0.75>S.I.>0.30 (*dashed lines & open circles*), S.I.< 0.3 (points omitted because of phase inaccuracy). *Outer circle:* SI=1.0 (perfect synchronization). *Inner circle:* S.I.=0.75 (high synchronization). *Center:* SI=0 (no synchronization) Response phase and synchronization were calculated from PZC histograms (see Fig. 6C and Methods).

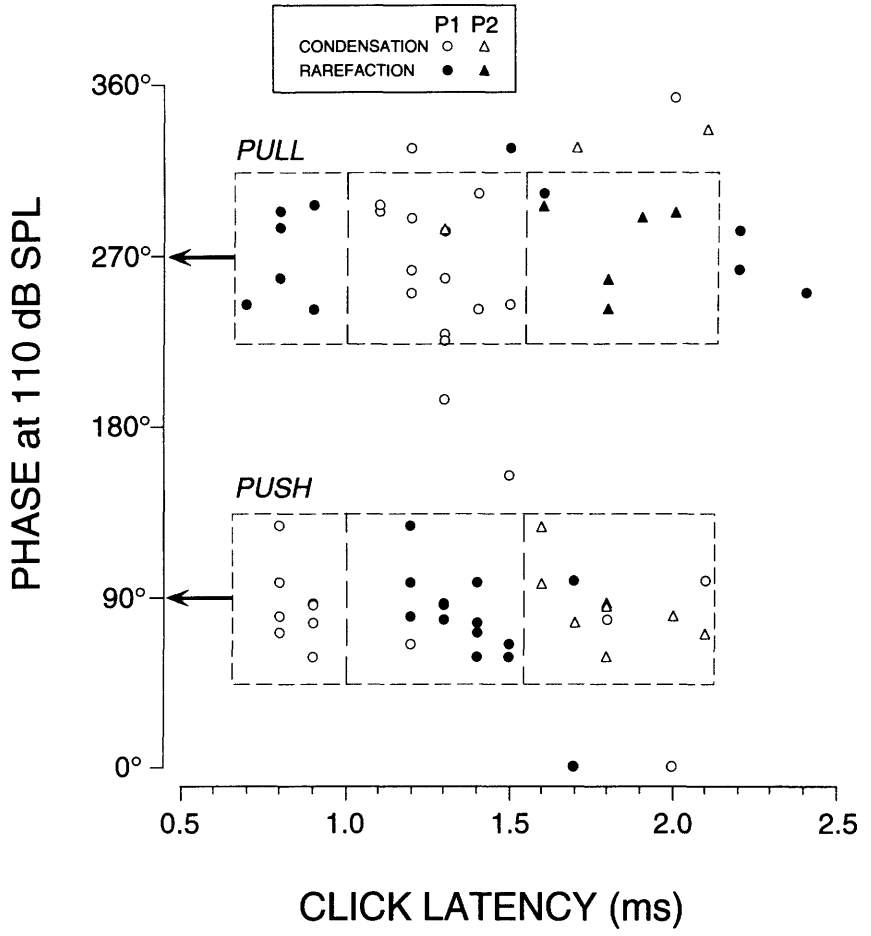

FIGURE I–11. Relationship between click latency and preferred phase for tonal stimulation. Each *symbol* indicates the latency of a peak in a click PST histogram (see Fig. 3) accumulated in response to condensation (*open symbols*) or rarefaction (*filled symbols*) clicks. Initial peaks (*P1*) are represented by *circles* while any secondary peaks (*P2*) are represented by *triangles*. The *upper dashed boxes* and *lower dashed boxes* are regions of identical size, centered on 270° and 90° respectively, in which each corresponding sub-region contains an almost homogeneous population of points. PULL units (*top boxes)* responded with shortest latency to rarefaction clicks and had preferred phases which clustered around 270°. PUSH units *(bottom boxes)* responded with shortest latency to condensation clicks and had preferred phases which clustered around 90°. Response phases were calculated from PZC histograms (see Fig. 6C and Methods). Latency information was taken from all PST maxima that exceeded by 100% the average background activity during the 80-ms pre-click interval. This criterion was occasionally met by a second peak but not a first peak (*triangle* with no corresponding *circle*). Units that responded to tone bursts but not to clicks are not included.

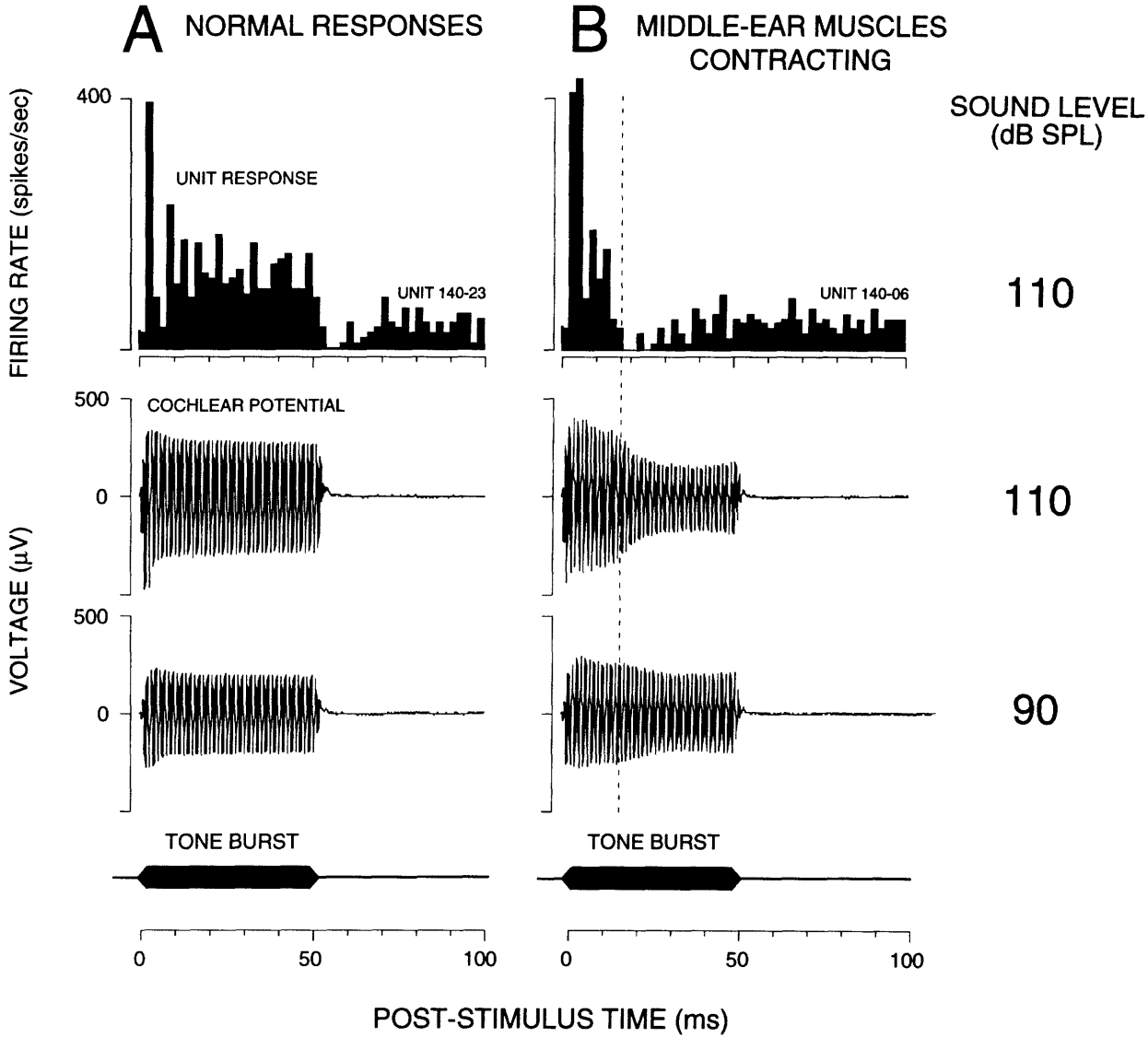

FIGURE I–12. Effect of middle-ear muscle (MEM) contraction on the acoustic responsiveness of vestibular neurons. *A*, The *top panel* shows a PST histogram with the typical (continuous) response of ARID units to intense tone bursts in the absence of the acoustic MEM reflex. *B*, PST histogram showing the response pattern observed in three consecutive ARID units recorded while the acoustic MEM reflex was active. *Bottom panels* show the cochlear response potentials produced by tone burst stimulation at two sound levels. The sharp reduction in middle-ear transmission caused by MEM contraction is shown beginning at 15 ms (*B, dashed line*).

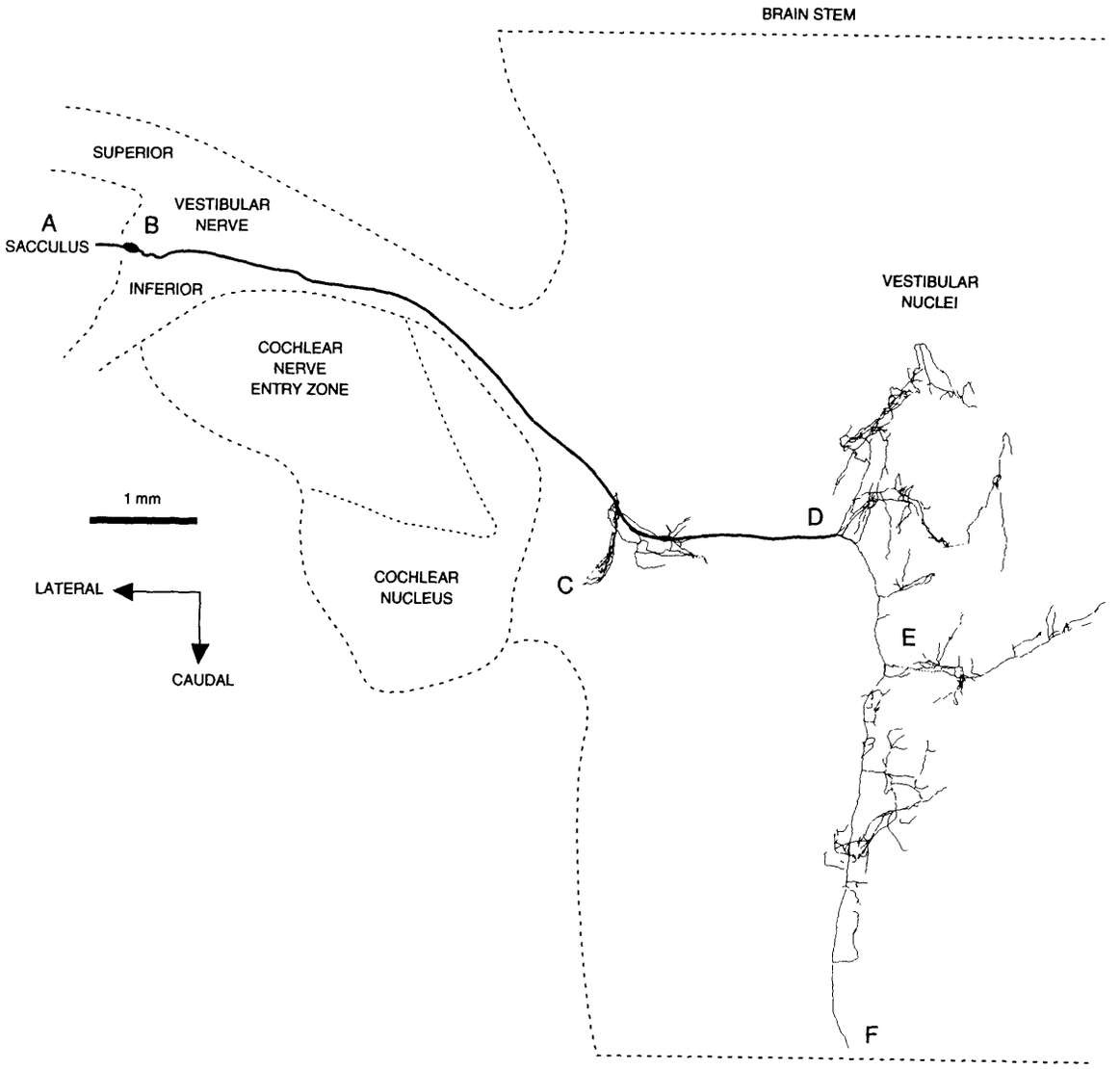

FIGURE I–13. Reconstruction of an intracellularly labeled ARID unit showing its peripheral projection to the saccule (*A*), its cell body (*B*), and its central projections to the brain stem (*C-F*). Neural processes were traced from near horizontal sections using a camera lucida (x10, 0.45 n.a. objective). Two cells were intentionally labeled in this case and could be separated based on marked differences in labeling intensity. The lightly-labeled fiber faded out just prior to the bifurcation of the dark fiber in the vestibular nuclei (*D*) and was therefore not reconstructed. Presumed connectivity is indicated by *dashed lines* (e.g. *E*) which represent sections lost during histological processing. The fiber was not completely reconstructed because it extended beyond the caudal edge of the tissue block (*F*). The boundary of the cochlear nucleus was estimated from low-power tracings in the 3 sections containing the nearby neural arborization (*C*). The fiber is shown collapsed along its dorsal-ventral dimension (4.32 mm) as are the partially schematized brain-stem and nerve boundaries. Differences in line thickness do not represent differences in labeling intensity.

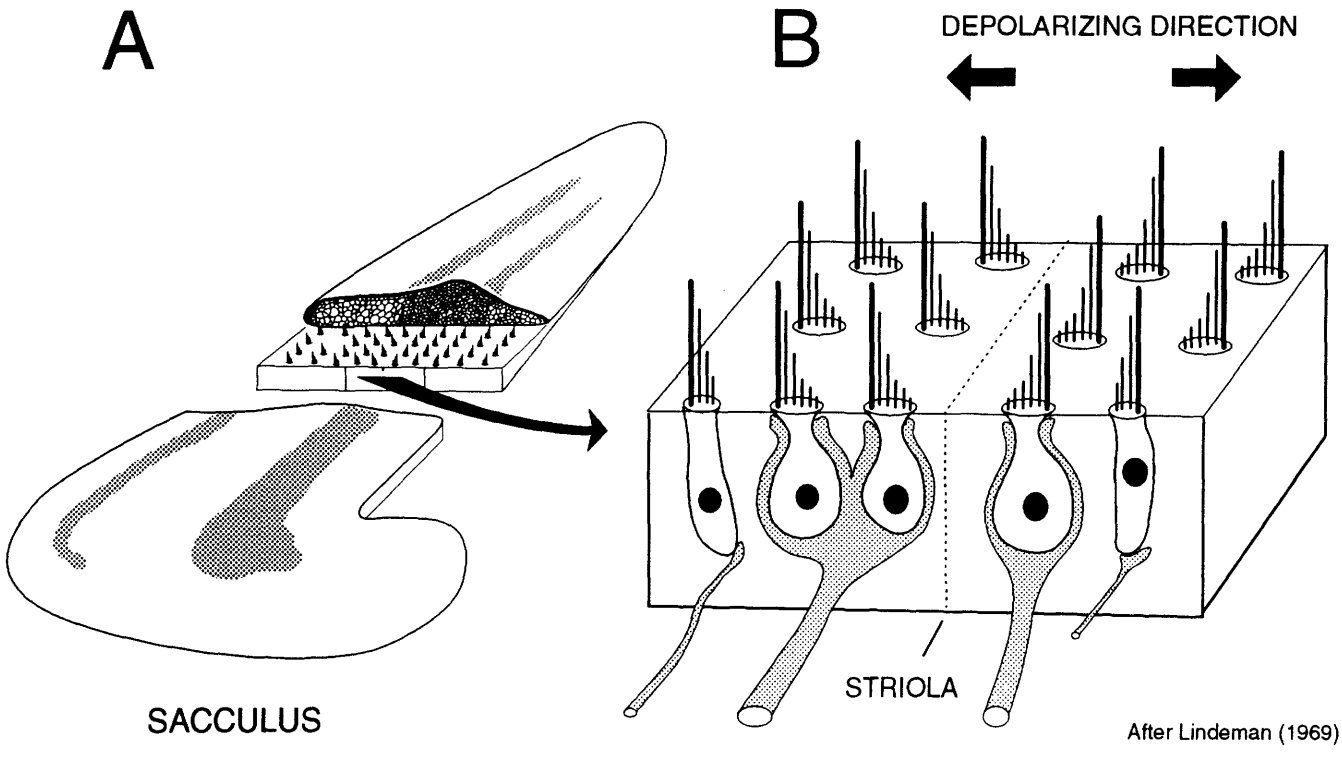

FIGURE I–14. Schematic representation that shows the general shape of the mammalian saccular sensory epithelium (*A*) and the morphological polarization of its hair cells (*B*). Saccular hair cells are divisible into two classes which are morphologically polarized in opposite directions with a boundary along the longitudinal axis (striola) of the macula. Flask-shaped Type I hair cells with chalice-like afferent endings predominate near the striola (*B*). Some of these may exhibit variable directions of morpological polarization (*not shown*). Figure adapted from Lindeman, 1969.

II. TUNING: IMPLICATIONS FOR MAMMALIAN HEARING MECHANISMS

II. INTRODUCTION

We have studied a class of primary vestibular afferent neurons in the cat which respond robustly to sounds at moderately high sound levels (Chapter I). These findings support conclusions about the normal acoustic responsiveness of vestibular elements based on the presence of sound-evoked gross potentials after chemical elimination of cochlear hair cells (Aran *et al.*, 1979; Cazals *et al.*, 1979; Cazals *et al.*, 1980; Cazals *et al.*, 1982; Cazals *et al.*, 1983; Didier & Cazals, 1989). A variety of physiological and anatomical evidence suggests that these cells arise in the saccule, and project to brain stem regions both within and outside the traditional boundaries of the vestibular nuclei (Chapter I).

Acoustically responsive saccular neurons make up an auditory pathway distinct from that originating in the cochlea. Because the acoustic responsivity of the saccule pre-dates the evolution of the mammalian cochlea (Lowenstein & Roberts, 1951; Moffat & Capranica, 1976; Saidel & Popper, 1983), its mechanisms may have played a role in the evolution of mammalian hearing. In this report, we describe the frequency response (tuning) characteristics of saccular neurons and discuss possible mechanisms for this tuning. We relate the response thresholds and frequency ranges of these units to existing auditory mechanisms in mammals and lower vertebrates (Moffat & Capranica, 1976). In particular, we show the similarites between the tuning of these vestibular units and the low-frequency tails in the tuning curves of cochlear afferent neurons (Kiang & Moxon, 1974). We propose a number of hypotheses regarding the evolutionary development of cochlear tuning mechanisms and the relationship of those mechanisms to the action of the middle-ear muscles.

II. METHODS

Treatment of experimental animals was in accordance with protocols approved by the Committees on Animal Care at the Massachusetts Institute of Technology and the Massachusetts Eye & Ear Infirmary. Adult cats were induced and maintained under anesthesia by intraperitoneal injection of diallylic barbiturate in urethane as previously described (Kiang *et al.*, 1965). Except where noted, surgical preparation, sound stimulation and neural recording were performed as described previously (Chapter I).

Sound Stimulation. Sounds were delivered through a metal acoustic assembly sealed against the bony tympanic ring (Kiang *et al.*, 1965). The standard sound source was a 1-in. condenser earphone (Brüel & Kjaer 4132) which was rigidly fixed to the acoustic assembly.

In an experiment designed to test the possibility of direct bone vibration, a second earphone (Beyer DT-48) was connected in parallel to the acoustic assembly through a 4-cm flexible polyethylene tube (Fig. 5A). A small metal probe tube ending near the tympanic membrane (omitted in Fig. 5A) was connected to a 1/4-in. condenser microphone (Brüel & Kjaer 4135) which measured the levels produced by both sound sources as a function of frequency. The maximal sound level delivered was 115 dB *re:* 20 μPa (sound pressure level or SPL).

Neural Recording. Single-unit recordings were made from primary vestibular afferent neurons in the inferior vestibular nerve using glass micro-pipettes (2M KCl) as previously described (Chapter I). The recording site was near the junction of the inferior and superior vestibular nerves. Access was obtained by aspirating the overlying cerebellum and drilling away the roof of the internal auditory meatus (Wilson *et al.*, 1977; Liberman & Brown, 1986). In one experiment, drilling was avoided, and units were recorded centrally at the exit of the vestibular nerve from the internal auditory meatus.

Unit Search Paradigm. Spike discharges were fed to a speaker for audio monitoring. Impaled units were detected by a drop in DC potential or the detection of "spontaneous" spikes. In early experiments, all encountered units were tested with intense noise bursts and units which exhibited audible increases in discharge rate were studied further. We determined that all responsive units had irregular background activity and responded with a rate increase to 800 Hz tone bursts at 115 dB SPL. In experiments reported here, we used these two properties as defining criteria. Each unit with audible irregularity was tested with an 800 Hz tone burst at 115 dB SPL. If it exhibited audible increases in discharge rate, it was classified as acoustically responsive and studied further.

Tuning Curves. We measured thresholds as functions of sound frequency ("tuning curves"; see Fig. 1) using an automated algorithm designed for cochlear afferent neurons (Kiang *et al.*, 1970). Sound stimuli consisted of tone bursts (0.1 to 48 kHz) of 50-ms duration with a 2.5 ms $\cos^2$-shaped rise-fall time. Stimuli were delivered at a rate of 3 bursts/sec rather than the standard 10 bursts/sec used for cochlear afferent neurons (Kiang *et al.*, 1970). The sound frequency was initally set at 48 kHz and decremented in 1 dB frequency steps (between each threshold determination) until 3 kHz was reached, whereupon 0.5 dB frequency steps were used down to 100 Hz (Fig. 1). Sounds as intense as 115 SPL dB were tested except at frequencies where this level was beyond the maximal output of the acoustic system (Fig. 1).

Each tuning curve underwent 3-point smoothing (triangular weighting) before being analyzed further. We defined "best frequency" (Fig. 1) to be the frequency which produced a response at the lowest absolute sound level ("best threshold"). To assess tuning curve

sharpness, we used the statistic Q_{10} (Fig. 1), defined as the best frequency divided by the tuning curve bandwidth 10 dB above best threshold.

II. RESULTS

Acoustically responsive vestibular neurons were first noted during experiments in which cochlear efferent fibers were being recorded near the vestibulo-cochlear anastomosis (Bundle of Oort) in the inferior vestibular nerve (Chapter I). Search stimuli for cochlear efferent fibers consisted of high-level noise bursts, which were found to excite robust responses in some vestibular afferents. Most vestibular neurons that we encountered had regular background discharges and did not show sound-evoked increases in firing rate. A fraction of the irregular vestibular units did show increased firing rates to sound (between 0 and 100% of the irregular units in different electrode penetrations). We refer to these as Acoustically-Responsive Irregularly Discharging (ARID) units (Chapter I).

ARID vestibular afferents were recorded in the inferior vestibular nerves of 21 cats. Responses to tone bursts and clicks have been previously described (Chapter I). We focus here on "frequency response" data from 57 units recorded in 3 ears in 3 cats. Frequency response ("tuning curve", e.g. Fig. 1) was assessed with an automated algorithm previously applied to cochlear afferents (Kiang *et al.*, 1970) and efferents (Liberman & Brown, 1986).

Tuning

ARID units responded to moderately intense sounds (rate change at ≤115 dB SPL) over a frequency band extending from 100 Hz to 2.5 kHz (Fig. 2). Minimum thresholds were near 90 dB SPL (Fig. 2), although units synchronize to low frequency tones at levels 10-15 dB lower than their rate thresholds (Chapter I). Best frequencies are between 500 and 1000 Hz (Figs. 2-3). There was a slight tendency for units with higher best frequencies to have higher thresholds (Fig. 3).

Tuning curves of ARID units were relatively broad (Fig. 4) in comparison to cochlear afferent and efferent units with similar best frequencies (Liberman & Brown, 1986). We assessed sharpness of tuning using the statistic Q_{10} (Fig. 1) and found values generally ≤1.0 for ARID units. In contrast, cochlear afferents and efferents with similar best frequencies have Q_{10} values ≥1.0 (Liberman & Brown, 1986). ARID units with lower best thresholds and lower best frequencies tended to have sharper (higher Q_{10}) tuning curves (Fig. 4). However, we were able to obtain a Q_{10} in only 14 of 57 units because best thresholds in the remaining units were within 10 dB of the maximal earphone output.

Is Activation by Bone -Conducted Vibrations?

A control experiment was performed to determine whether ARID units were responding to earphone vibrations coupled through the metal housing and bony tympanic ring (Fig. 5). We added a second earphone connected to the acoustic assembly through a flexible plastic tube. The tube was inserted to provide vibration isolation and reduce the coupling of vibration from earphone to skull.

Units responded to the two sound sources with similar tuning at similar sound pressures (Fig. 5B), suggesting that the relevant physical variable was sound pressure near the tympanic membrane and not the amplitude of bone vibration. We conclude that the adequate sound stimulus for these units is conducted through the tympanic membrane (and middle ear) rather than through the surrounding temporal bone.

Is the Response Influenced by Temporal Bone Drilling?

In one ear, we recorded from units in the main vestibular nerve root at its exit from the internal auditory meatus without drilling the temporal bone. We obtained tuning curves from several acoustically responsive vestibular afferents (Fig. 6). Tuning curves from two such units are shown in Fig. 6.

II. DISCUSSION

Acoustically-responsive primary neurons are found commonly in the inferior vestibular nerve of the anesthetized cat; available physiological and anatomical evidence (including intracellular labeling) suggests that most of these cells arise in the saccule (Chapter I). These neurons respond to moderately high sound levels with best frequencies in a narrow portion of the acoustic frequency spectrum – both properties which differentiate them from the population of cochlear afferent neurons (Fig. 7). Fig. 7 compares the best threshold and best frequencies for the two known classes of acoustically-responsive irregularly-discharging afferents (cochlear and vestibular) now demonstrated in mammals.

The cat saccule contains two principle groups of hair cells which are morphologically polarized in opposite directions, and ARID units fall into two opposing classes based on their preferred polarities for acoustic stimulation with clicks and their preferred response phases for tones (Chapter I; Young *et al.*, 1977). A simple explanation for these two dichotomies is that ARID units are activated through the normal mechanical stimulation of hair cell stereocilia and the two physiological classes of ARID units correspond to the two anatomical classes of saccular hair cells (Chapter I).

Other evidence supports the hypothesis that hair cells supplying ARID units are stimulated by fluid motions created as the stapes is displaced within the oval window. An earlier study showed that some vestibular units synchronize more effectively to air-borne sounds than to direct skull vibration (Young *et al.*, 1977). We previously observed that the attenuation of ossicular transmission by middle-ear muscles sharply reduces ARID discharges (Chapter I). These observations are supported by the result shown in Fig. 5, which suggests that ARID units respond to sound pressure at the tympanic membrane (and hence middle-ear transmission) rather than to vibration of the surrounding temporal bone. Acoustic sensitivity of ARID units also seems likely to be related to their presumed origin in the saccule (Chapter I), which lies on the medial wall of the vestibule directly opposite the oval window (Lindeman, 1973).

One hypothesis proposed to explain the acoustic sensitivity of vestibular neurons (Young *et al.*, 1977) is that their response to audio-frequencies is an upward extension of their low-frequency dynamic sensitivity to gravito-inertial stimuli (Fernández & Goldberg, 1976a-c). This hypothesis is somewhat discredited by the observation that these units are unmistakably *tuned* to a narrow range of audio-frequencies, i.e. they do not have monotonically decreasing thresholds toward lower frequencies. Because thresholds rise toward both low and high frequencies, it seems unlikely that these neurons are involved in the detection of either infrasound or ultrasound, as has been recently suggested (Lenhardt *et al.*, 1991).

Possible Mechanisms of Tuning in ARID Units.

One possible mechanism to account for the tuning of these vestibular units is that a part of each hair cell is embedded in a physical substrate that has a mechanical resonance. The relatively small differences in best frequency among ARID units (Fig. 7) would then be accounted for by local variations in the resonance characteristics of a vibrating mass. The two obvious candidates for such a vibrating mass in the saccule would be the sensory epithelium, in which the cell bodies are embedded, and the otolithic membrane which surrounds the stereocilia (Lindeman, 1973).

Other possibilities for tuning mechanisms include those intrinsic to each hair cell. For example, tuning may arise from a mechanical resonance in the hair cell stereocilia, as in the alligator lizard basilar papilla (Weiss *et al.*, 1978). Arguing against this possibility is the observation that general tuning characteristics are similar for semicircular canal and otolith units (Young *et al.*, 1977), yet crista stereocilia are more than three times as long as macular stereocilia (Spoendlin, 1970).

Another possibility is that tuning arises from an intrinsic electrical mechanism in the cell membrane, as in the turtle cochlea (Crawford & Fettiplace, 1981) and bullfrog sacculus (Lewis & Hudspeth, 1983). Systematic variations in electrical tuning among different hair cells are well documented in the turtle cochlea (Crawford & Fettiplace, 1981) and might account for the limited range of best frequencies observed in ARID units (Fig. 7).

Vestibular Units in Other Vertebrates Exhibit Similar Tuning Characteristics

When tuning characteristics are compared, ARID units of saccular origin look similar to vestibular units from a wide range of vertebrates. Some semicircular canal units in the squirrel monkey can be made to synchronize to tones at very high levels, and these units exhibit tuning characteristics similar to those shown in Fig. 2 (Young *et al.*, 1977). Units from the fenestrated pigeon semicircular canal also exhibit similar tuning characteristics (Wit *et al.*, 1984). Perhaps the most intriguing similiarity we have noted is between ARID units in the cat and saccular units in the toad (Moffat & Capranica, 1976), which resemble each other in terms of both best thresholds and best frequencies (Fig. 8). Strong similarities are also noted in the broad ($Q_{10}<1.0$) frequency response characteristics of saccular fibers in the goldfish, which are tuned to 800-1000 Hz (Furukawa & Ishii, 1967).

Tuning similarities among vestibular nerve fibers across the entire vertebrate line may be coincidental, but it may also result from the evolutionary propagation of an auditory mechanism that has survival value for vertebrates. We propose the following simple hypothesis to account for the presence of low-frequency (BF 500-1000 Hz), broad ($Q_{10}<1.0$) tuning in sensory receptors of varying size and shape in many species:

Hypothesis 1: Low frequency, broad tuning results from an intrinsic hair cell mechanism that persisted throughout the vertebrate line.

ARID Tuning Curves Resemble Tails of Cochlear Afferent Tuning Curves.

As shown in Fig. 9, tuning curves of normal cochlear afferents have 2 distinct regions – a sharp 'tip' at the unit's characteristic frequency and a broad 'tail' with a minimum at low frequencies (Kiang & Moxon, 1974). ARID tuning curves are less sharp ($Q_{10}\leq1.0$) than the tips of cochlear afferent tuning curves ($Q_{10}\geq1.0$) (Kiang *et al.*, 1965). However, the frequency range and tuning of ARID units resemble the tails of cochlear tuning curves (Fig. 9). As a consequence of this similarity, some effort was expended in early experiments to rule out the possibility that we were recording from high-frequency cochlear afferent neurons with aberrant courses through the inferior vestibular nerve. We routinely scanned units for responses to higher frequencies (up to 48 kHz) in part to rule out this possibility. ARID units

turned out to be distinguishable from cochlear afferent neurons based on their lack of high-frequency tuning curve tips (Fig. 1), extremely rapid responses to clicks (Chapter I) and their spontaneous activity patterns (Chapter III). ARID units were confirmed to be primary vestibular afferent neurons by intracellular labeling (Chapter I).

The cochlea is a relatively late evolutionary development, appearing in full form only in mammals, and thought to be derived from the inferior portion of the labyrinth (containing the saccule and lagena in lower vertebrates) (Wever, 1974). Because cochlear hair cells are derived from vestibular hair cells (Wever, 1974), they may have retained intrinsic tuning mechanisms developed earlier. The fact that the tips and tails of cochlear afferents (Fig. 9) make up components which are separable based on lesions (Kiang *et al.*, 1970) suggests the following hypothesis:

Hypothesis 2: The tips of cochlear afferent tuning curves represent the mechanical tuning of the basilar membrane at the unit's characteristic place, whereas the tails represent an intrinsic tuning mechanism in cochlear hair cells identical to that in vestibular hair cells.

Differences in absolute threshold between ARID tuning curves and cochlear tuning curve tails (Fig. 9) may simply reflect differences in the effectiveness of sound wave transmission to different parts of the membranous labyrinth. Hypothesis 2 suggests that mechanisms underlying the tails of cochlear tuning curves might be fruitfully addressed (in isolation from the tips) by elucidating the tuning mechanism of ARID vestibular units in the cat or even the saccular units of lower species such as the toad (Fig. 8).

Possible Roles in Hearing.

The moderately high thresholds of ARID units (Fig. 8) makes them suitable candidates for afferents neurons which trigger high-level sensations and reflexes (Guinan & McCue, 1987). Despite assumptions to the contrary (Borg *et al.*, 1990), the afferent neurons which trigger all acoustic reflexes remain unknown. Neuroanatomical knowledge of acoustic reflexes involving neck muscles (Townsend & Cody, 1971), peri-ocular muscles (Galambos *et al.*, 1953), and middle-ear muscles (Guinan & McCue, 1987) is so crude (Borg, 1973a; Joseph *et al.*, 1985) that we cannot even say for sure whether the primary afferent neurons enter the brain through the cochlear or vestibular nerves.

Do Vestibular Units Contribute to the Reflex Activation of the Middle-Ear Muscles?

Stapedius motoneurons in the cat have broad tuning curves ($Q_{10} \leq 1.0$) with best thresholds and best frequencies for sound activation (Kobler *et al.*, 1992) near those of ARID units (Fig. 10). One difference in tuning characteristics between stapedius motoneurons and ARID vestibular units and is that some stapedius motoneurons have an additional high frequency response region near 10 kHz (Fig. 10). This observation suggests that stapedius motoneurons receive acoustic input from another source, but does not rule out the possiblity that ARID units make contributions. Differences in response threshold at low frequencies (Fig. 10) could be accounted for if stapedius motoneurons discharged when ARID units began synchronizing to tones (Chapter I), a phenomenon that occurs at sound levels 10-15 dB below tuning curve thresholds.

Were Middle-Ear Muscles Designed to Regulate Acoustic Vestibular Responses?

Contraction of the middle-ear muscles reduces sound transmission through the middle ear and has its predominant effect on low frequencies (Pang & Peake, 1986). The responses of vestibular units to sound are sharply attenuated during contraction of the middle-ear muscles (Chapter I). These observations, together with similarities in frequency response between ARID units and stapedius motoneurons (Fig. 10), suggest a novel hypothesis for the function of the middle-ear muscles.

Hypothesis 3: Middle-ear muscle characteristics were developed in part to regulate the responses of vestibular neurons to loud sounds, so as to limit disequilibrium.

We note, for example, that the frog has an acoustically responsive sacculus (Lewis *et al.*, 1982) and a highly developed middle-ear-muscle mechanism (Wever, 1979). Referring to this mechanism, Wever stated:

> The frog thus achieves a degree of control of sound reception that probably is unmatched among vertebrate ears. The purpose of the middle ear mechanism is no doubt the protection of the inner ear receptors ... from overstimulation by sounds, including the animal's own cries and the intense clamor produced by a group of frogs calling in chorus. (Wever, 1979).

Acoustic triggering of this mechanism may have once been accomplished entirely by vestibular neurons (through negative feedback) with any or all of the sensing function subsequently taken over by the developing cochlea. However, very little information is

currently available about the presence (or absence) of acoustic middle-ear muscle reflexes in sub-mammalian vertebrates (Wever, 1979).

Evolutionary Relationship of Middle-ear Muscles and Auditory Afferents.

The fact that middle-ear muscles existed prior to the origin of the cochlea (Wever, 1979), raises the possibility that their presence helped guide cochlear evolution. Recent experiments on the middle-ear muscles (Pang, 1988) suggests that the primary assistance they provide to mammalian hearing is one of anti-masking, i.e. they prevent low-frequency sounds at high levels from interfering with cochlear reception of high-frequency sounds such as speech (Borg, 1973b; Borg & Zakrisson, 1974). Intense low-frequency sounds interfere with frequency discrimination because all cochlear afferents have some inherent sensitivity to low frequencies. The tails of tuning curves (Kiang & Moxon, 1974)(Fig. 9) are an obvious manifestation of this sensitivity, and these (as noted above) resemble the tuning curves of ARID units (Fig. 9). We therefore propose the following hypothesis.

Hypothesis 4: Middle-ear muscle were implemented to regulate the low-frequency acoustic responses of vestibular units and subsequently aided the evolution of the cochlea by allowing the incorporation of hair cells with intrinsic low-frequency sensitivity (tuning curve tails) into a structure with sharp, mechanical tuning at many frequencies (tuning curve tips).

Conclusion

The demonstration that primary vestibular afferents in mammals respond to sound within the normal range of hearing introduces a second auditory pathway which must be considered when inferences are made about the evolutionary origin and neural organization of acoustic sensations and behaviors. Knowledge of the acoustic threshold and frequency response of this pathway should help to clarify its possible contributions.

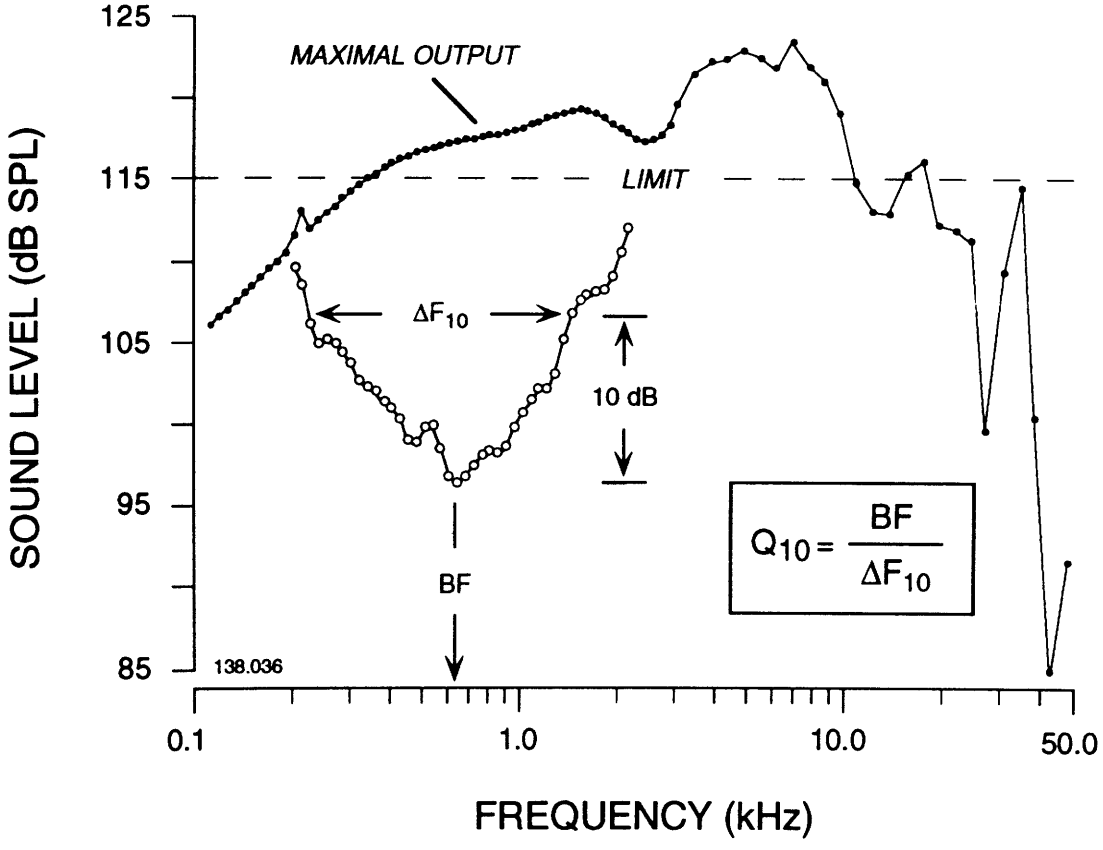

FIGURE II–1. Frequency response (tuning curve) of an acoustically responsive vestibular afferent neuron. *Open circles* represent frequencies at which a threshold was obtained. *Filled circles* describe the maximal sound output of the earphone (measured near the tympanic membrane) and the frequencies tested. The maximal sound level tested was ≤115 dB SPL (*dashed line*) but was restricted by the maximal output of the acoustic system at some frequencies (e.g. <350 Hz). Statistics obtained from each smoothed tuning curve included the lowest threshold (*best threshold, BT*), its frequency (*best frequency, BF*), and a measure of tuning curve sharpness (Q_{10}). Values for Q_{10} were obtained (*inset box*) by dividing BF by ΔF_{10} (the bandwidth of the tuning curve at 10 dB above BT) .

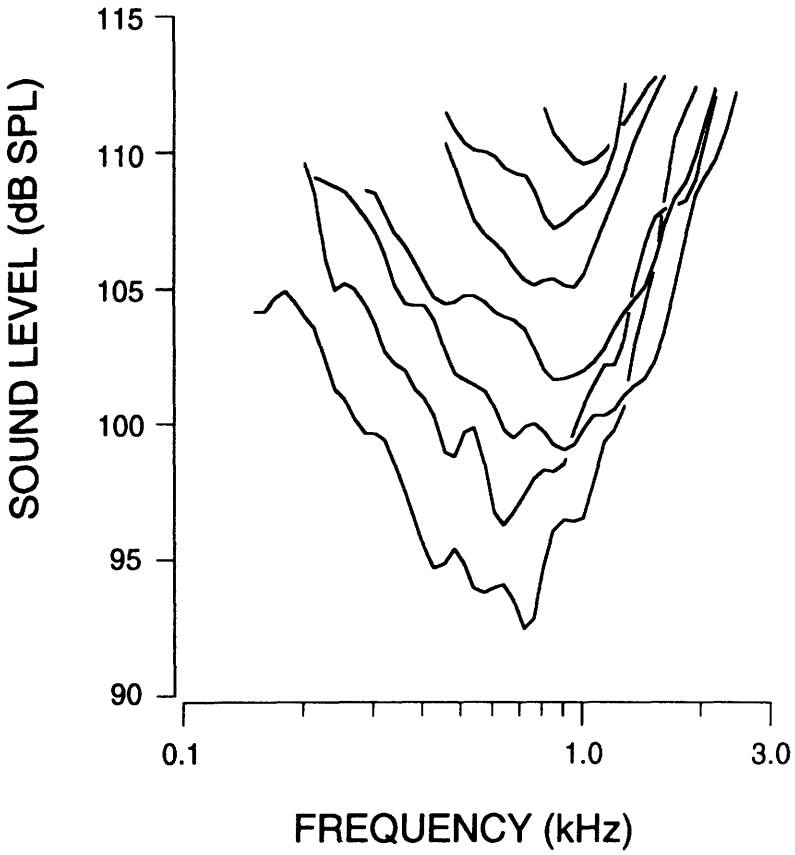

FIGURE II–2. Tuning curves for 7 acoustically responsive vestibular neurons from 3 ears selected to show a range of thresholds.

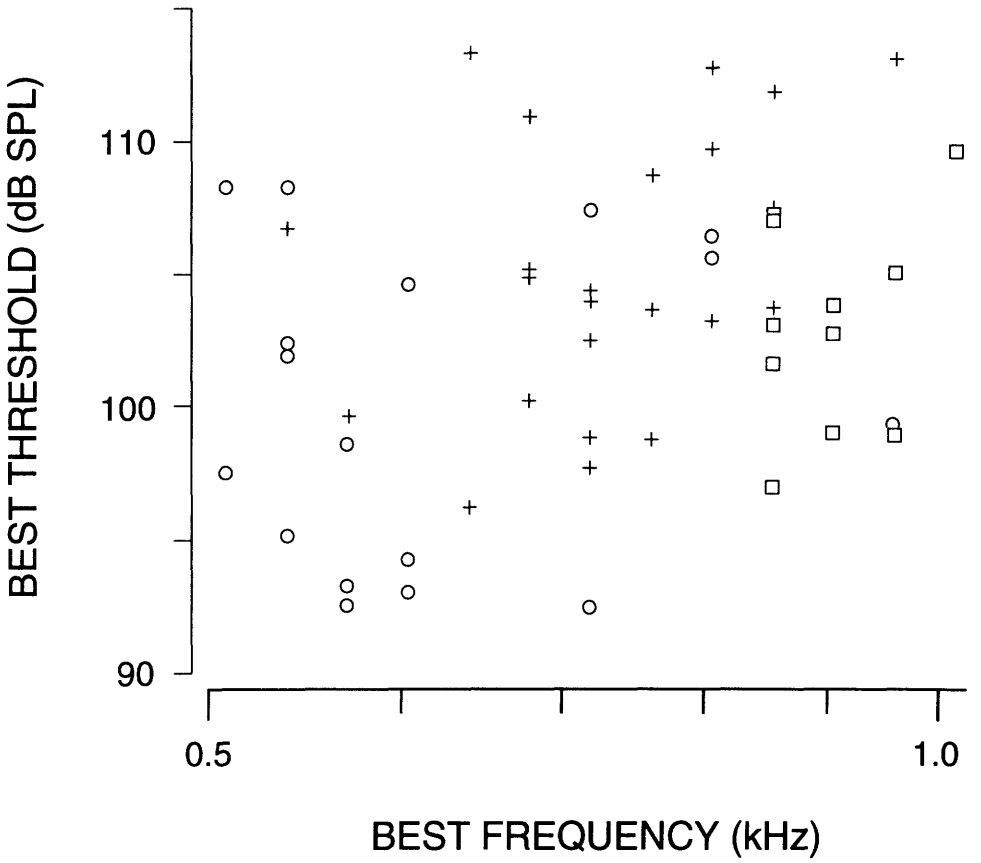

FIGURE II–3. Relationship of best threshold and best frequency for acoustically responsive vestibular units. Each *symbol* type represents one ear.

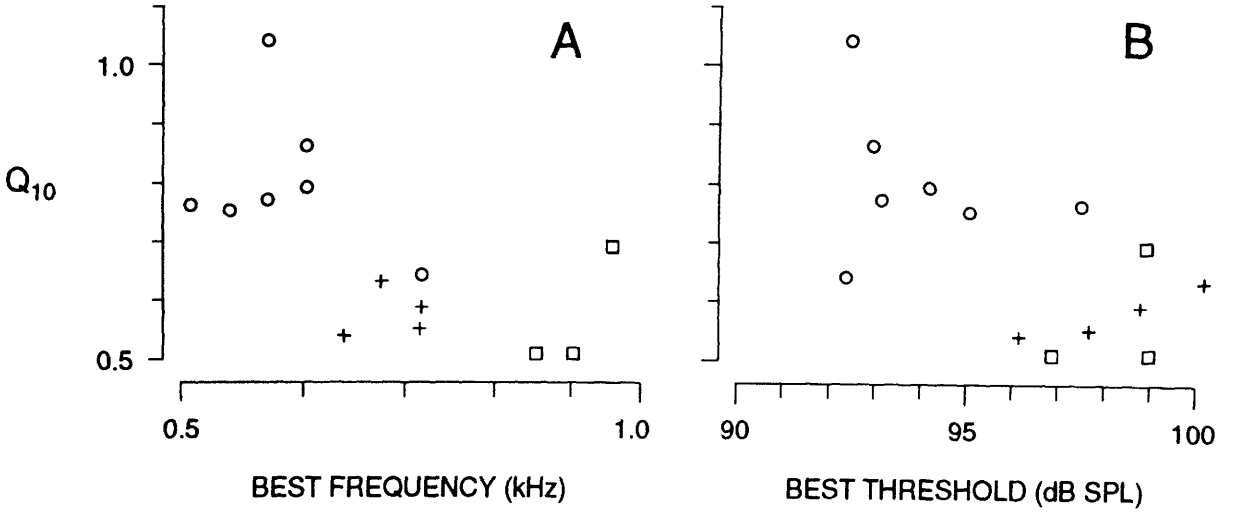

FIGURE II–4. Sharpness of tuning (Q_{10}) versus best frequency (*A*) and best threshold (*B*) for all units which had Q_{10} values. Q_{10} values were not obtained in most units because their best thresholds were within 10 dB of the upper sound limit in one or both side bands. Same *symbols* as Fig. 3.

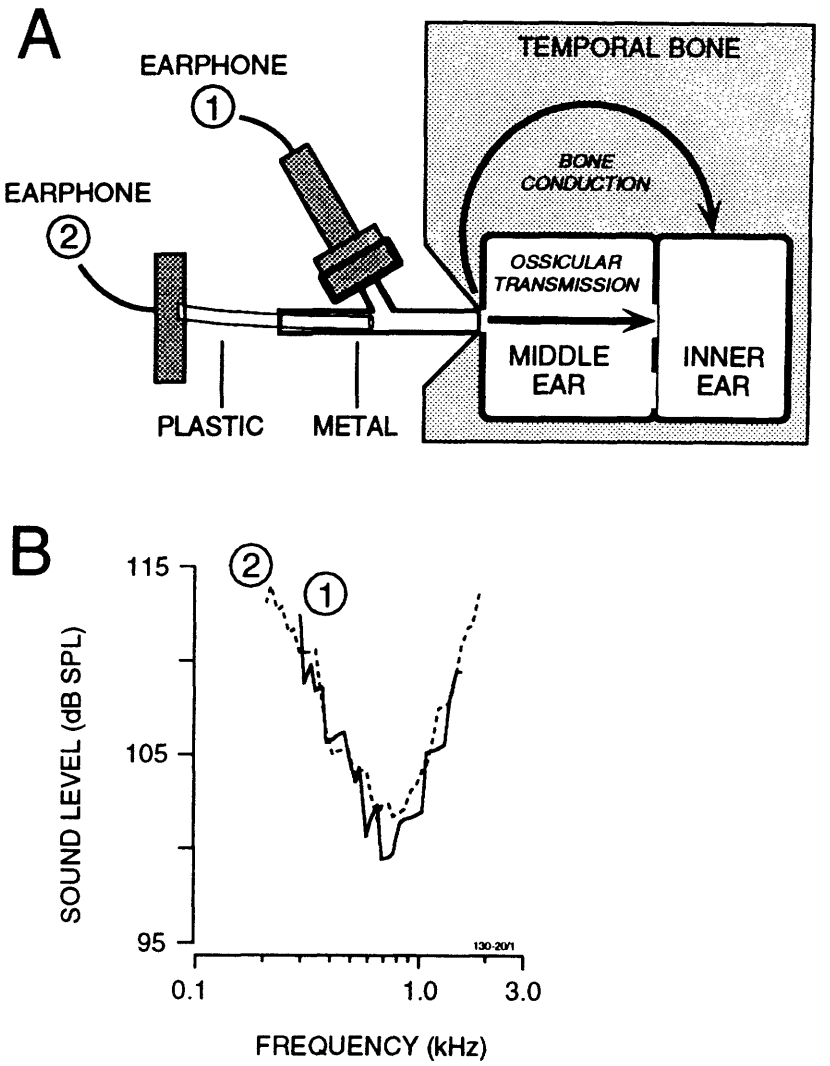

FIGURE II–5. Arrangement and results of a control experiment to test whether ARID units are activated by bone conduction or ossicular transmission. *A*, Schematic showing a special acoustic system using two earphones. Earphone 1 (the standard sound source) is rigidly attached to the metal assembly which is pressed against the bony tympanic ring at the entrance to the middle ear. Earphone 2 is connected by a 4-cm flexible plastic tube to the metal assembly. *B*, tuning curves from the same unit with each earphone.

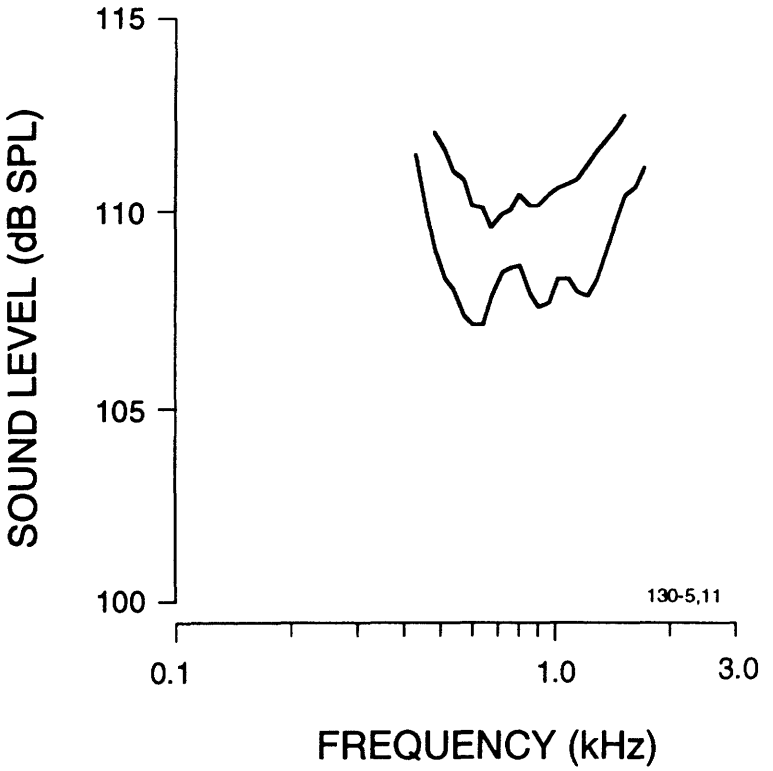

FIGURE II–6. Tuning curves from 2 acousically-responsive primary vestibular neurons recorded in the main vestibular nerve root without drilling the temporal bone.

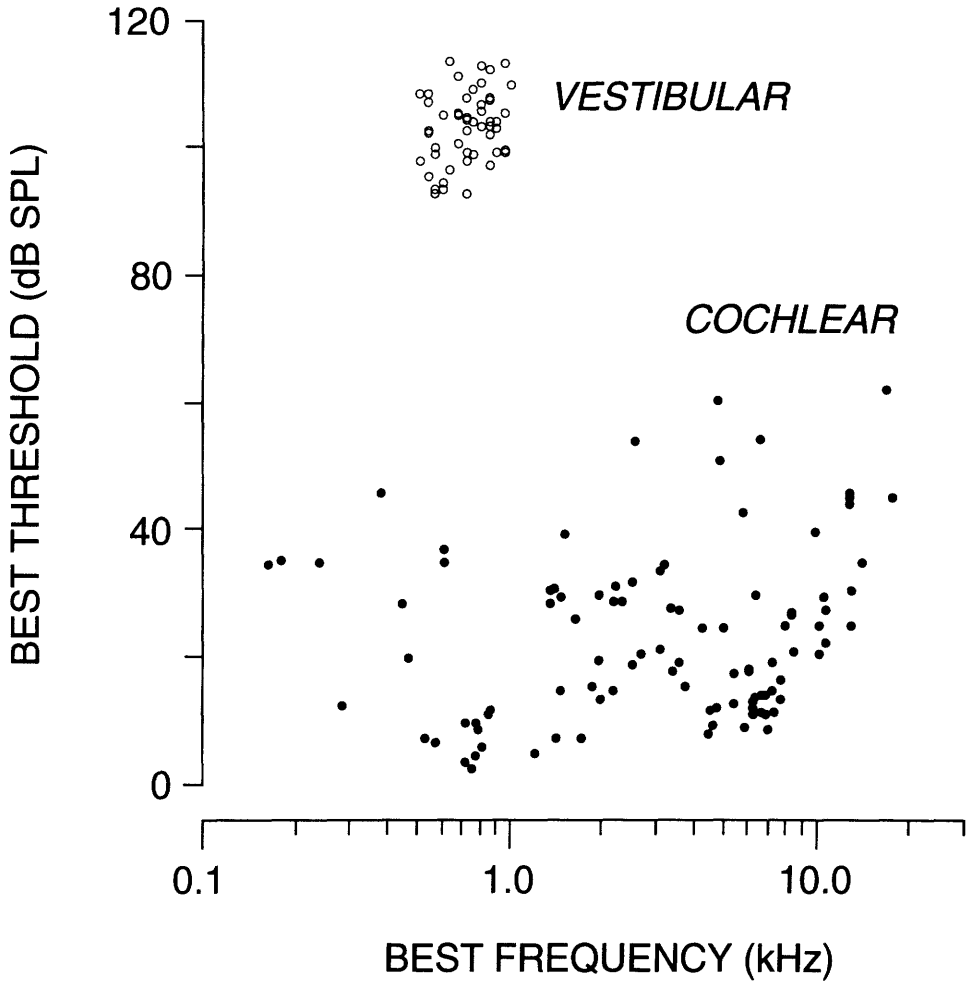

FIGURE II–7. Best thresholds and best frequencies for acoustically responsive primary afferent neurons arising in the cat's vestibular and cochlear systems. *Open circles*, acoustically responsive irregularly discharging (ARID) vestibular units recorded in the inferior vestibular nerves of 3 ears. *Filled circles*, data from cochlear afferent neurons in one ear of a similar experimental preparation (taken from Fig. 2 of Guinan & Gifford,(1988)).

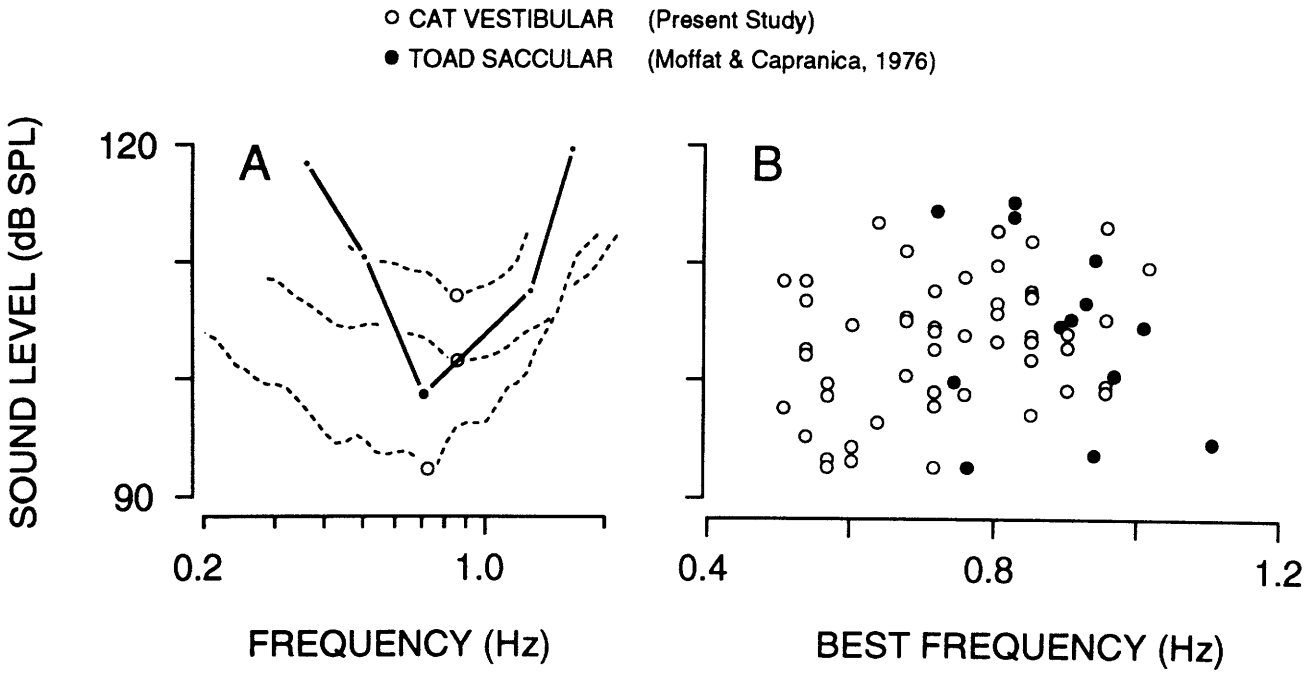

FIGURE II–8. Direct comparison of frequency and sound level response ranges for cat ARID vestibular units and toad saccular units. All data on the toad sacculus were taken from Moffat & Capranica (1976). *A*, tuning curves from one toad saccular unit (*solid curve*) and 3 ARID units (*dashed curves*; from Fig. 2). *B*, Best frequencies and best thresholds for toad saccular units (*filled circles*) and cat ARID units (*open circles*). Note that the frequency scale in *B* is linear.

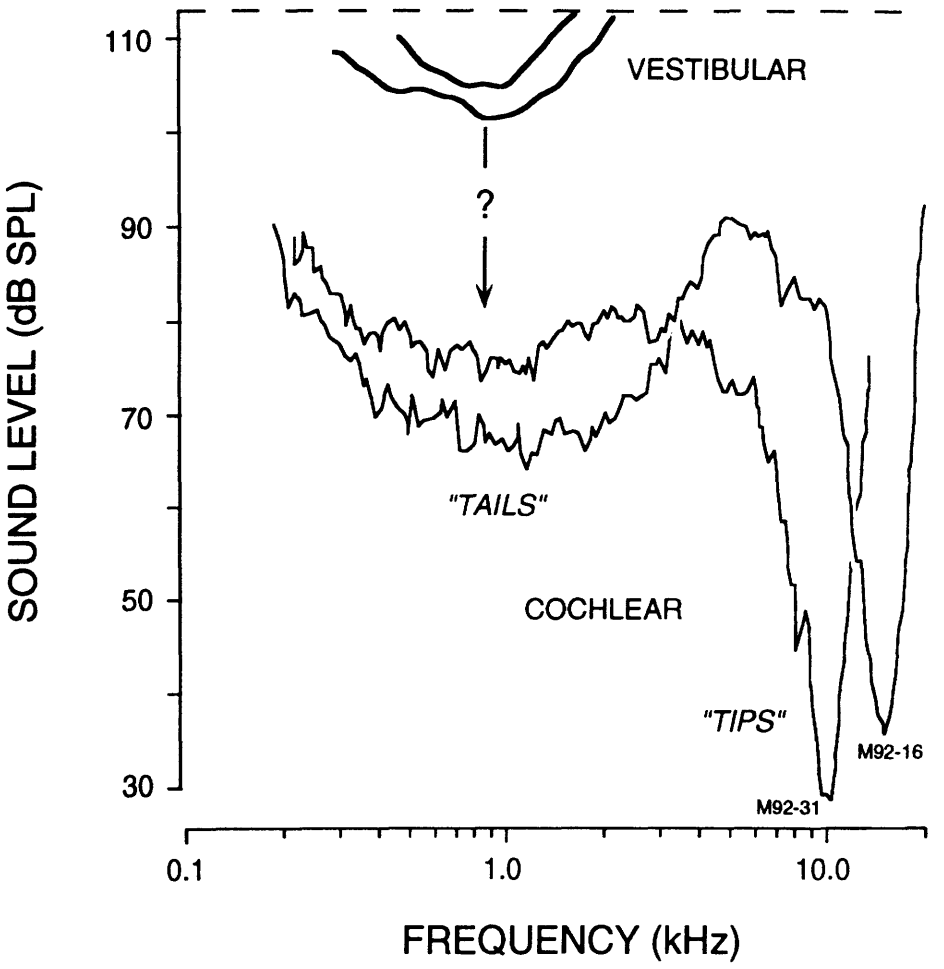

FIGURE II–9. Direct comparison of frequency ranges for ARID vestibular units and the tails of cochlear tuning curves with high CFs. ARID unit tuning curves taken from Fig. 2. Cochlear afferent tuning curves were taken from (Kiang & Moxon, 1974). Tuning curves were chosen from both data sets to emphasize similarities rather than differences.

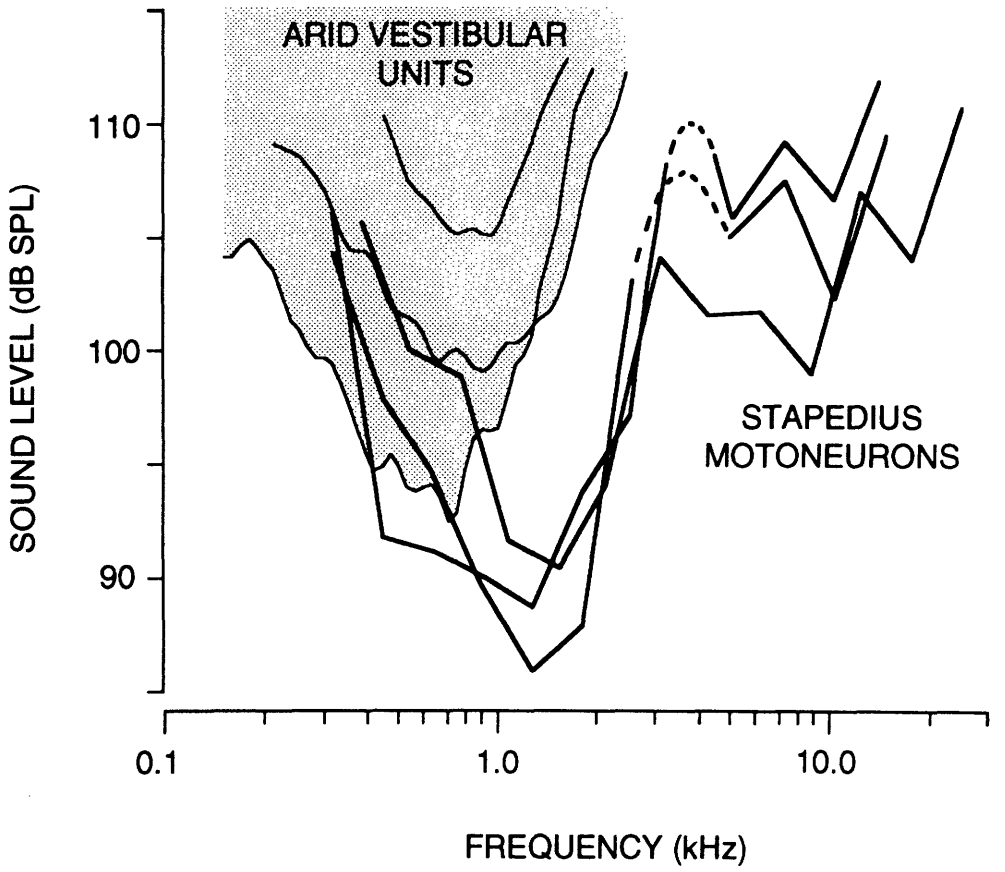

FIGURE II–10. Direct comparison of tuning curves for ARID vestibular units (*thin lines, shaded area*) and stapedius motoneurons of the cat (*thick lines*). ARID unit tuning curves were taken from Fig. 2. Stapedius motoneuron tuning curves were obtained using a similar tuning curve algorithm from unit recordings in peripheral nerve branches of cats anesthetized with Ketamine and paralyzed with Flaxedil (from Fig. 8 in (Kobler et al., 1992)). *Dashed lines* indicate that the upper limit of the acoustic system was exceeded.

III. SPONTANEOUS ACTIVITY OF ACOUSTICALLY-RESPONSIVE VESTIBULAR NEURONS

III. INTRODUCTION

The goals of this chapter are three-fold but modest. They are (1) to describe the spontaneous discharge properties of acoustically-responsive vestibular units, (2) to place these properties into the context of the large body of data available from other eighth nerve units in the cat (Walsh *et al.*, 1972), and (3) to summarize relationships between the spontaneous activity and acoustic discharge properties of these units.

III. METHODS

Methods were as described previously (Chapter I-II) with the following additions. Spontaneous activity was measured during a 20-sec period soon after contact with a unit and, if possible, for a longer (usually 5-min) period after acoustic responses were assessed. The background activity during presentation of acoustic clicks (Chapter I) was also measured and used as an intermediate check for the presence of injury discharge during data gathering. Each run of spontaneous activity had to be free of sudden changes in rate (signal of injury) for the data to be further analyzed. Only runs containing 600 or more spikes were included. The longest spontaneous activity run available for each unit was analyzed (range 20-1500 s).

Inter-spike interval histograms were constructed from the event-times measured as described previously (Chapter I). The standard bin-width was 5 ms. All statistics (except the mode) were calculated from the raw event times. The mode was taken as the midpoint of the bin with the most intervals. Skew values were calculated as described elsewhere (Walsh *et al.*, 1972).

III. RESULTS

Selection criteria. Spontaneous activity was initially assessed in 57 acoustically responsive vestibular units recorded in three ears in three different cats (Chapter I). To increase the reliability of the data, we applied a number of criteria which data had to meet in order to be analyzed further. First, a unit's spike had to be large enough to insure perfect triggering of the event timer (57/57 units). Second, units had to exhibit little or no injury discharge, the hallmarks of which were rapid variations in firing rate (well described by Walsh *et al.* (1972) and commonly seen here). Forty out of 57 units met this criterion. Injury discharge was assessed in part by comparing mean rates during the spontaneous

activity measurement with a short (20-sec) run of spontaneous activity at the time of initial contact and measurements of background activity during the presentation of acoustic clicks. Third, units had to produce at least 600 recorded spikes (30/40 units).

Comparison of Acoustically Responsive Vestibular Units to Other Eighth Nerve Afferents

Firing patterns. Fig. 1 shows the basic types of spontaneous firing patterns observed in afferent units in the cat's eighth nerve. Regular discharge patterns (e.g. Fig. 1B) are observed in the majority of vestibular units recorded in the inferior vestibular nerve. Irregular patterns are exhibited by cochlear units (Fig. 1A) and a minority of vestibular units (Fig. 1C). Cochlear units (with irregular discharge patterns) can be distinguished statistically from irregular vestibular neurons by examining the mode of the unit's inter-spike interval histogram (Fig. 1D). Cochlear units have modes which are almost always <10 ms, whereas vestibular units have modes >10 ms. The tendency for cochlear units to have short intervals between adjacent spikes (Kiang *et al.*, 1965) can be seen in Fig. 1A and detected with considerable reliability by the experimenter listening to the amplified spike discharges played through a loudspeaker (Walsh *et al.*, 1972).

Likewise, a regular vestibular unit can be detected statistically by the fact that its interval histogram is symmetric so that the mode is at the mean interval and hence is inversely related to firing rate (Fig. 1D). Regular units can also be detected audibly because they sound like running internal-combustion motors.

Irregular vestibular units have interval histograms that are skewed to the right (postive skew values) and have modes that fall between regular units and cochlear units (Fig. 1D). The acoustically responsive irregularly discharging (ARID) vestibular units recorded here are shown plotted on top of data collected in a more thorough study of spontaneous activity in the eighth nerve of the cat (Walsh *et al.*, 1972). This study offers an unusually good data base in that it was undertaken in an almost identical preparation in our laboratory. Fig. 1D shows that the modes of ARID units are similar to those of other irregular vestibular units.

Fig. 2 shows an example of an inter-spike interval histogram from an ARID unit. Notice that it closely resembles the interval histogram for an irregular vestibular unit shown in Fig. 1D (*inset*). We accumulated interval histograms for all units and calculated statistics for each (Fig. 2, *inset*). Coefficient of variation (CV) was defined as the SD of the intervals divided by the mean interval.

Discharge Variability. Fig. 3 shows a measure of inter-spike interval variability (skew) obtained from 143 units recorded in the cat's vestibular nerve (Walsh *et al.*, 1972). Skew values were calculated as described by Walsh *et al.* (1972). Audible determination of irregularity has been previously found to correlate strongly with skew values >0.9 (Walsh *et*

al., 1972). Again, the population of ARID units is virtually indistinguishable from other irregular (high skew) vestibular units (Walsh *et al.*, 1972).

We compared the relationship between skew and coefficient of variation (CV) in ARID units (Fig. 4). CV is the most common measure of inter-spike interval variability applied to vestibular units (Fernández *et al.*, 1972; Loe *et al.*, 1973; Goldberg *et al.*, 1990a). We again found substantial overlap with the vestibular units in the previous study (Fig. 4). Note, however that while some exceptionally irregular vestibular units seen by Walsh *et al.*(1972) had skew and CV values that overlapped with those of cochlear units, ARID units were more likely to do so (Fig. 4, *arrow).* This small difference is due to differences in unit selection criteria. The four ARID units in the upper right of Fig. 4 (high skew, high CV) had mean discharge rates <8 spikes/s, and Walsh *et al.*(1972) did not examine units with rates <10 spikes/s. Units with low spontaneous rate have higher CV and skew values (see below).

As shown in Fig. 5A, ARID vestibular units have inter-spike interval distributions in which the mean and standard deviation are highly correlated (Loe *et al.*, 1973). As mean interval increases, measures of variability such as CV also increase (Figs. 5A-B).

Spike Generation in ARID Vestibular Neurons.

The strong correlation between mean and SD (Fig. 5) in ARID vestibular units suggests that there may be a simple probabilistic description for their firing properties. In Fig. 6, I have fitted the inter-spike interval histogram from Fig. 2 with a probability density function from the Erlang family (Drake, 1967). This Erlang process is not memoryless; it can be derived simply by measuring the times between arrivals in a Poisson process and erasing every other arrival, i.e. it describes the distribution of 2nd order inter-arrival times for a Poisson process (Drake, 1967). The mean and standard deviation are linearly related (Drake, 1967).

The shape of inter-spike interval histograms for ARID units strongly resembles an Erlang process that begins after some finite time delay, which amounts to 9 ms in Fig. 6. A simple sequential description for the behavior of the unit shown in Fig. 6 would be as follows: (1) the unit fires; (2) it becomes unresponsive for 9 ms; and (3) two subsequent arrivals from a Poisson event generator are required to make the unit fire again. Further analysis seems warranted in this area, but it will not be pursued here.

Relationship of Spontaneous Activity and Acoustic Responses in ARID Vestibular Neurons

We looked for a relationship between acoustically-evoked and spontaneous discharge properties of ARID units. Fig. 7 shows the relationship between mean spontaneous rate and the best frequencies and thresholds obtained from tuning curves (Chapter II). No obvious relationship was found. There was a slight tendency, however, for more irregular (higher CV) units to have lower acoustic thresholds (Fig. 8).

III. DISCUSSION

The goals of this chapter are three-fold and modest. We have (1) described the spontaneous discharge properties of acoustically-responsive irregularly discharging (ARID) vestibular units, (2) placed these properties into the context of the large body of data available from other eighth nerve units in the cat (Walsh *et al.*, 1972), and (3) summarized relationships between the spontaneous activity and acoustic discharge properties of these units.

Discharge Patterns of ARID Vestibular Units.

We conclude that ARID units are indeed "irregular" as defined statistically using measurements of skew (Walsh *et al.*, 1972) and coefficient of variation (Fernández *et al.*, 1972). Moreover, there are no compelling statistical features (Figs. 1-4) that distinguish them from other high-skew (irregular) vestibular units recorded in cats by Walsh *et al.* (1972). This negative finding is interesting for several reasons. First, Walsh *et al.* (1972) tested vestibular units for responses to sound:

> In the present series of experiments, none of the 25 Class I [high-quality] vestibular units tested responded to clicks even at high stimulus levels, whereas every auditory [cochlear] unit responded to clicks or tones.

They do not mention whether these acoustically unresponsive units were regular or irregular. Nor do they mention the levels tested. It is probable that by "high stimulus levels", they meant high levels for cochlear neurons (Kiang *et al.*, 1965). These levels could still be well below the click levels necessary to elicit responses from ARID vestibular units (Chapter I). Walsh *et al.* (1972) did record from many irregular afferents in the superior portion of the vestibular nerve (the inferior division was not studied in detail) and yet saw no acoustically responsive vestibular units. We conclude that either (1) they did not use high enough stimulus levels, or (2) acoustically responsive vestibular units are not common in the superior

division of the nerve, which supplies the utricle, 2 semicircular canals, and a small portion of the saccule (Retzius, 1884).

Relationship of Spontaneous Activity and Acoustic Responses in ARID Vestibular Neurons

We found no correlation between the mean spontaneous rate and the acoustic response threshold at the best frequency – a correlation well established for acoustically responsive neurons in the cochlea (Liberman, 1978). However, the two variables would have to be highly correlated to be apparent in pooled data (30 units) from 3 ears over the narrow 25 dB acoustic threshold range found in ARID units (compare with the 70-80 dB range observed among cochlear neurons; Liberman, 1978). Similary, no relationship was found between mean spontaneous rate and best frequency, but, again, the best frequency range for ARID units spans only one octave.

The finding of a weak correlation between discharge variability (CV) and acoustic threshold is provocative. Irregular vestibular afferents are more sensitive than regular afferents to low-frequency mechanical stimuli and have response gains (mechanical sensitivities) that rise with frequency (Goldberg & Fernández, 1975). This feature may boost their responses to audio-frequencies, but cannot account for the tuned responses observed in ARID vestibular units (Chapter II).

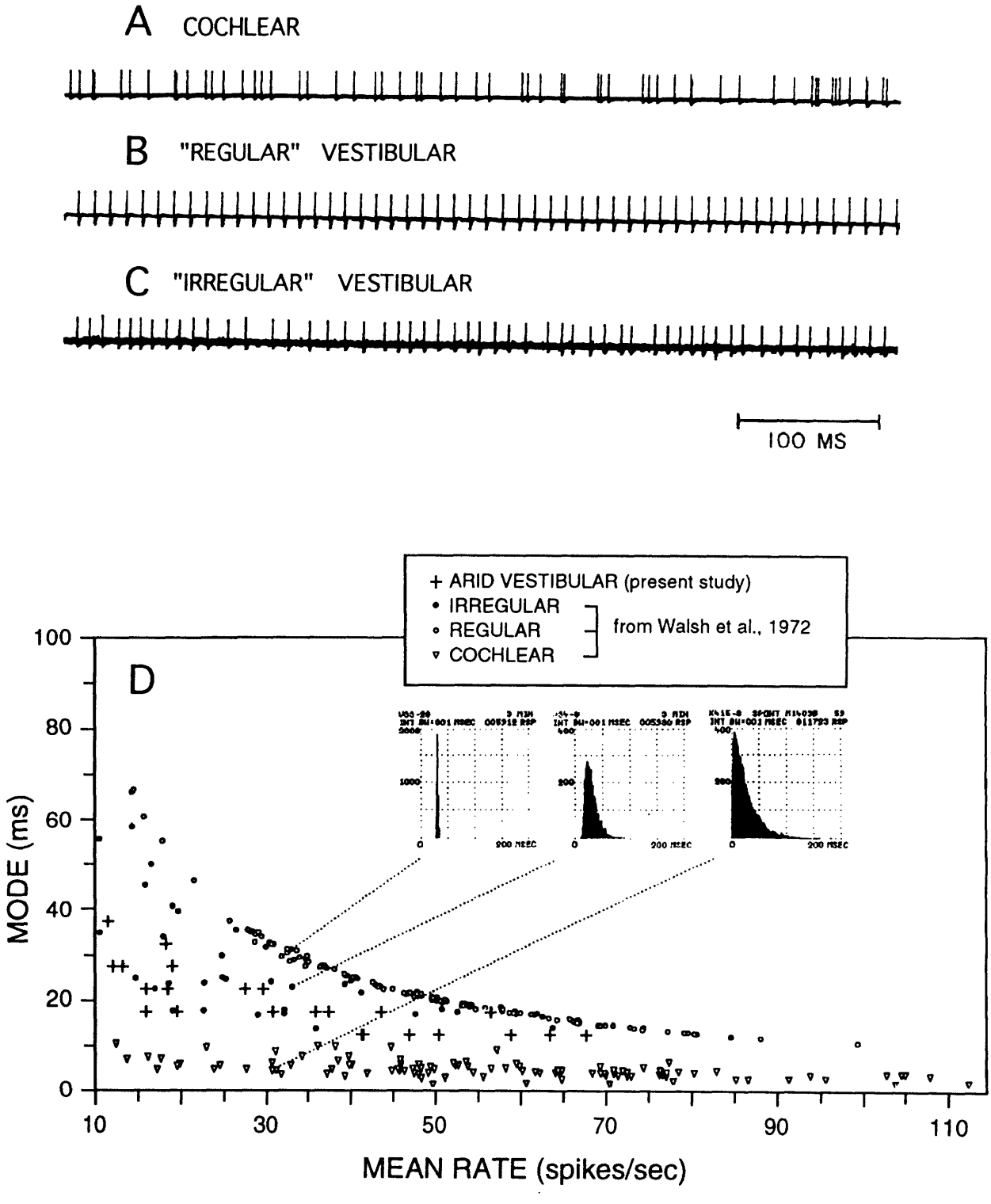

FIGURE III-1. Some firing properties of acoustically responsive irregularly discharging (ARID) vestibular units compared with units recorded in the eighth nerve by Walsh *et al.* (1972). Samples of spontaneous discharge activity in a cochlear unit (A), "regular" vestibular unit (*B*), and "irregular" vestibular unit (*C*). Modes of interval histograms plotted against rates of spontaneous discharge for eighth-nerve units. See *upper inset* for legend. The *lower insets* are sample interspike-interval histograms for the three eighth nerve units indicated by *dotted lines. A-C, Figure 2 of* Walsh *et al.* (1972). *D*, Modified *Figure 6 of* Walsh *et al.* (1972).

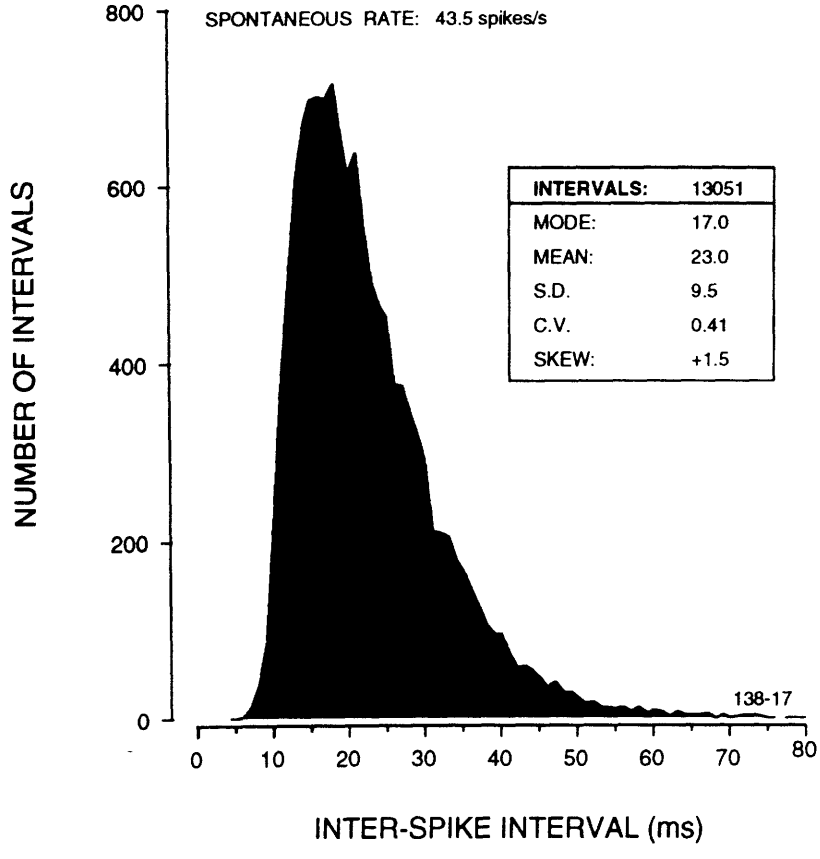

FIGURE III-2. Sample inter-spike interval histogram for an ARID vestibular unit. Accumulation time: 5 mins. Bins: n = 80, width = 1 ms.

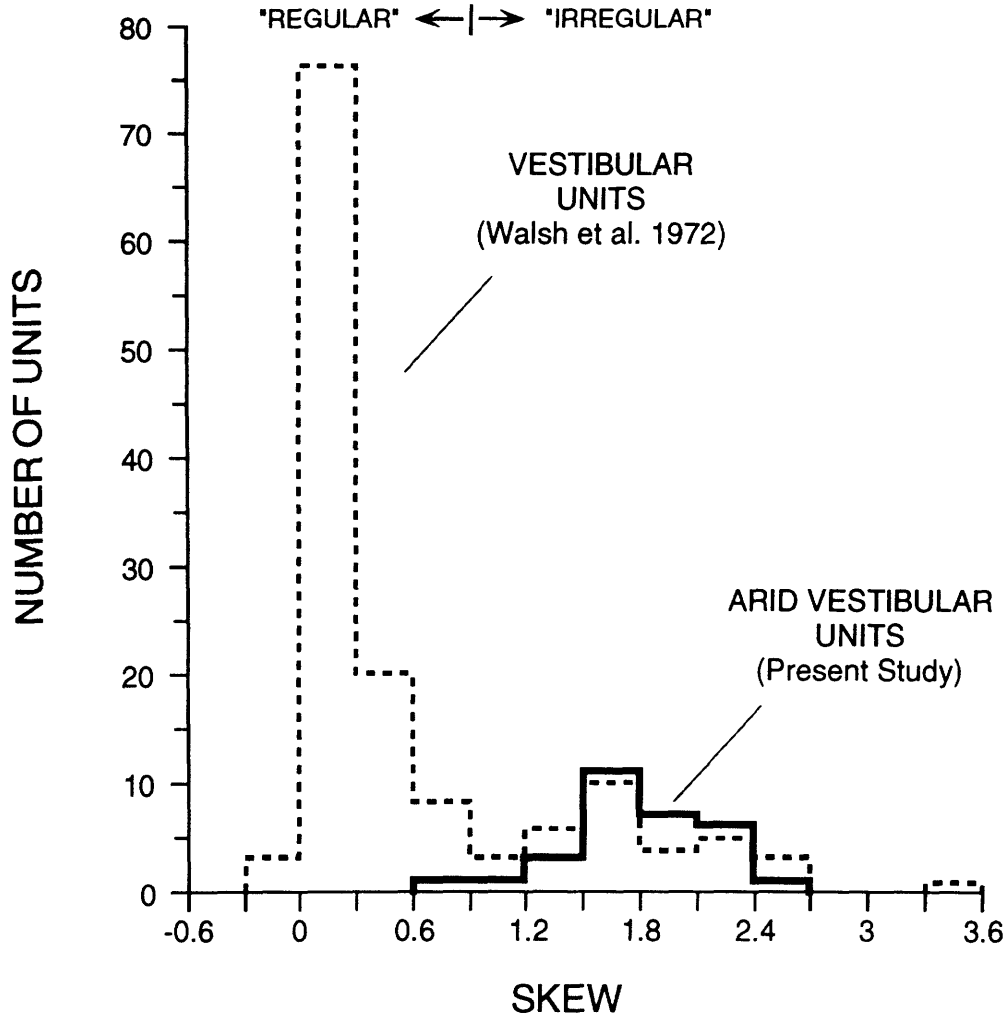

FIGURE III-3. Skew values of acoustically responsive irregularly discharging (ARID) vestibular units compared to other vestibular units. *Dashed lines* represent a bimodal histogram of skew values from 143 vestibular units recorded by Walsh *et al.* (1972). *Solid lines* represent a histogram of skew values from 30 ARID units. Bin width is 0.3 ms. Adapted from *Figure 3 of* Walsh *et al.*, 1972.

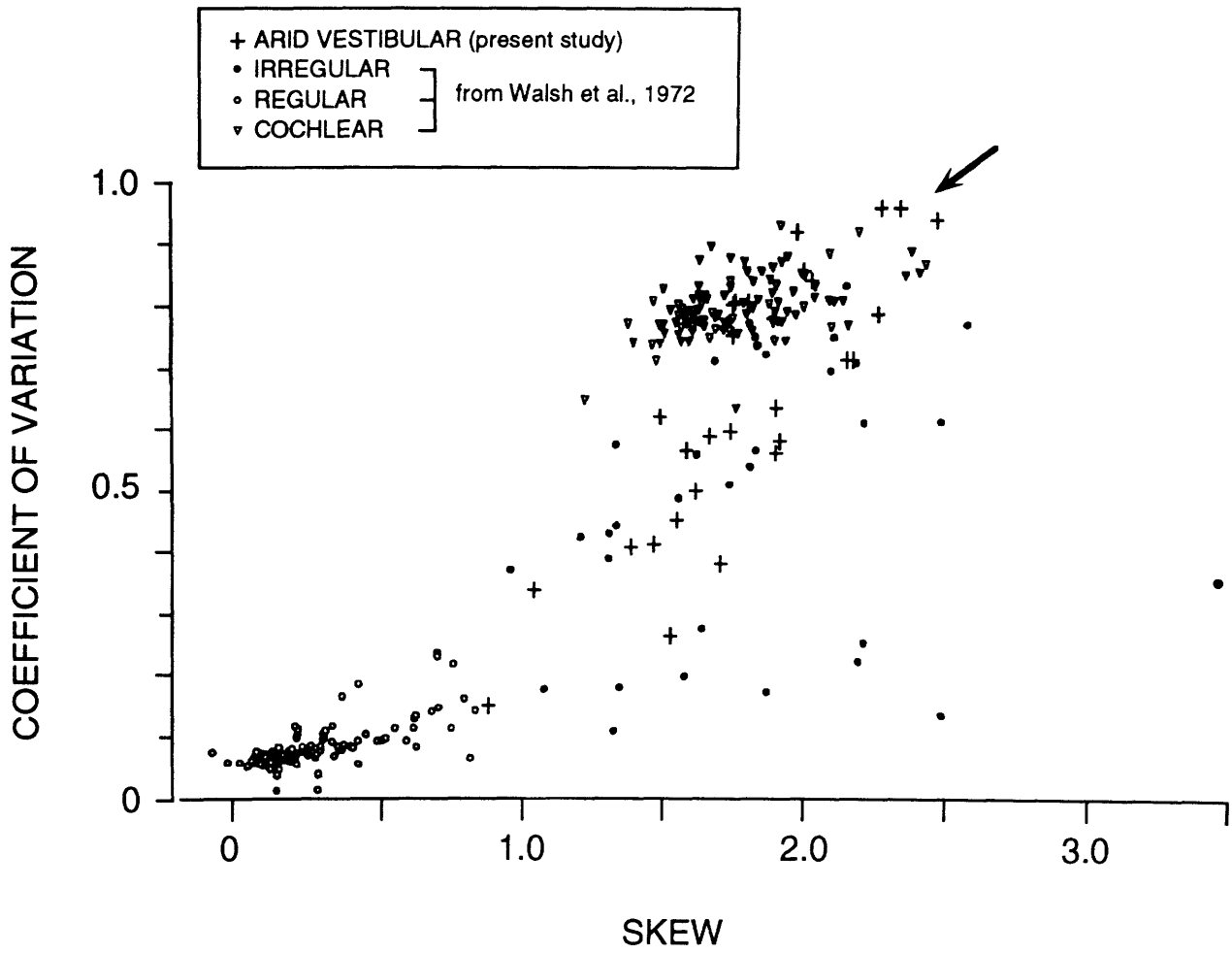

FIGURE III-4. Measures of inter-spike interval variability (coefficent of variation and skew) for ARID vestibular units compared with units recorded in the eighth nerve by Walsh *et al.* (1972). See *inset* for legend. Modified *Figure 4 of* Walsh *et al.* (1972).

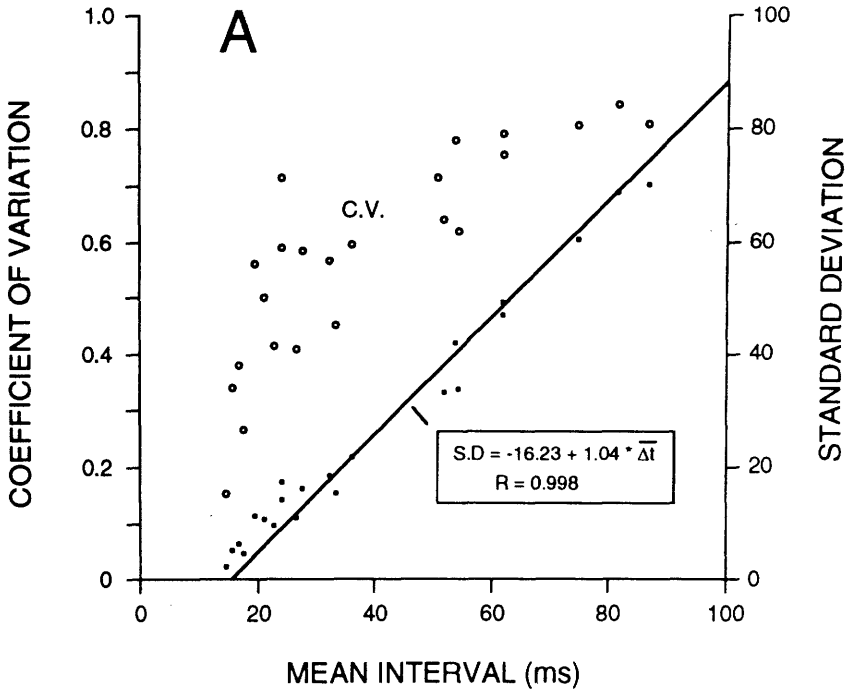

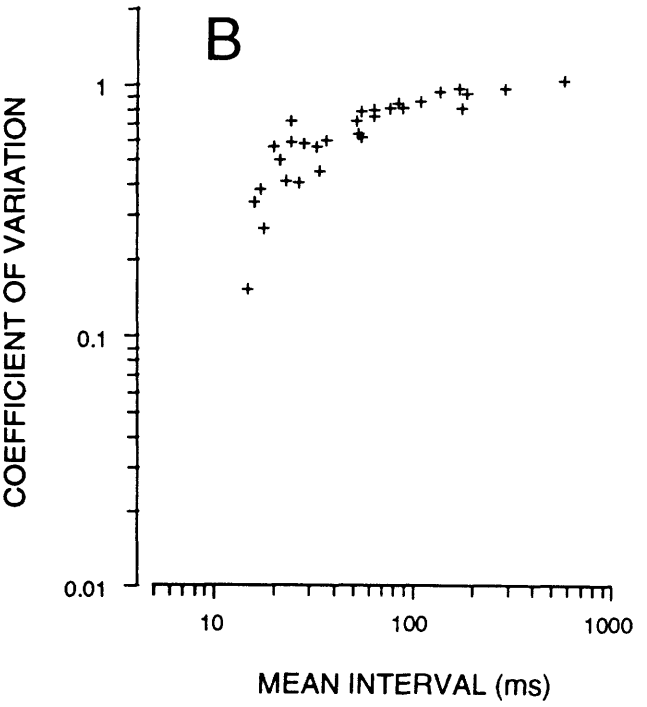

FIGURE III-5. Relationship of mean, SD and coefficent of variation (CV) of inter-spike intervals for ARID vestibular units. Each *symbol* represents a different unit. *A*, Mean and SD are highly correlated in ARID units (see *inset* for linear regression). *Open circles* indicate CV *Filled circles* indicate SD. *B*, Coefficient of variation and mean interval plotted on a log-log axis for comparison with vestibular units from chinchilla utricle recorded by Goldberg *et al.* (1990).

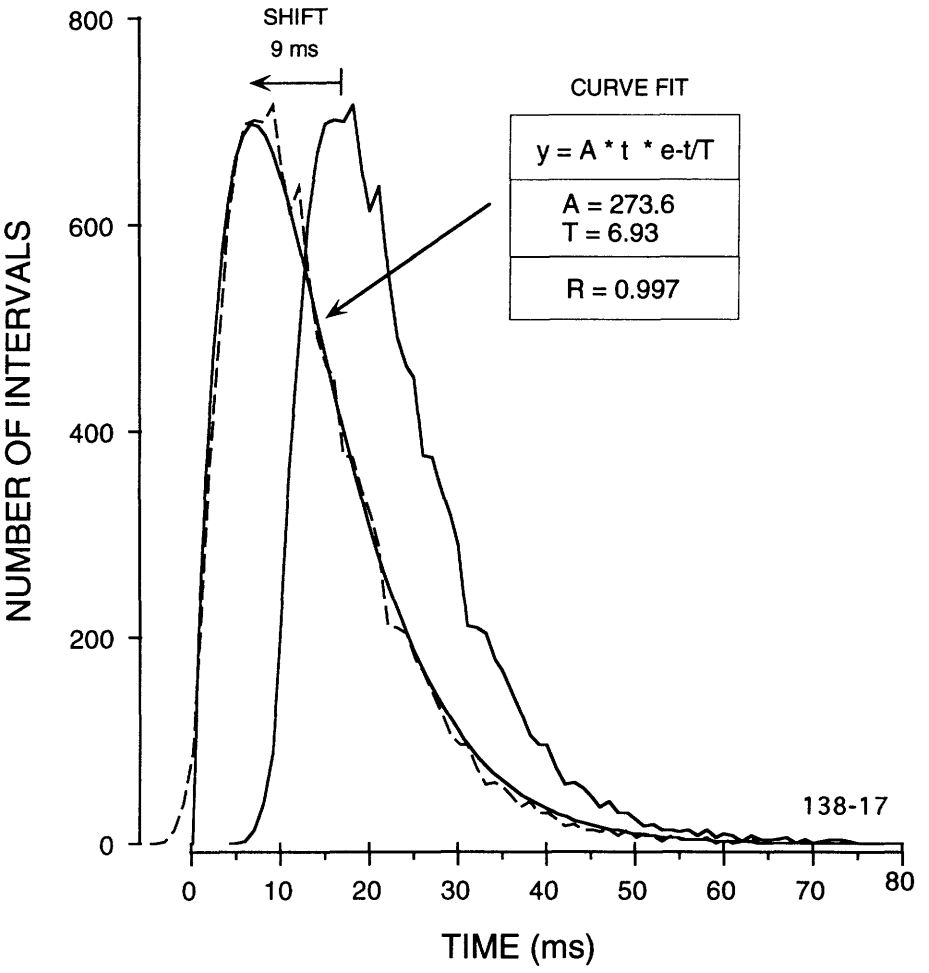

FIGURE III-6. Curve fit of an ARID unit inter-spike interval histogram with an Erlang probability density function (Drake, 1967). The original histogram is shifted left by 9 ms and then fit well with a simple function for t >0 (see *inset*). The statistics for this Erlang function can be obtained by measuring the arrival of events in a Poisson process and throwing away every other event (Drake, 1967). Same histogram shown in Fig. 2.

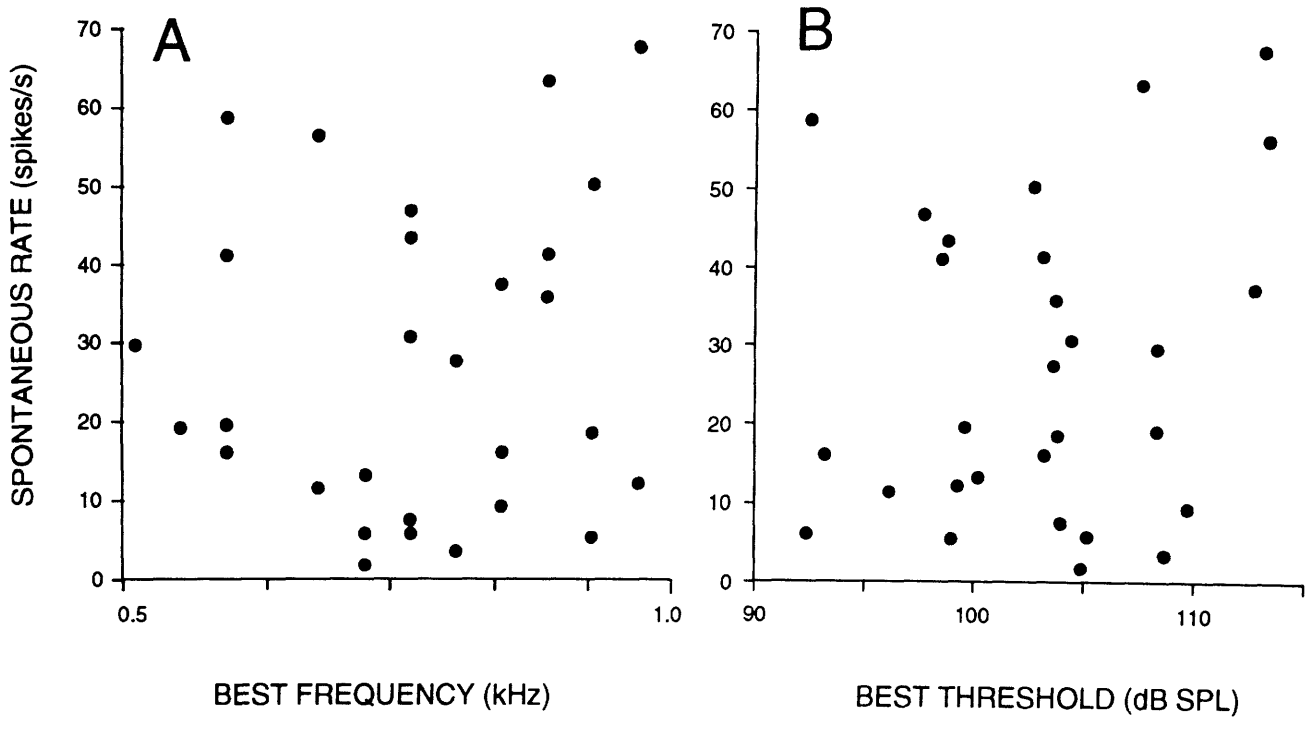

FIGURE III-7. Scatterplots of mean spontaneous firing rate and acoustic response characteristics for ARID vestibular units. Each *symbol* in a panel represents a different unit. Best frequency (*A*) and best threshold (*B*) were obtained from tuning curves

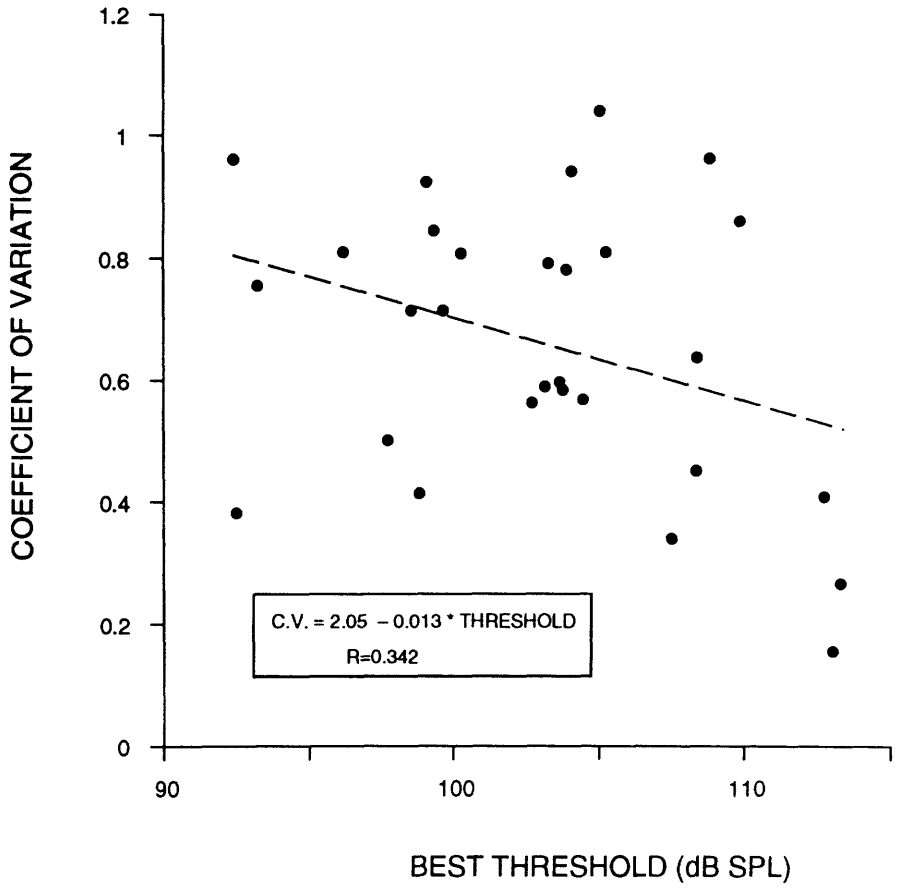

FIGURE III-8. Relationship between coefficient of variation and best threshold for ARID vestibular units (see *inset* for linear regression). Each *symbol* in a panel represents a different unit. Best thresholds were obtained from tuning curves (Chapter II).

IV. INFLUENCE OF EFFERENT STIMULATION ON ACOUSTICALLY-RESPONSIVE VESTIBULAR NEURONS IN THE CAT

IV. INTRODUCTION

Sensory organs of the mammalian inner ear are influenced by the activity of efferent neurons which have cell bodies in the brain stem (Fig. 1) (Galambos, 1956; Warr, 1975; Goldberg & Fernández, 1980). The only previous study of vestibular efferent stimulation in the cat suggested that efferents exert a weak inhibitory influence on the background spike activity of vestibular afferents (Dieringer *et al.*, 1977). However, vestibular efferent stimulation was subsequently shown to exert an overwhelmingly excitatory influence on vestibular afferents in the squirrel monkey (Goldberg & Fernández, 1980). An explanation advanced for this apparent discrepancy (Goldberg & Fernández, 1980) is that the small number of shocks used in the cat study (Dieringer *et al.*, 1977) was ineffective in activating the vestibular efferent system. We have recently demonstrated a strong excitatory influence of efferent stimulation on vestibular afferents in the cat (McCue & Guinan, 1993), and have found that these effects are similar in most respects to those observed in the squirrel monkey (Goldberg & Fernández, 1980).

Relationships between neurons and hair cells in the vestibular end organs are schematized in Fig. 2. A leading hypothesis to account for the excitatory influence of efferent stimulation on vestibular afferents is that such influences are exerted directly on afferent dendrites (a post-synaptic effect) rather than on hair cells (a pre-synaptic effect) (Goldberg & Fernández, 1980). This explanation reconciles the observation that activation of direct efferent synapses on hair cells in other sense organs produces an inhibition of afferent discharge (Flock & Russell, 1973a; Klinke & Galley, 1974).

The influence of efferent stimulation on the normal response of vestibular afferents to mechanical stimuli has been well studied in only a few species, notably squirrel monkey (Goldberg & Fernández, 1980) and toadfish (Boyle & Highstein, 1990). Results in both species suggest that the predominant result of efferent activation is to elevate the background discharge rate, yet reduce the response to mechanical stimuli. One rationale put forward for these effects is that elevation of background rate prevents units from being silenced during any phase of the stimulus cycle and allows them to transduce stimuli in both directions through increases and decreases in rate (Goldberg & Fernández, 1980; Boyle & Highstein, 1990).

Effects of efferent stimulation on vestibular afferent responses to mechanical stimuli have only been examined for low-frequency (<50 Hz) rotations and tilts – the adequate

stimuli for organs of equilibrium and balance. We have recently studied a class of irregularly-discharging vestibular afferent neurons in the cat which respond to sound (up to 2500 Hz) at moderately high levels (Chapter I-II). These neurons have given us an opportunity to examine the effects of efferent excitation on hair cell responses at audio-frequencies.

Our findings are somewhat different from those reported for stimuli at lower frequencies in different species (Goldberg & Fernández, 1980; Boyle & Highstein, 1990). We find that the effect of efferent stimulation is to amplify responses to acoustic stimuli (increase the gain). No apparent improvement in the bidirectionality of the response is seen. We have also obtained evidence in vestibular afferents for multiple driving mechanisms that can be differentially influenced by efferent stimulation. We relate these findings to the neural and mechanical structure of the vestibular sensory epithelium (Spoendlin, 1966; Baird *et al.*, 1988; Fernández *et al.*, 1988; Fernández *et al.*, 1990; Goldberg *et al.*, 1990a-b). Lastly, we discuss the possible relationship of our results to the analogous post-synaptic efferents in the cochlea (lateral olivocochlear neurons). A preliminary report of this work has been presented (McCue & Guinan, 1993).

IV. METHODS

Surgical preparation, anesthesia, sound stimulation, and neural recording were performed as described previously (Chapter I) with the following modifications.

Surgical Preparation. Middle ear muscle tendons were cut bilaterally. After posterior craniectomy, both the lateral and medial parts of the cerebellum were aspirated to expose the dorsal surfaces of the temporal bone and brain stem. The roof of the internal auditory meatus was drilled away to reveal the junction of the inferior and superior vestibular nerves as described previously (Chapter I).

Sound Stimulation. Acoustic stimuli consisted of 100-ms tone bursts (2.5 ms $\cos^2$-shaped rise-fall time) at a frequency of 800 Hz, which is near the best frequency for acoustically responsive vestibular neurons (Chapter II).

Efferent Stimulation. The cochlear and vestibular efferent axons travel together in bundles at the dorsal surface of the brain stem (Fig. 1). Electrical stimulation of the efferent bundles was accomplished using an 8-conductor linear electrode array (0.5 mm separation between tips) oriented rostro-caudally at the midline of the dorsal brain stem (Gifford & Guinan, 1983). The optimal electrode pair for vestibular efferent stimulation was determined by maximizing the inhibitory effects of cochlear efferent stimulation on the click-

evoked compound action potential of the cochlear nerve as previously described (Gifford & Guinan, 1983).

Shocks stimuli were bursts of 0.3 ms rectangular voltage pulses filtered through a transformer to remove D.C. components. Each shock burst lasted 0.4 sec (shock rate: 200/s). A standard stimulus sequence was obtained by delivering 64 shock bursts at 1.5 sec intervals (Figs. 4-5). Shock amplitude was fixed at 1 dB below the level which initiated a visible twitch of any muscle (typically 1-3 volts).

Recording. Single units were recorded using 2M KCl micro-pipettes inserted into the inferior vestibular nerve (Fig. 1) as described (Chapter I). Shock-evoked electrical artifact picked up by the recording micro-electrode was minimized using a grounded aluminum-foil shield suspended between the stimulating and recording electrodes.

Event Timing and Analysis. Spikes, stimulus triggers, and the positive-going zero crossings of stimulus voltage waveforms were timed with μsec accuracy by special-purpose event-timing hardware. Event times were used to calculate post-stimulus time (PST) histograms (e.g. Figs. 3 & 5) from which rate measurements were made (Fig. 6). Rates were measured during the first 50 ms of each PST and the last 50-ms of each stimulus (sound or shock) period. Calculated rates (Fig. 6) were used to construct rate-level functions (Figs. 7-8). The method for calculating synchronization index and response phase have been described elsewhere (Chapter I).

Measurement Protocol. All vestibular neurons with audible irregularity in rate were tested for acoustic responses as previously described (Chapter I). Detection of acoustically responsive units initiated a standard measurement protocol. First, a tuning curve was taken (Chapter I) followed by a 20-sec measurement of background activity. A stimulus sequence was then initiated consisting of shocks alone (64 shock bursts at 1.5 sec intervals). Sound-alone sequences were then alternated with concurent sound/shock sequences. Brief rest periods were inserted occasionally to permit any shock-evoked response to return to baseline. Typically, sound levels were tested in the order: 110, 100, 90, 80, 105, 95, 85 dB SPL. Shock amplitude remained fixed throughout. A complete data set (all sound levels tested) required a unit holding time >15 minutes.

IV. RESULTS

Acoustically-responsive irregularly-discharging (ARID) vestibular afferents have been found commonly in the inferior vestibular nerves of cats (Chapter I). We recorded the background and sound-evoked responses from ARID vestibular units while stimulating vestibular efferent neurons (Fig. 1). Shocks were applied at the dorsai surface of brain stem

(Galambos, 1956; Goldberg & Fernández, 1980). The influence of efferent stimulation on ARID vestibular neurons was examined in 8 cats with similar results. We report here the results of 15 representative units recorded in one ear.

Influence of Efferent Stimulation

Efferent stimulation at shock rates of 200/sec caused increased firing rates in all vestibular neurons examined. No evidence for inhibition was found in our study of ARID vestibular neurons nor in our cursory examination of other nearby vestibular afferents. Excitatory effects were more prominent in irregularly discharging units than in regularly discharging units, and were similar in many respects to those previously observed in squirrel monkey vestibular neurons (Goldberg & Fernández, 1980). As shown in Fig. 3, ARID vestibular units responded to brief bursts of efferent shocks with increased firing rates that depend on shock amplitude.

Two excitatory components with different time-courses were noted. A fast component was evident as the firing rate rose and fell with each 50-ms shock burst (Fig. 3). A slower component was also evident as the background firing rate increased with each successive shock burst (over a 20-40 sec period) and then decayed back to its baseline activity over a comparable time period. The slow component of the efferent response is shown in Fig. 4, which summarizes the responses of 4 ARID vestibular units to our standard efferent stimulus paradigm. Shock bursts of 0.4 sec duration were delivered at 1.5 sec intervals, and the firing rate was measured in intervals during and following each shock burst (Fig. 4, inset). The slow (20-40 sec) buildup of background activity was evident in 12/13 units tested (Fig. 4). The fast response component rose and fell with each shock burst (Fig. 3), and its amplitude remained constant throughout the stimulus sequence, despite the sometimes dramatic rise and fall of the slow response component (Fig. 4).

Influence of Sound.

The effects of sound on the discharges of ARID vestibular units have been reported (Chapter I-II). Fig. 5A shows a response to 800 Hz tone bursts as the sound level was increased in 5 dB steps. Rate increases were rarely observed in ARID units at sound levels <90 dB SPL, although units tended to synchronize to low-frequency tones at levels as low as 80 dB SPL. As sound level was raised above 90 dB SPL, firing rates increased monotonically. No plateau was ever observed up to the maximal sound levels tested (115 dB SPL), despite the frequent occurence of firing rates near 400 spikes/s (Fig. 5A).

Influence of Efferent Stimulation on Acoustic Responses.

Firing Rate. Fig. 5B shows the influence of efferent stimulation on sound-evoked responses in a vestibular afferent neuron. Results using a standard shock paradigm of constant amplitude are shown. Efferent shocks raised the background activity with a fast component (seen in each panel) and slow component (compare background rates in Fig. 5A & B). At sound levels <90 dB SPL, little or no changes in mean firing rate occurred in response to the tone bursts. As level was increased, sound evoked responses made their first appearances at levels similar to those seen in the absence of shocks (Fig. 5A). Acoustic responses were superimposed on the crest of shock responses (Fig. 5B) with maximal firing rates clearly elevated.

We measured absolute and evoked rates as shown in Fig. 6 and plotted the results as functions of sound level ("rate-level functions") for each unit. Fig. 7 shows results from 4 units chosen to illustrate a range of evoked firing rates. Efferent stimulation elevated the rate-level functions for ARID vestibular units (Fig. 7A-D), but had little or no effect on the additional activity evoked by sound (Fig. 7E-H). In particular, efferent stimulation did not significantly shift the acoustic response thresholds (Fig. 7E-H), despite causing impressive increases in background activity (Fig. 7A-D) . Results from all units are summarized in Fig. 8, which shows the mean acoustic response and its elevation by efferent stimulation (Fig. 8A). Also shown is the lack of efferent influence on the mean afferent activity evoked specifically by sound (ΔRate, Fig. 8B).

Phase Locking. Each ARID vestibular unit has a strong tendency to fire at a preferred phase of the stimulus cycle (synchronize or phase-lock) in response to low frequency tones (Chapter I). Fig. 9 shows post-zero-crossing (PZC) histograms that relate the occurrence of spikes to positive-going zero-crossings of the earphone voltage waveform. The PZC histograms in Fig. 9 were calculated for the unit shown in Fig. 5 using only spikes which occurred during the tone burst. At the lowest sound levels tested (80-85 dB SPL), the unit in Fig. 9 displays a clear synchronization with no sound-evoked mean rate change (Fig. 5). At these low sound levels, this unit fired throughout the stimulus cycle (Fig. 9, 80 dB SPL), while at higher sound levels it synchronized so strongly that its instantaneous firing rate was zero for much of the stimulus cycle (Fig. 9, 110 dB SPL).

The influence of efferent stimulation on phase-locking of this ARID vestibular unit is shown in Fig. 9B. At 80 dB SPL, the unit responded throughout the stimulus cycle (Fig. 9A, left). The net result of efferent stimulation was an amplification of both AC and DC components, with greater fluctuations in firing rate amplitude throughout the stimulus cycle. There was little or no change in the sharpness of the peaks and hence no change in synchronization (Fig. 9B, left). At higher stimulus levels (Fig. 9B, 110 dB SPL), a similar

amplification occurred. More spikes occurred at particular phase of the stimulus cycle, but little or no change in the sharpness of the peaks was noted. The preferred response phase also did not shift with efferent stimulation.

From data such as that shown in Fig. 9, we measured synchronization and response phase as functions of sound level in the presence and absence of efferent stimulation. Fig. 10 shows these results for the same 4 units whose rate characteristics are shown in Fig. 7. Except in one unit which showed a consistent phase advancement (Fig. 10F), efferent stimulation induced little or no shift in synchronization or phase (Fig. 10).

Phase Separation ("Peak Splitting") Induced by Efferent Stimulation.

As sound level was increased from 90 to 110 dB SPL, most ARID vestibular units underwent >30° advancement in their response phase (Fig. 10E-H) (Chapter I). The origin of this phenomenon was clarified somewhat by examining the influence of efferent stimulation on the phase change. A sizable fraction of units (6/14) had responses which had two distinct peaks at high sound levels during efferent stimulation (Fig. 11).

We refer to the preferred phases at 90 and 110 dB SPL, in the absence of efferent stimulation, as *Phase 1* and *Phase 2* respectively (Fig. 11). For the unit shown in Fig. 11, efferent stimulation at 90 dB SPL augmented the existing response at *Phase 1.* At 110 dB SPL, a response was observed at *Phase 2* (Fig. 11B). Application of efferent stimulation at 110 dB SPL caused peaks to occur at *Phase 1* and *Phase 2* simultaneously (Fig. 11A).

Fig 12 shows another example of a unit in which efferent stimulation caused a split peak in the PZC histogram Also shown is the response phase for the first 500 spikes recorded during tone burst stimulation (Fig. 12A,C). Fig. 12C is representative of the whole spike cohort for this unit and shows that the two components at different phases contributed more or less steadily to the flow of spikes – that one component did not dominate or drop out during data collection.

We interpret the findings in Figs. 11-12 to suggest that ARID units are driven by two mechanisms with different response phases and that the mechanism with the more rapid response (more positive phase) predominates at high sound levels. The results are consistent with efferent stimulation augmenting the mechanism producing *Phase 1* and/or inhibiting the mechanism producing *Phase 2.*

We note that one unit in the present sample of 14 was the only unit that we have ever observed (including 57 units sampled in a previous study; Chapter I) which exhibited a clearly split peak at 110 dB SPL in the absence of efferent stimulation. For this unit, efferent stimulation completely inhibited *Phase 1*, producing one clear peak at *Phase 2* (the opposite of the efferent effect on peak-splitting observed in Figs. 11-12). Half of the units in our

sample (7/14) had no split peaks with efferent stimulation, including the units whose data are shown in Figs. 7 & 10.

IV. DISCUSSION

Mechanism of Efferent Influence

In the last few years, the anatomy of neural elements in the mammalian vestibular end organs has been substantially clarified (Fernández *et al.*, 1988) and correlations with physiological responses made (Baird *et al.*, 1988; Fernández *et al.*, 1990; Goldberg *et al.*, 1990b). The majority of mammalian vestibular afferents, both regularly and irregulary discharging, are *dimorphic units* (Fig. 2A) that have calyceal endings around Type I hair cells and variable numbers of branches to Type II hair cells (Baird *et al.*, 1988; Goldberg *et al.*, 1990b). A minority of afferents (1-10%) are pure *calyx* neurons which end only around Type I hair cells and have irregular discharges (Baird *et al.*, 1988; Goldberg *et al.*, 1990b). The remaining vestibular afferents (2-20%) are *bouton* neurons – small fibers that terminate solely on Type II hair cells (Baird *et al.*, 1988; Goldberg *et al.*, 1990b). As shown in Fig. 2, efferent endings in the vestibular end organs are primarily on Type II hair cells (VE-II) and on the afferent dendrites of Type I hair cells (VE-I) (Wersäll, 1956). Both of these endings have ultrastrutural characteristics of chemical synapses (Spoendlin, 1970).

In the lateral line organs (Flock & Russell, 1973b), direct efferent synapses on hair cells cause hyperpolarization and result in the inhibition of afferent discharge (a pre-synaptic effect). Indirect evidence suggests that outer hair cells in the cochlea are also hyperpolarized by direct efferent synapses (Fex, 1967). The hypothesis that Type II vestibular hair cells and their bouton units behave similarly is supported by the fact that efferent inhibition is rarely observed in recorded vestibular units (<1% of units in the squirrel monkey, Goldberg & Fernández, 1980) and bouton units are difficult to record from and label intracellularly (Baird *et al.*, 1988; Goldberg *et al.*, 1990b). Conversely, the widespread excitatory effect of vestibular efferent stimulation is consistent with the existence of calyces (Fernández *et al.*, 1988) studded with efferent synapses (Wersäll, 1956) in most vestibular afferents. Thus, the leading hypothesis is that vestibular efferents exert an inhibitory pre-synaptic effect on hair cells (Flock & Russell, 1973b) and excitatory post-synaptic effect on afferent dendrites (Goldberg & Fernández, 1980).

Influences of Efferent Stimulation on the Background Firing Rate

We found that efferent shock bursts raised the background firing rates of acoustically responsive irregularly discharging (ARID) vestibular afferents in the cat (Figs. 3-4). This excitatory effect had a fast component which rose and fell with efferent shock bursts over 10-

20 milliseconds (Fig. 3) and a slow components which built up over 20-40 seconds and then decayed during repeated shock bursts. Both components are similar to the influences of efferent stimulation observed previously in irregular vestibular units in the squirrel monkey (Goldberg & Fernández, 1980).

The fast excitatory component has a time course consistent with a direct synaptic effect on the afferent dendrite (Goldberg & Fernández, 1980), but the mechanism of the slow component is less obvious. Speculation have been made with regard to slow EPSPs, buildup of extracellular K^+, or long lasting (seizure-like) discharges of efferent neurons (Goldberg & Fernández, 1980). Another possibility is that the two effects represent the action of two different neurotransmitters, e.g. acetylcholine and CGRP (Sewell & Starr, 1991).

Influences of Efferent Stimulation on Acoustic Responses: Mean Firing Rate

We found that efferent stimulation raised the mean firing rates of acoustically responsive vestibular neurons without appreciably shifting their acoustic thresholds or the amplitude of their sound-evoked responses (Figs. 5 & 7). The net effect was a vertical shift of the rate-level curve for each unit, as schematized in Fig. 13A. For units with low background activity, this shift could amount to a 4-fold or more increase in discharge rate (Fig. 7B).

Influences of Efferent Stimulation on Acoustic Responses: Phase-Locking & Gain

Another set of interesting phenomena were noted when we examined efferent influences on the phase-locking responses of afferent neurons. At the lower sound levels tested (e.g. 80 dB SPL), units tended to respond to each stimulus cycle with a sinusoidal modulation of firing rate (Fig. 9) that did not fall to zero during any phase of the stimulus cycle. At these sound levels, efferent stimulation raised the background firing rate and simultaneously increased the magnitude of firing rate fluctuations (Figs. 9 & 14A). The amplitude of firing rate modulation for a sinusoidal acoustic stimulus can be described by an AC "gain," and its variation with efferent stimulation can be compared with observations made using low frequency mechanical stimuli in different preparations (Goldberg & Fernández, 1980; Boyle & Highstein, 1990). As schematized in Fig. 14A-B, the efferent induced enhancement in gain at audio-frequencies contrasts sharply with the observed gain reductions at low frequencies (<50 Hz) in toadfish afferents (Fig. 14C) and in the majority of squirrel monkey afferents (Goldberg & Fernández, 1980). However, a few vestibular afferents in the squirrel monkey did exhibit gain enhancement similar to Fig. 14A. These were units whose discharge rates were driven close to zero (but not completely abolished) by low-frequency (≤2 Hz) sinusoidal stimulation (Goldberg & Fernández, 1980).

Acoustic stimuli strongly modulate the extra activity generated by efferent stimulation in ARID vestibular units (Fig. 9). At high sound levels, the acoustic stimulus always drove the afferent firing rate to zero over much of the stimulus cycle (Figs. 9 & 14B). This observation indicates that the efferent mechanism that generates increased activity in the afferent ending does not add spikes independently of the acoustic stimulus, as might be suggested by the apparent summation of discharge rates generated by sound and efferent stimulation (Figs. 5 & 13).

We did not see an example of efferent excitation biasing the afferent response upward to higher firing rates and improving the bidirectionality of the transduction process (Fig. 14D). This observation in other species has been advanced as a rationale for efferent-induced increases in afferent firing rate, but it is apparently not important in vestibular units responding to audio-frequencies in the cat (Fig. 14D). Modulation of efferent induced activity such as that seen here at high sound levels (Fig. 14B) has been previously observed in a few squirrel-monkey vestibular afferents that had no background discharge (Goldberg & Fernández, 1980).

The efferent mechanism for gain enhancement (Fig. 14) in vestibular afferents is unclear. One possible explanation is that efferent synapses on calyces change membrane resistance. Hair cell transmitter release, both spontaneous and sound-evoked, would be more effective in spike generation if the afferent's membrane resistance was increased by efferent stimulation. The net effect would be an amplification of all afferent activity with little change in the tendency of discharges to synchronize (Figs. 9-10).

Peak Splitting

ARID vestibular neurons display a characteristic 30° advancement in the phase of their response to sound as level increases from 100 to 110 dB SPL (Fig. 10). This phenomenon might be due to a smooth advancement in the afferent driving mechanism, e.g a level-dependent change in the mechanical oscillation of the hair cell. The remarkable ability of efferent stimulation to produce responses at two phases (Fig. 11) suggests several alternate hypotheses for phase advancement.

One hypothesis, patterned after the putative interaction of outer and inner hair cells in the cochlea (Brown *et al.*, 1983), is that efferent stimulation changes the mechanical behavior of the sensory epithelium by inducing a mechanical change in Type II hair cells (Ashmore, 1987; Denk & Webb, 1992). This could indirectly affect the responses of Type I hair cells and produce or eliminate responses at different phases, e.g. by altering mechanical distortion (Gifford & Guinan, 1983).

Another 2-component hypothesis is that the hair cell and calyx are coupled through both chemical synapses and electrically conductive junctions, as has been suggested by the presence of certain membrane specializations (Spoendlin, 1966). A level dependent transition from slow chemical conduction to fast electrical conduction would advance the response phase, and could help explain the extremely short latencies (≤0.8 ms) exhibited by ARID vestibular units to intense acoustic clicks (Chapter I). If efferent stimulation were to improve chemical transmission or to undermine electrical transmission at high levels, it could bring out highly synchronized responses to both transmission modes (Fig. 11).

Another 2-component hypothesis is suggested by the morphology of vestibular units with irregular discharges (Fig. 2A). Studies using intracellular labeling suggest that the large majority of irregular neurons are dimorphic, having a calyx around one or more Type I hair cells and bouton endings on one or more Type II hair cells (Baird *et al.*, 1988; Goldberg *et al.*, 1990b). Even afferents with no bouton endings likely receive input from Type II hair cells via direct synapses on the outer calyceal surface (Ross *et al.*, 1986; not shown in Fig. 2). If afferent excitation from Type I hair cells predominated at low sound levels and Type II hair cells had more phase lead and predominated at high levels, a smooth level-dependent phase advancement would be observed in the responses of most units. Efferent stimulation would be expected to hyperpolarize Type II hair cells through direct efferent synapses (Fex, 1967; Flock & Russell, 1973b) (Fig. 2A), thus inhibiting their contributions, while efferent endings on calyces amplify responses. The net effect might be to bring contributions from the two hair cell types into balance at higher sound levels and show responses at both phases.

Comparison with Efferent Influences on Cochlear Afferents

The influence of efferent stimulation on acoustic responses has been previously studied in cat cochlear nerve fibers (Fex, 1967)(Wiederhold & Kiang, 1970; Guinan & Gifford, 1988a-c), but this is the first such study of acoustic responses of vestibular nerve fibers. As we have previously demonstrated (Chapter I), most (if not all) of the acoustically responsive vestibular neurons reported here come from the saccule, the sensory organ in the inferior part of the labyrinth which is thought to have given rise to the cochlear duct during vertebrate evolution (Wever, 1974). The evidence presented here thus represents the first opportunity to compare efferent influences on two sensory systems that have similarities in anatomy, physiology and evolutionary origin.

Anatomy. As shown in Fig 2B, cochlear hair cells are similar to vestibular hair cells in that they are of two morphological types: flask-shaped inner hair cells and cylindrical outer hair cells. Efferent endings are also arranged similarly, being found on outer hair cells

(Kimura & Wersäll, 1962; Spoendlin & Gacek, 1963) and on the afferent dendrites under inner hair cells (Smith, 1961; Smith & Rasmussen, 1963).

Cochlear efferent neurons are divided into 2 classes based on their central origins and peripheral projections (Warr & Guinan, 1979). Medial olivocochlear (MOC) efferents end on outer hair cells and have cell bodies near the medial superior olive (Guinan *et al.*, 1983). Lateral olivocochlear (LOC) neurons end on afferent dendrites under inner hair cells and have cell bodies near the lateral superior olive (Guinan *et al.*, 1983).

Physiology. Electrical stimulation of MOC neurons most likely hyperpolarizes (Fex, 1967) and induces a mechanical change (Brownell *et al.*, 1985) in cochlear outer hair cells which in some way decreases the acoustic responses of inner hair cells (Brown *et al.*, 1983). The principal effect is to raise the acoustic threshold of inner-hair-cell afferents (Wiederhold & Kiang, 1970; Guinan & Gifford, 1988), i.e. to shift their rate-level functions to higher levels (Fig. 13B).

Because they are unmyelinated, LOC axons are probably not excited by the shock stimuli commonly used for efferent stimulation (Guinan *et al.*, 1983; Gifford & Guinan, 1987). LOC neurons make up the largest group of cochlear efferents (Warr, 1975; Warr & Guinan, 1979; Warr *et al.*, 1986), yet their effects on inner hair cell afferents remain unknown (Gifford & Guinan, 1987). Anatomical similarites in the arrangment of neural elements in vestibular end organs (Fig. 2A) and the cochlea (Fig. 2B) suggest that the post-synaptic effect of LOC neurons may parallel the post-synaptic effect of vestibular efferents studied here (Figs. 13B & 14A-B). The analogy is attractive because of the possible homologous relationship of the systems, as well as the likelihood that both types of efferents are influencing hair cell responses to audio-frequencies.

One hint that LOC neurons exert effects similar to those observed here comes from lesion experiments in which cochleas were chronically de-efferented (Liberman, 1990). The principal physiological abnormality noted was that the spontaneous rates of cochlear afferent neurons were lower than expected (Liberman, 1990). This reduction in background activity could easily have resulted from the removal of a tonic LOC excitation on cochlear afferents.

Consequences and Predictions. The data presented here should be of use in attempts to understand the LOC system. According to the proposed analogy, LOC stimulation would be expected to elevate the background firing rate of cochlear afferent neurons without shifting their rate thresholds or mean sound-evoked firing rates (cf. Fig. 7). The net effect would be an LOC-induced vertical shift in afferent rate-level function which would complement the horizontal shift created by MOC activation (Fig. 13B). Gain enhancements (increased AC modulation of tone responses) would also be expected in afferent responses to sound at

frequencies (<5000 Hz) which elicit synchronization of cochlear afferents (Kiang *et al.*, 1965; Johnson, 1980) (cf. Fig. 14).

Despite a lack of change in the sound-evoked rate threshold, the sound-evoked compound action potential of the cochlear nerve might increase under LOC activation owing to the enhanced, synchronized response to brief sounds. LOC activation simulated pharmacologically (e.g. by application of transmitter candidates) or initiated electrically (e.g by stimulating LOC cell bodes) should be observable in the electrical "noise" generated by increased background activity in cochlear nerve afferents.

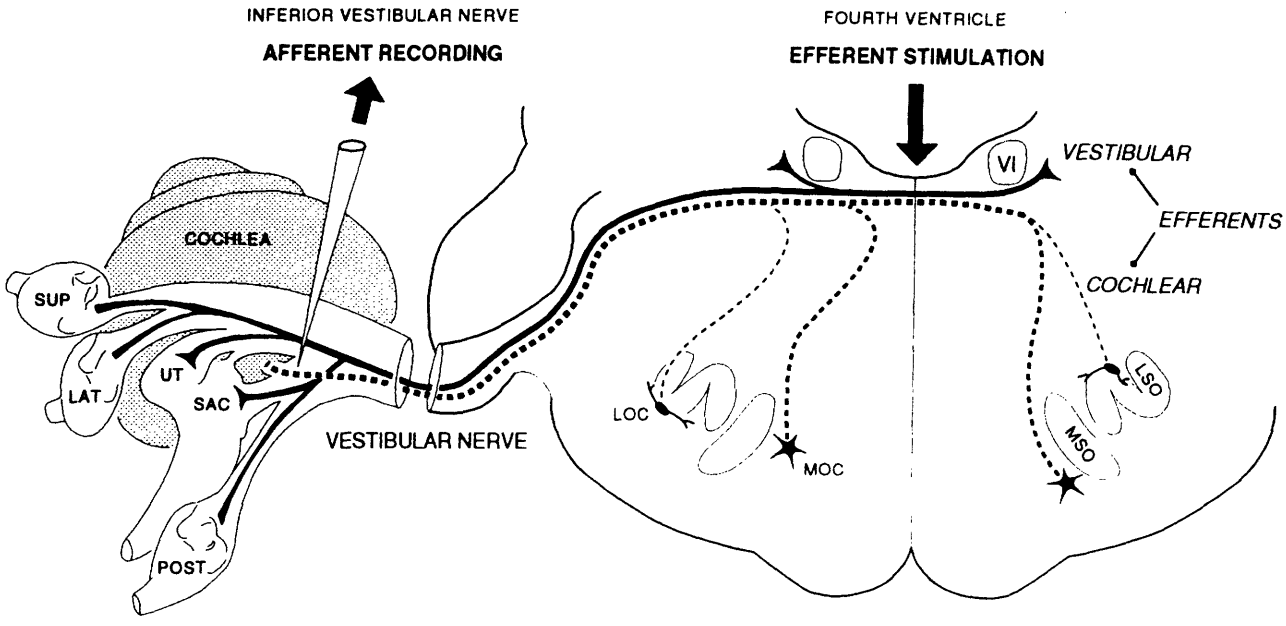

FIGURE IV–1. Schematic of the brain stem and labyrinth in the cat, showing the recording site in the inferior vestibular nerve (*pipette*) and the locations of cochlear efferent neurons (*dashed lines*) and vestibular efferent neurons (*thick solid lines*). The *shaded area* represents the cochlea. The *unshaded areas* at left represent the vestibular apparatus, which consists of two otolith organs (*SAC* = saccule and *UT* = utricle) and three semicircular canals (*SUP* = superior, *LAT* = lateral, *POST* = posterior). Vestibular efferents arise bilaterally near the abducens (*VI*) nuclei. Cochlear efferent neurons also arise bilaterally and are divided into 2 groups based on the locations of their cell bodies (Warr & Guinan, 1979). The medial olivocochlear neurons (*MOC*) arise near the medial superior olive (*MSO*); the lateral olivocochlear neurons (*LOC*) arise near the lateral superior olive (*LSO*). Cochlear efferents leave the brain stem in the vestibular nerve and reach the cochlea through the vestibulocochlear anastomosis, a fiber tract that leaves the vestibular nerve near the recording site. Both cochlear and vestibular efferents can be electrically stimulated at the floor of the fourth ventricle, where their axons travel in proximity.

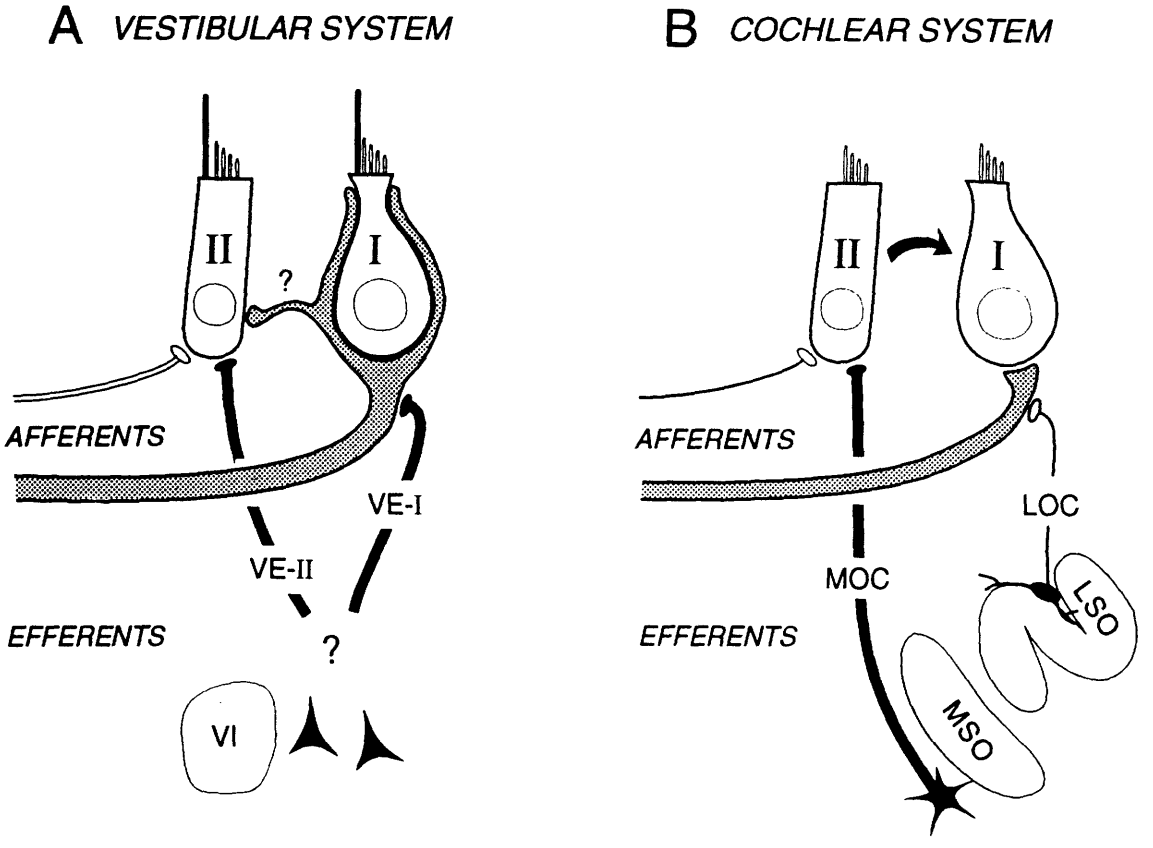

FIGURE IV–2. Schematic showing relationships of hair cells and neurons in the vestibular (*A*) and cochlear (*B*) systems. Each system contains flask-shaped cells (Type I or inner hair cells) and cylindrical cells (Type II or outer hair cells), each of which has afferent innervation. Efferent neurons synapse on the afferent dendrites under Type I hair cells (VE-I or LOC efferents), or directly on Type II hair cells (VE-II or MOC efferents). *A*, Type I vestibular hair cells are supplied by myelinated afferent neurons which form a chalice around the cell and which often branch to synapse on Type II hair cells. Type II vestibular hair cells are innervated by small myelinated afferents with bouton endings. Vestibular efferent neurons may branch to innervate both kinds of hair cells and may therefore exert VE-I and VE-II effects. *B*, Type I cochlear hair cells are supplied by a number of afferent neurons, each with a small ending. Type II cochlear hair cells have unmyelinated afferents. The efferent innervation to the two hair cell regions is separate in the cochlea, with myelinated efferents (MOC) directly synapsing on Type II hair cells and unmyelinated efferents (LOC) synapsing on Type I afferent dendrites. MOC stimulation induces a change (probably mechanical) in Type II hair cells that can affect Type I hair cells (*B, curved arrow*). Action of LOC neurons on cochlear afferents has not been demonstrated. ***Abbreviations:*** *VE-I*, vestibular efferent ending on Type I afferent dendrite; *VE-II* - vestibular efferent ending on Type II hair cell. *VI*, abducens nucleus; *MSO*, medial superior olive; *LSO*, lateral superior olive; *LOC*, lateral olivocochlear neurons; *MOC*, medial olivocochlear neurons.

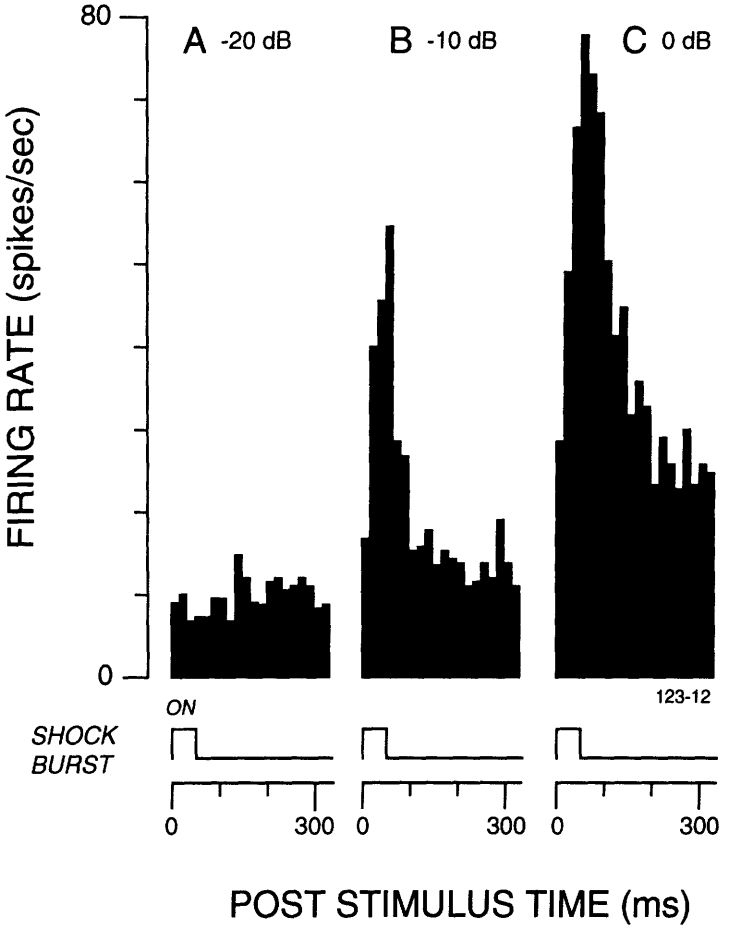

FIGURE IV–3. Influence of electrical stimulation on the discharge of an acoustically responsive vestibular neuron. Post-stimulus time (PST) histograms show unit discharge rates at three efferent shock levels (*top*). Stimuli were 50-ms shock trains (shock rate - 200/s; 128 bursts at 333 ms intervals). Bins: n = 20, width = 16.5 ms.

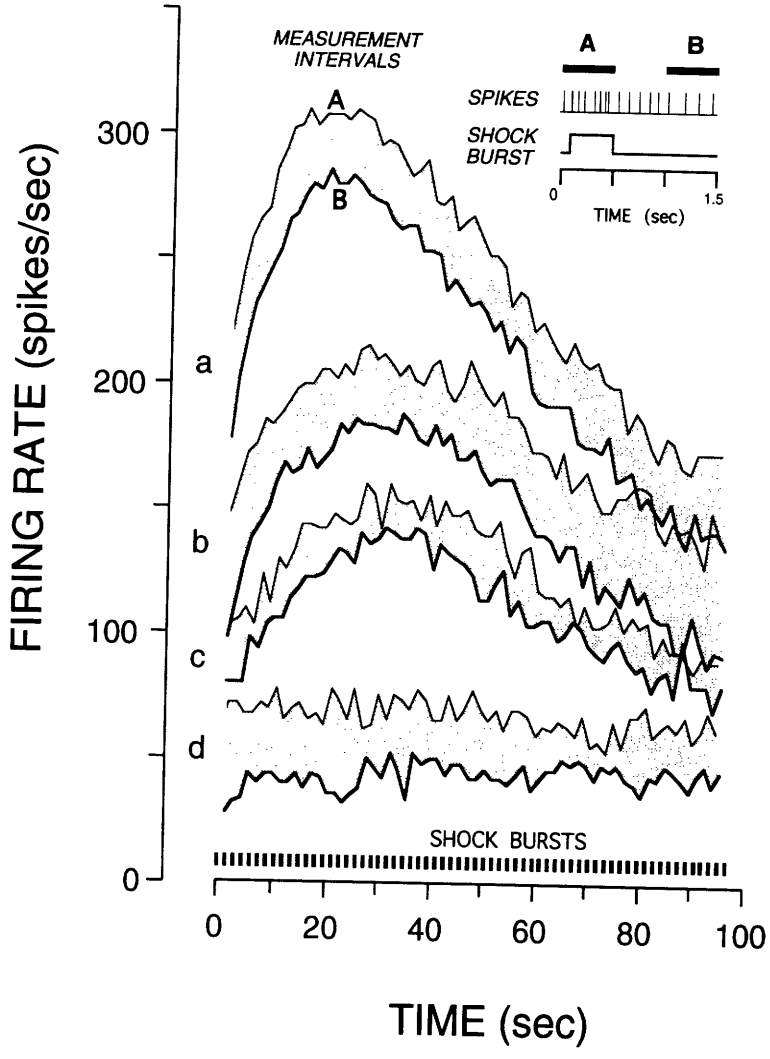

FIGURE IV–4. Slow and fast excitation components elicited in 4 ARID vestibular neurons (*a-d*) by efferent stimulation. Units were selected to show a range of evoked rates. Stimuli were repeated 0.4 sec shock bursts (shock rate - 200/s; 64 bursts at 1.5 sec intervals) as shown (*bottom & inset). Thick lines* show the slow (20-40 sec) buildup and decay of mean rate in measurement interval B (*inset*). *Thin lines* show the firing rate during measurement interval A (*inset*). The fast component of each excitatory response (*height of shaded area*) usually varied less than the slow component (*thick line*).

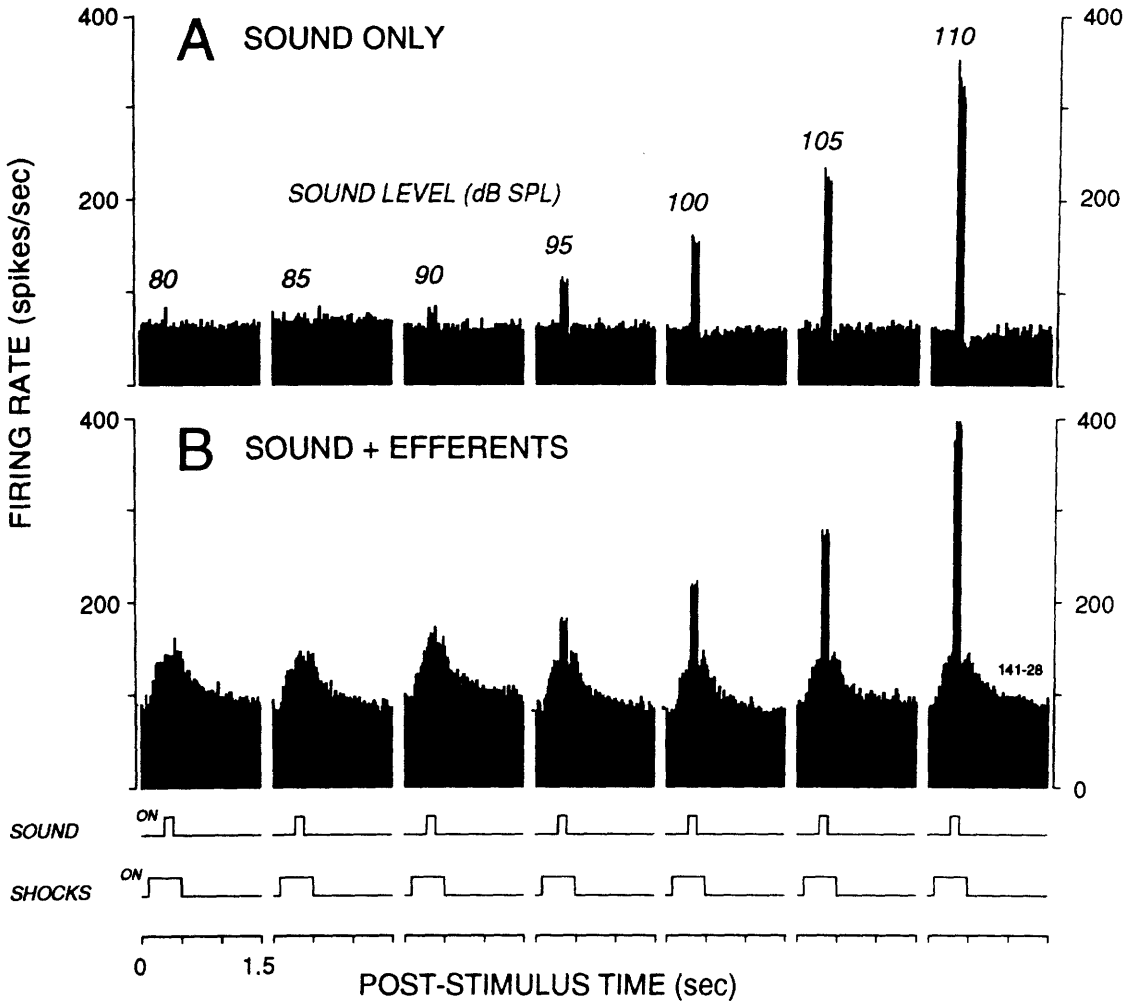

FIGURE IV–5. Influence of sound and efferent stimulation on the firing rate of an acoustically responsive vestibular neuron. *A*, PST histograms show spike rate elicited by an 800-Hz tone burst of 0.1 s duration at 7 sound levels. *B*, PST histograms show spike rate elicited during presentation of sound (as in *A*) with concurrent shock bursts to the efferent bundles. Stimulus presentation times are represented in the bottom *traces*. The sound stimulus was a 0.1 sec tone burst. Each shock burst lasted 0.4 sec (shock rate: 200/s; 64 bursts at 1.5 sec intervals). The difference in background activity between histograms in *A* and *B* represents a time average of the slow excitatory response (see Fig. 4). Bins: n = 75, width = 20.0 ms.

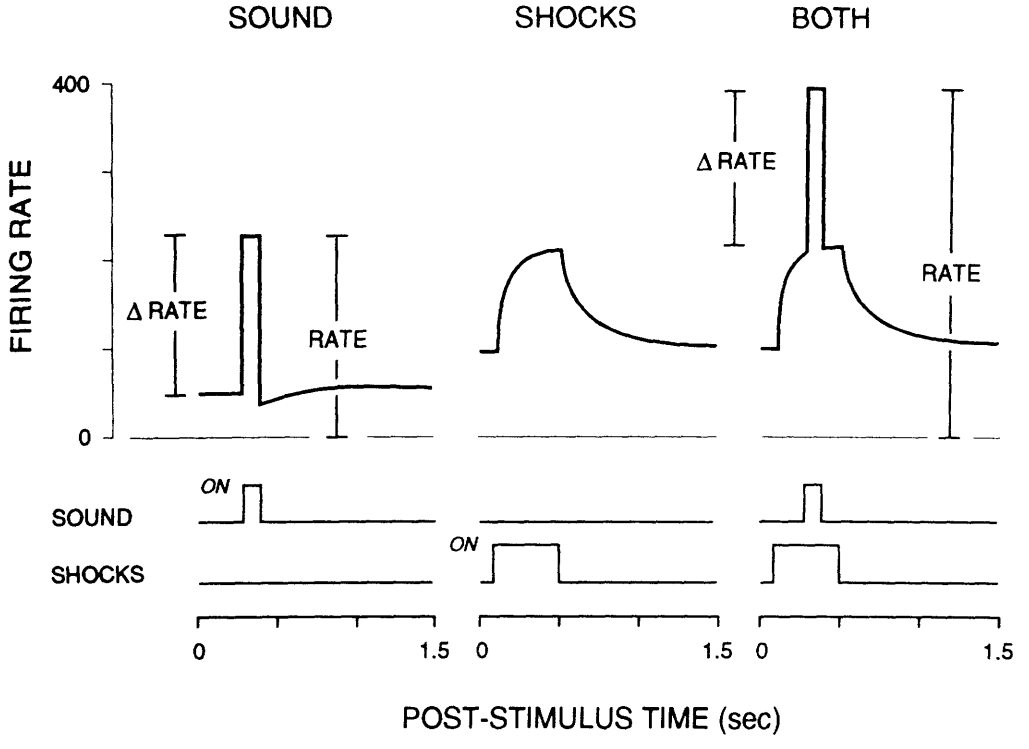

FIGURE IV–6. Measurement of evoked firing rates (*Rate*) and firing rate changes (*ΔRate*) from PST histograms. Calculations of Rate and ΔRate were made from average measurements taken from each PST during three 50-ms time periods beginning at t = 0, 350, & 450 ms.

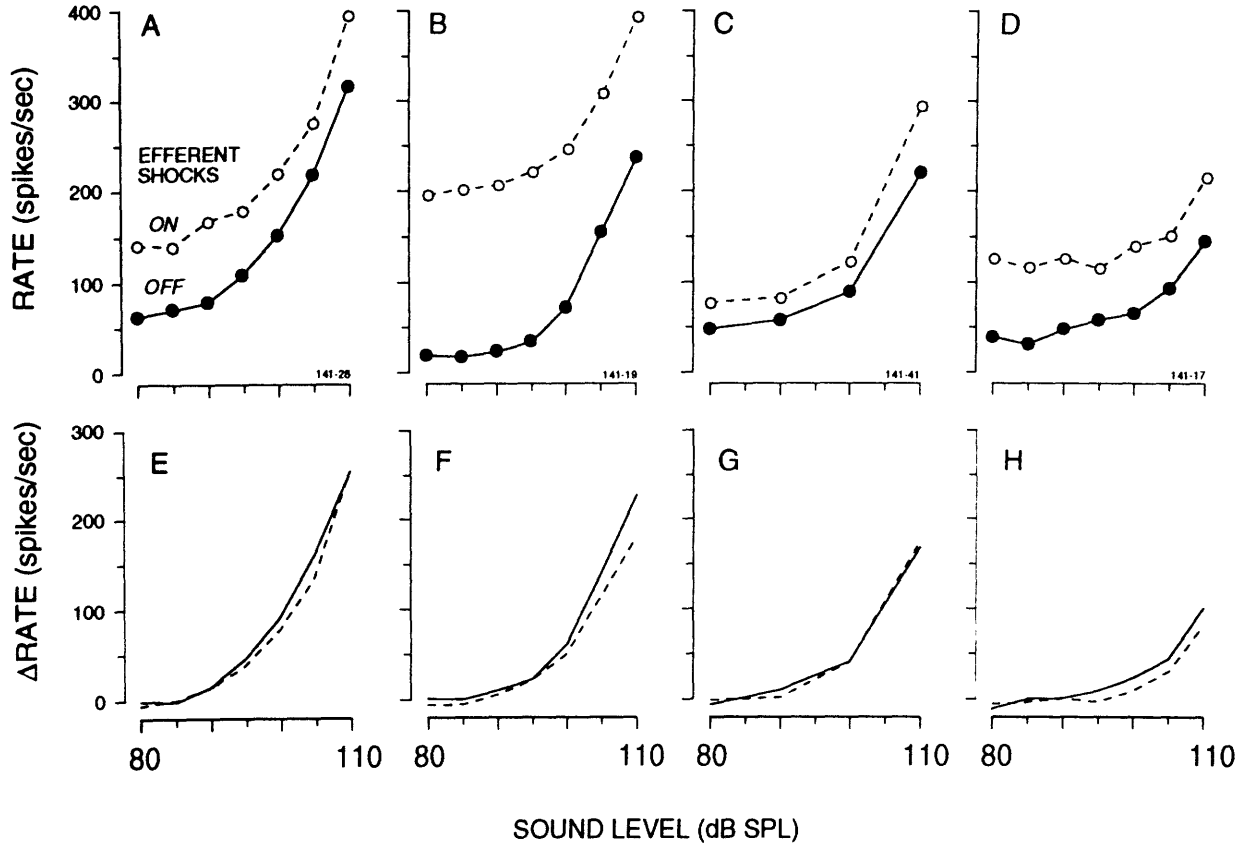

FIGURE IV–7. Influence of efferent stimulation on the acoustically evoked firing rates of 4 vestibular neurons. Each *column* shows data from a different unit. Measurements of absolute rate (*Rate, A-D*) and sound-evoked rate change (*ΔRate, E-H*) were made from PST histograms taken at each sound level as shown in Fig. 6. *Solid lines* show rates elicited by sound only. *Dashed lines* show rates elicited during concurrent delivery of sound and efferent shocks. Stimulus conditions were identical to Fig. 5.

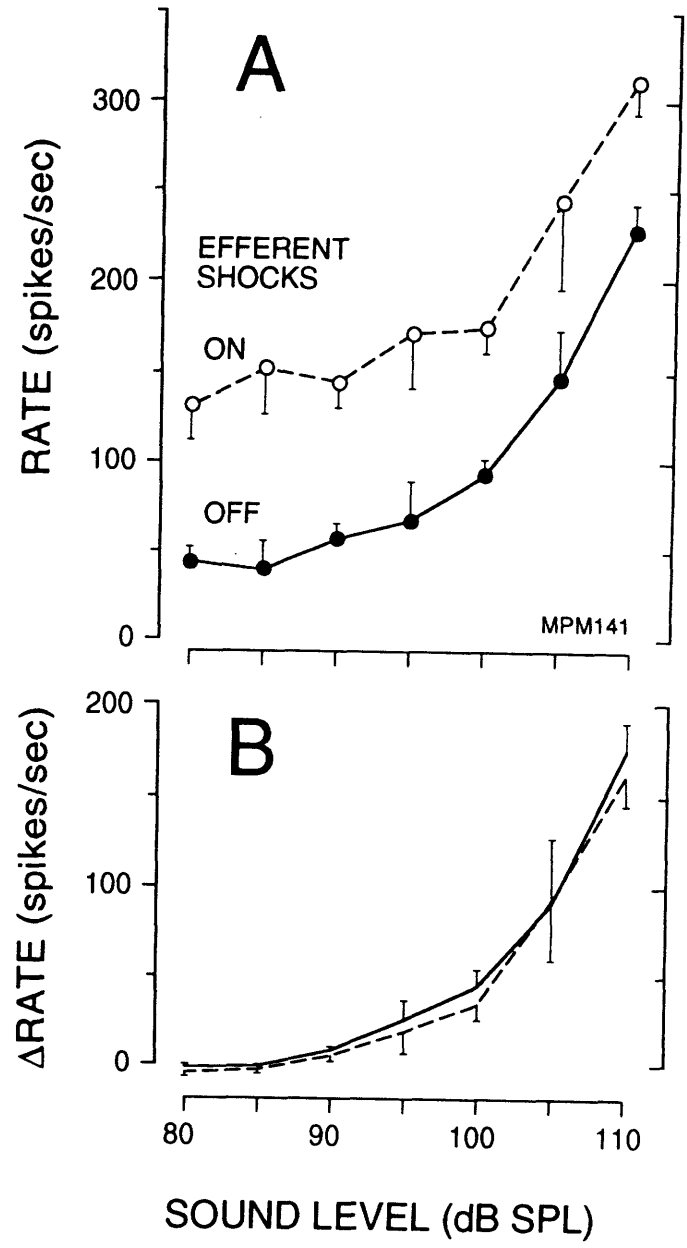

FIGURE IV–8. Mean influence of efferent stimulation on the acoustically evoked firing rates of vestibular neurons from one ear. Measurements of absolute rate (*Rate, A*) and sound-evoked rate change (*ΔRate, B*) were made from PST histograms taken at each sound level as shown in Fig. 6. *Solid lines* show mean rates elicited by sound only. *Dashed lines* show mean rates elicited during concurrent delivery of sound and efferent shocks. *Symbols* in *A* indicate which sound levels were tested. *Vertical bars* indicate SEM. The number of units tested was higher at "even" sound levels, ranging from n=15 at 110 dB SPL to n = 5 at 80 dB SPL. Only 3 units were tested at "odd" sound levels.

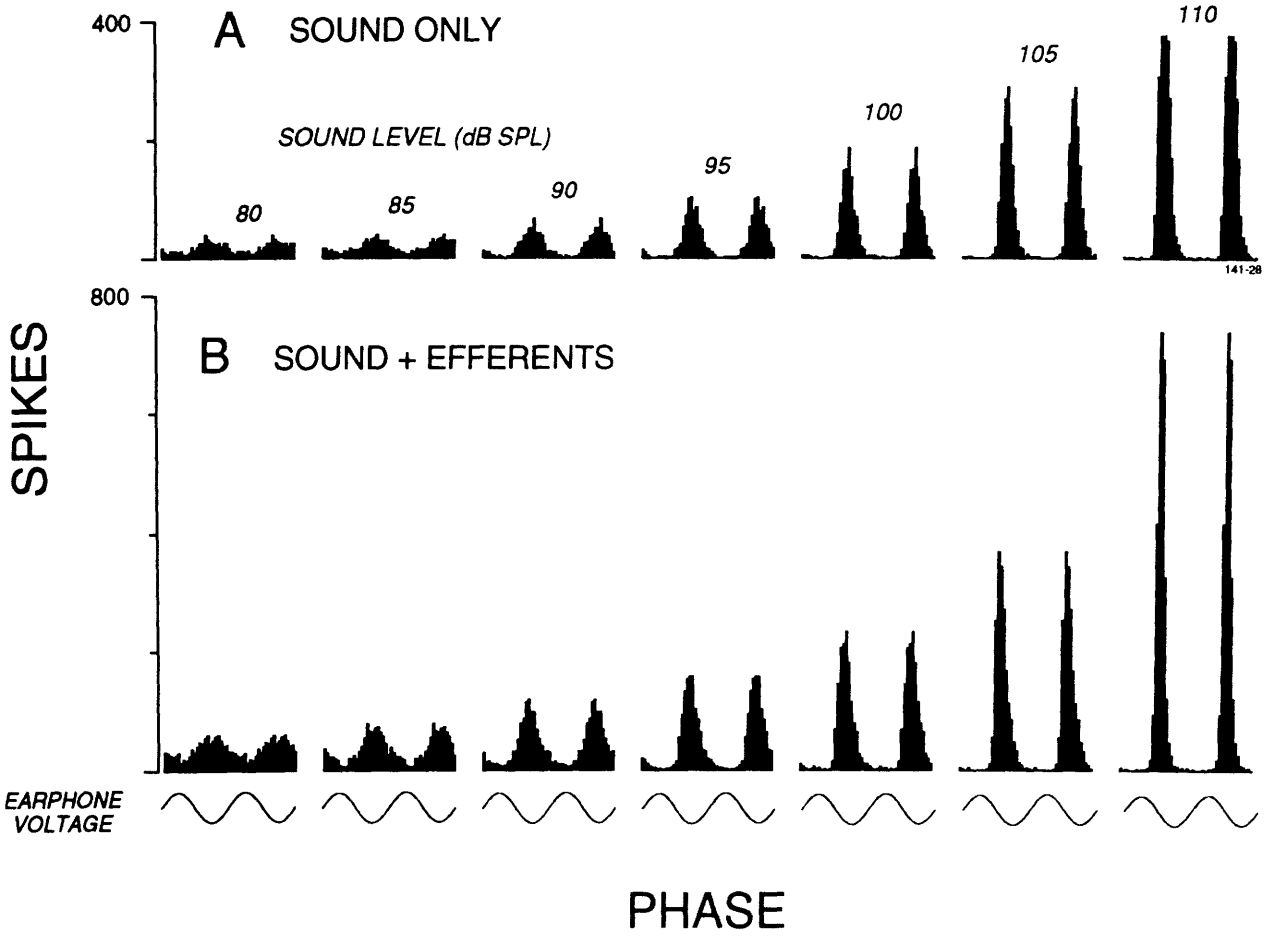

FIGURE IV–9. Influence of sound and efferent stimulation on phase-locking in an acoustically responsive vestibular neuron. PZC histograms show phase locking to an 800-Hz tone burst at increasing sound levels with efferent shocks OFF (*A*) and ON (*B*). Earphone voltage waveforms are shown at *bottom*. Unit, stimulus conditions and event data (during sound stimulation) are the same as Fig. 5. The *ordinate* is the total number of spikes occuring in each bin during 5120 tone cycles. The second response cycle is a duplicate of the first cycle and is added to emphasize sinusoidal amplitude variations. Bins: n = 50, width = 50 μs.

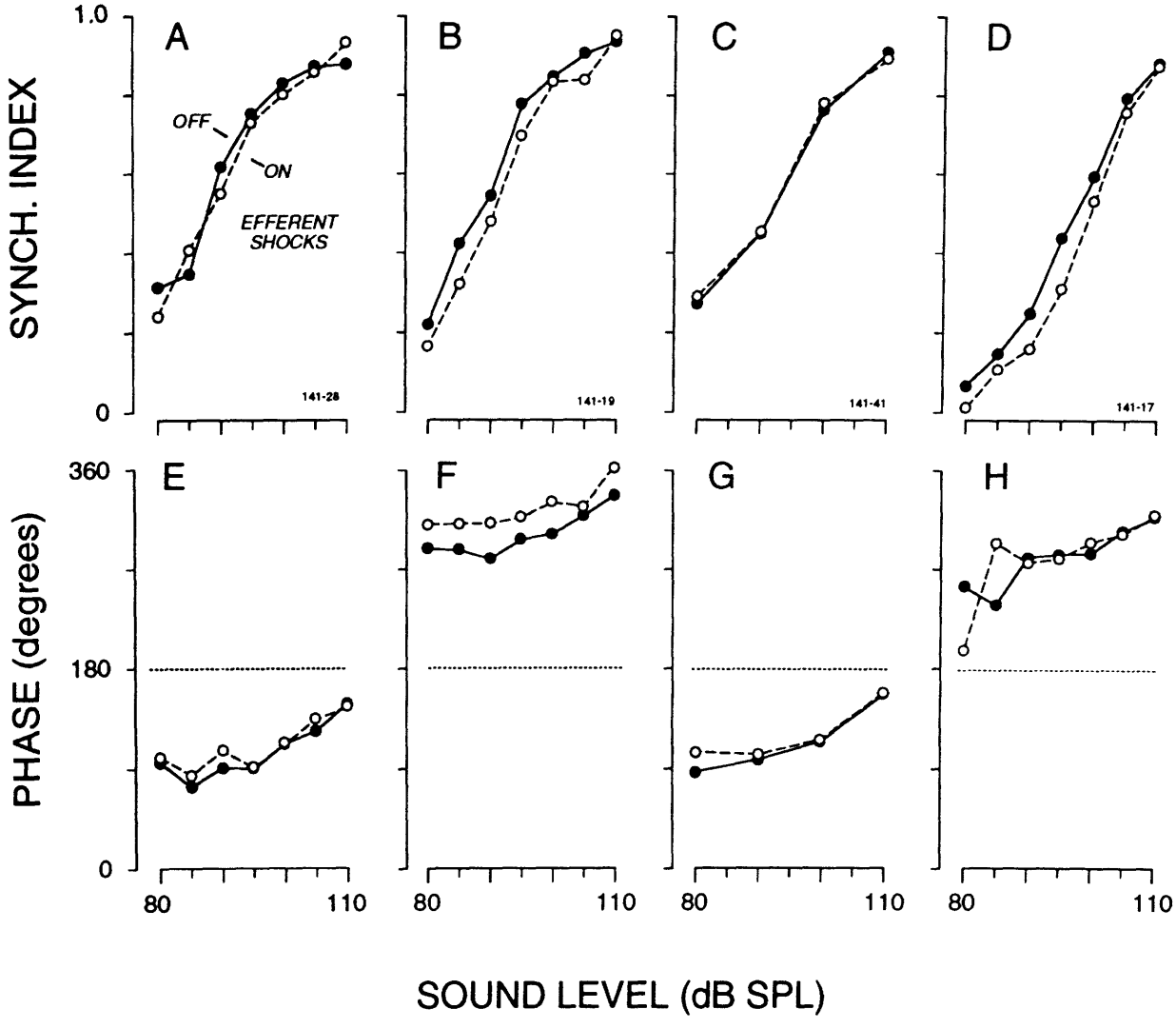

FIGURE IV–10. Influence of efferent stimulation on phase-locking in 4 vestibular neurons. Each *column* shows data from a different unit. Measurements of synchronization index (*A-D*) and phase (*E-H*) were made from Fourier transforms of PZC histograms (e.g. Fig. 9). Values were obtained in response to sound with efferent shocks OFF (*solid lines*) and ON (*dashed lines*). *Symbols* indicate which sound levels were tested. Units, stimulus conditions and data (during tone burst presentation) are identical to those in Fig. 7. The *dotted line* at 180° in *E-H* emphasizes our previous finding (McCue & Guinan, 1994a) that ARID units fall into two classes with preferred response phases approximately 180° apart (*E,G* = PUSH units; *F,H* = PULL units). Note that most ARID units exhibit a phase shift of about 30° between 100 and 110 dB SPL (*E-H*).

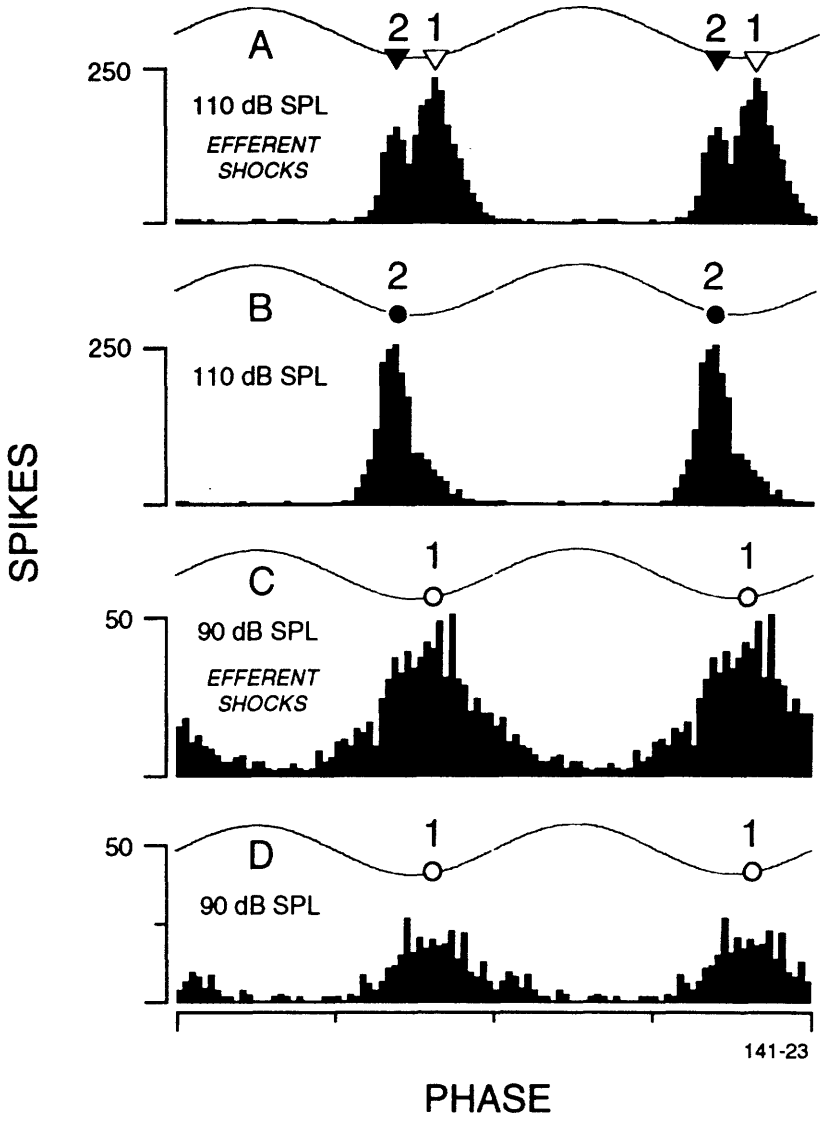

FIGURE IV–11. "Peak-splitting" of acoustic responses during efferent stimulation. *A-D*, PZC histograms obtained at 110 dB SPL with efferent stimulation ON (*A*) and OFF (*B*) and at 90 dB SPL with efferent stimulation ON (*C*) and OFF (*D*). *Circles* indicate phases calculated from Fourier transforms of PZC histograms. *Triangles* indicate the two local maxima of the histogram in *A*. *B & D* show the ≥30° phase advance (*Phase 1* -> *Phase 2*) which usually occurs in ARID units between 90 and 110 dB SPL (see Fig. 10E-H). At 90 dB SPL, efferent stimulation augments the response at *Phase 1* (*C-D, open circles*). At 110 dB SPL, the response occurs at *Phase 2* (*B*), and efferent stimulation causes reappearance of a response component at *Phase 1* (*A*). Stimulus conditions identical to Fig. 5. PZC histograms as in Fig. 9. The *ordinate* is the total number of spikes occuring in each bin during 5120 tone cycles.

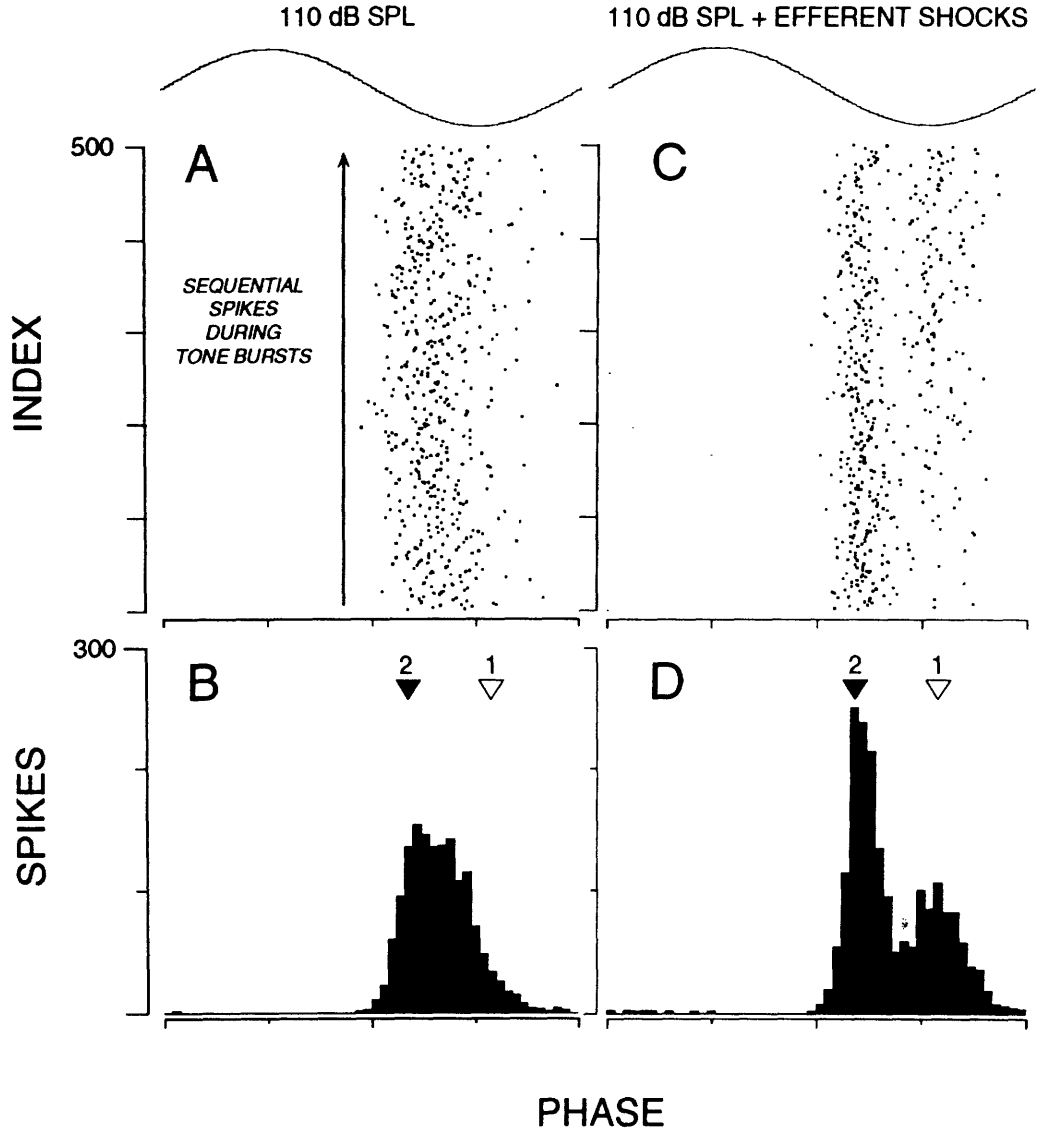

FIGURE IV–12. Another example of peak-splitting during efferent stimulation. *A* & *C*, response phases of the first 500 spikes occuring during the sound stimulus (110 dB SPL) with efferent stimulation OFF (*A*) and ON (*C*). *B* & *D*, PZC histograms of all spikes occuring during the sound stimulus interval with efferent shocks OFF (*B*) and ON (*D*). *Triangles* in *B* & *D* indicate the two local maxima of the histograms. *C* shows that the peaks are not composed of long runs of spikes at *Phase 1* alternated with runs at *Phase 2*. The *ordinate* in *B* & *D* is the total number of spikes occuring in each bin during 5120 tone cycles.

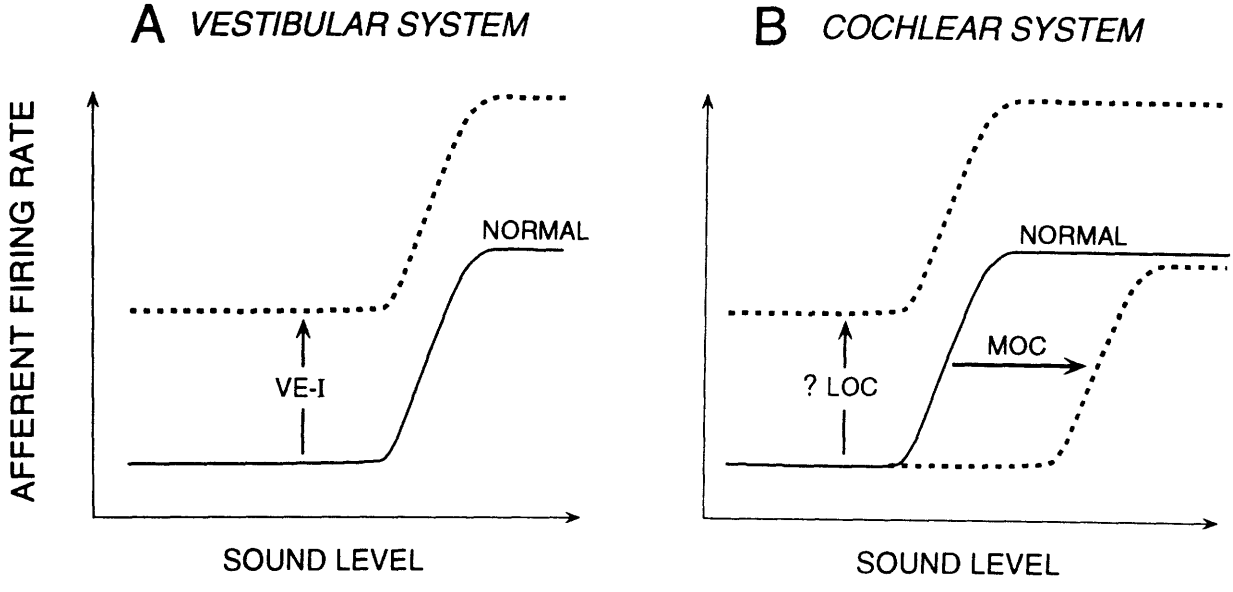

FIGURE IV–13. Schematic showing possible analogies between the interactions of efferent and afferent neurons in the vestibular (*A*) and cochlear (*B*) systems. See Fig. 2 for anatomical arrangement and abbreviations. Rate-level functions are shown for spikes elicited with efferent stimulation OFF (*solid lines*) and ON (*dashed lines*). *A*, Stimulation of efferent endings on afferent dendrites (VE-I) increases the firing rate of vestibular units without shifting their acoustic thresholds (see Figs. 7-8). *B*, Stimulation of MOC neurons shifts the acoustic threshold of cochlear afferents by producing a change (probably mechanical) in Type II hair cells that affects Type I hair cells (Fig. 2B). The action of LOC neurons on cochlear afferents remains unknown, but the analogous neural connections (Fig. 2) suggests that LOC endings may work like VE-I endings, raising afferent firing rate without affecting rate threshold.

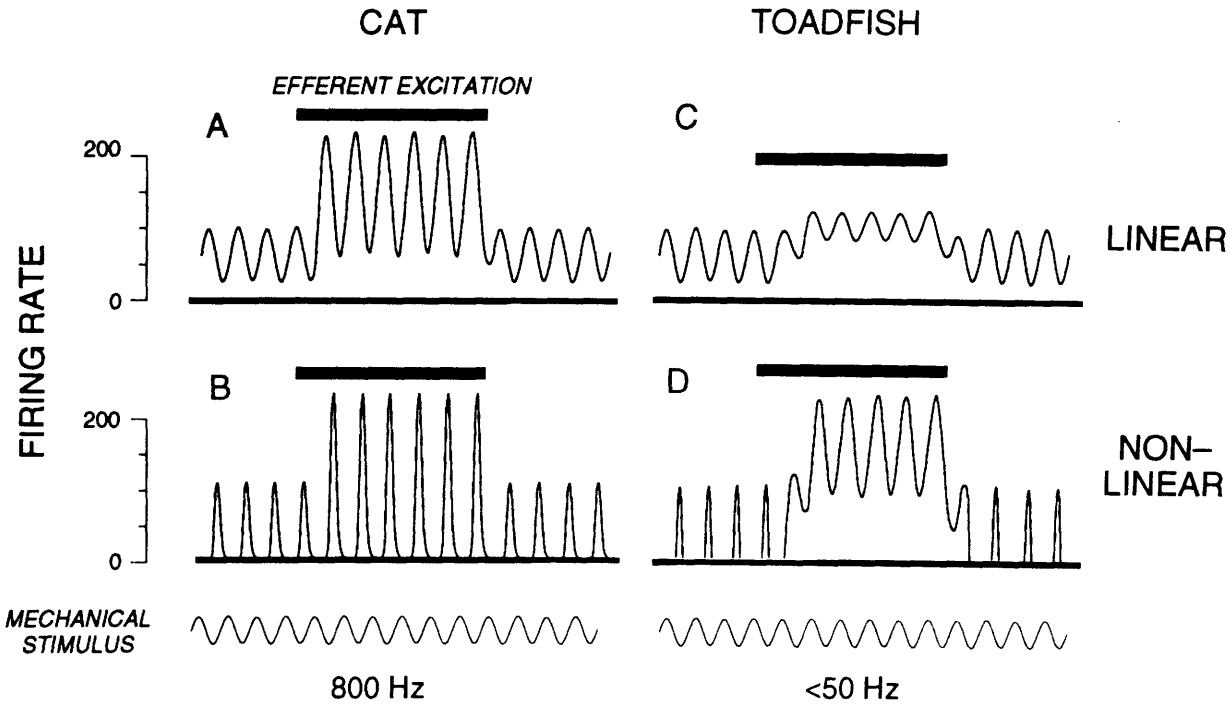

FIGURE IV–14. Schematic showing the different efferent influences on mechanically-evoked responses found in vestibular afferents in the cat (A-B) and toadfish (C-D). *A-C,* transduction mode of a mechanical stimulus in which the firing rate never falls to zero (*linear region*). *B-D,* transduction mode in which the firing rate falls to zero (*non-linear region*). *A-B,* In cat afferents stimulated by an 800 Hz tone, efferent stimulation increases the amplitude of both the AC and DC response components in both the linear and non-linear regions (Fig. 9). *C-D,* In toadfish afferents stimulated at low frequencies (<50 Hz) efferent stimulation elevates the DC component while reducing the AC component, making the transduction process bi-directional for units that operate in the non-linear region (*D*).

TOOLS

This is the first E.P.L. thesis rendered from Soup to Nuts on an Apple Macintosh system purchased and implemented against the advice of the E.P.L. Engineering Staff.

Principal Software

Function	*Program*	*Author*
Acoustic Calibration	Sweep 111.2	McCue
Data Aquisition	DAQ 146.0	McCue & Guinan
Data Analysis	Kaleidagraph 2.0	Synergy
Data Base Management	FileMaker Pro 2.0	Claris
Equipment Control	NI-DAQ 4.5.2	National Instruments
	NI-488 4.0.1	National Instruments
Figure Preparation	Canvas 3.0	Deneba
	Illustrator 3.0	Adobe
Programming Language	THINK C 5.0	Symantec
Reference Management	EndNote Plus 1.2	Niles & Associates
Scanning	DeskScan	Hewlett-Packard
Word Processing	Word 5.0	Microsoft

Principal Hardware

Function	*Device*	*Maker*
CPU	Quadra 950	Apple
	Quadra 800	Apple
	PowerBook 170	Apple
	Macintosh II	Apple
Data Acquisition	NB-A2000	National Instruments
	NB-DIO-32F	National Instruments
	NB-DMA2800	National Instruments
Event Timing	SpiGat	Brown
	E.P.L. Event Timer	Stefanov-Wagner/Cardarelli
Stimulus Timing	Brown Advanced Timing	Brown

REFERENCES

Aran, J.-M., Cazals, Y., Erre, J.-P. & Guilhaume, A. (1979). Conflicting electrophysiological and anatomical data from drug impaired guinea pig cochleas. *Acta Otolaryngol.* 87: 300-309.

Ashmore, J. F. (1987). A fast motile response in guinea-pig outer hair cells: The cellular basis of the cochlear amplifier. *J. Physiol.* 388: 323-347.

Baird, R. A., Desmadryl, G., Fernández, C. & Goldberg, J. M. (1988). The vestibular nerve of the chinchilla. II. Relation between afferent response properties and peripheral innervation patterns in the semicircular canals. *J. Neurophysiol.* 60: 182-203.

Borg, E. (1973a). On the neuronal organization of the acoustic middle ear reflex. A physiological and anatomical study. *Brain Res.* 49: 101-123.

Borg, E. (1973b). Stapedius reflex and speech features. *J. Acoust. Soc. Am.* 54: 525-527.

Borg, E., Counter, S. A., Engstrom, B., Linde, G. & Marklund, K. (1990). Stapedius reflex thresholds in relation to tails of auditory nerve fiber frequency tuning curves. *Brain Res.* 506: 79-84.

Borg, E. & Møller, A. R. (1975). Effect of central depressants on the acoustic middle ear reflex in rabbit. *Acta physiol. scand.* 94: 327-338.

Borg, E. & Zakrisson, J.-E. (1974). Stapedius reflex and monaural masking. *Acta Otolaryngol.* 78: 155-161.

Boyle, R., Goldberg, J. M. & Highstein, S. M. (1992). Inputs from regularly and irregularly discharging vestibular nerve afferents to secondary neurons in squirrel monkey vestibular nuclei. III. Correlation with vestibulospinal and vestibuloocular output pathways. *J. Neurophysiol.* 68: 471-484.

Boyle, R. & Highstein, S. M. (1990). Efferent vestibular system in the toadfish: action upon horizontal semicircular canal afferents. *J. Neurosci.* 10(5): 1570-1582.

Brown, M. C., Liberman, M. C., Benson, T. E. & Ryugo, D. K. (1988). Brainstem branches from olivocochlear axons in cats and rodents. *J. Comp. Neurol.* 278(591-603):

Brown, M. C., Nuttall, A. L. & Masta, R. I. (1983). Intracellular recordings from cochlear inner hair cells: Effects of stimulation of the crossed olivocochlear efferents. *Science.* 222: 69-72.

Brownell, W. E., Bader, C. R., Bertrand, D. & de Ribaupierre, Y. (1985). Evoked mechanical response of isolated cochlear outer hair cells. *Science.* 277: 194-196.

Burian, M. & Gstoettner, W. (1988). Projection of primary vestibular afferent fibres to the cochlear nucleus in the guinea pig. *Neurosci. Lett.* 84: 13-17.

Cazals, Y., Aran, J.-M., Erre, J.-P. & Guilhaume, A. (1980). Acoustic responses after total destruction of the cochlear receptor: brainstem and auditory cortex. *Science.* 210: 83-86.

Cazals, Y., Aran, J.-M., Erre, J.-P., Guilhaume, A. & Aurousseau, C. (1983). Vestibular acoustic reception in the guinea pig: a saccular function? *Acta Otolaryngol.* 95: 211-217.

Cazals, Y., Aran, J.-M., Erre, J.-P., Guilhaume, A. & Hawkins, J. E., Jr. (1979). "Neural" responses to acoustic stimulation after destruction of cochlear hair cells. *Arch Otorhinolaryngol.* 224: 61-70.

Cazals, Y., Aran, J.-M. & Erre, Y.-P. (1982). Frequency sensitivity and selectivity of acoustically evoked potentials after complete cochlear hair cell destruction. *Brain Res.* 231: 197-203.

Colebatch, J. G. & Halmagyi, G. M. (1992). Vestibular evoked potentials in human neck muscles before and after unilateral vestibular deafferentation. *Neurology.* 42: 1635-1636.

Crawford, A. C. & Fettiplace, R. (1981). *J. Physiol. (London).* 312: 377-412.

Denk, W. & Webb, W. W. (1992). Forward and reverse transduction at the limit of sensitivity studied by correlating electrical and mechanical fluctuations in frog saccular hair cells. *Hearing Res.* 60: 89-102.

Didier, A. & Cazals, Y. (1989). Acoustic responses recorded from the saccular bundle on the eighth nerve of the guinea pig. *Hearing Res.* 37: 123-128.

Dieringer, N., Blanks, R. H. I. & Precht, W. (1977). Cat efferent vestibular system: weak suppression of primary afferent activity. *Neurosci. Lett.* 5: 285-290.

Drake, A. W. (1967). Interarrival Times for the Poisson Process. Fundamentals of Applied Probability Theory. McGraw-Hill Book Co. pp. 137-140.

Fernández, C., Baird, R. A. & Goldberg, J. M. (1988). The vestibular nerve of the chinchilla. I. Peripheral innervation patterns in the horizontal and superior semicircular canals. *J. Neurophysiol.* 60: 167-181.

Fernández, C. & Goldberg, J. M. (1976a). Physiology of peripheral neurons innervating otolith organs of the squirrel monkey. I. Response to static tilts and long-duration centrifugal force. *J. Neurophysiol.* 39(5): 970-984.

Fernández, C. & Goldberg, J. M. (1976b). Physiology of peripheral neurons innervating otolith organs of the squirrel monkey. II. Directional selectivity and force-response relations. *J. Neurophysiol.* 39(5): 985-995.

Fernández, C. & Goldberg, J. M. (1976c). Physiology of peripheral neurons innervating otolith organs of the squirrel monkey. III. Response dynamics. *J. Neurophysiol.* 39(5): 996-1008.

Fernández, C., Goldberg, J. M. & Abend, W. K. (1972). Response to static tilts of peripheral neurons innervating otolith organs of the squirrel monkey. *J. Neurophysiol.* 35(6): 978-997.

Fernández, C., Goldberg, J. M. & Baird, R. A. (1990). The vestibular nerve of the chinchilla. III. Peripheral innervation patterns in the utricular macula. *J. Neurophysiol.* 63: 767-780.

Fex, J. (1967). Efferent inhibition in the cochlea related to hair-cell dc activity: study of postsynaptic activity of the crossed olivo-cochlear fibers in the cat. *J. Acoust. Soc. Am.* 41: 666-675.

Flock, Å. & Russell, I. J. (1973a). Inhibition by efferent nerve fibers: action on hair cells and afferent synaptic transmission in the lateral line canal organ of the burbot *Lota Lota. J. Physiol. (London).* 257: 45-62.

Flock, Å. & Russell, I. J. (1973b). The post-synaptic action of efferent fibres in the lateral line organ of the burbot *Lota Lota. J. Physiol. (London).* 235: 591-605.

Furukawa, T. & Ishii, Y. (1967). Neurophysiological studies on hearing in goldfish. *J. Neurophysiol.* 30: 1377-1403.

Gacek, R. R. & Rasmussen, G. L. (1961). Fiber analysis of the statoacoustic nerve of guinea pig, cat, and monkey. *Anat. Rec.* 139(4): 455-463.

Galambos, R. (1956). Suppression of auditory activity by stimulation of efferent fibers to the cochlea. *J. Neurophysiol.* 19: 424-437.

Galambos, R., Rosenberg, P. E. & Glorig, A. (1953). The eyeblink response as a test for hearing. *J. Speech & Hearing Disorders.* 18(4): 373-378.

Gifford, M. L. & Guinan, J. J., Jr. (1983). Effects of crossed-olivocochlear-bundle stimulation on cat auditory nerve fiber responses to tones. *J. Acoust. Soc. Am.* 74(1): 115-123.

Gifford, M. L. & Guinan, J. J., Jr. (1987). Effects of electrical stimulation of medial olivocochlear neurons on ipsilateral and contralateral cochlear responses. *Hearing Res.* 29: 179-194.

Goldberg, J. & Brown, P. B. (1969). Response of binaural neurons of dog superior olivary complex to dichotic tonal stimuli: some physiological mechanisms of sound localization. *J. Neurophysiol.* 32: 613-636.

Goldberg, J. M., Desmadryl, G., Baird, R. A. & Fernández, C. (1990a). The vestibular nerve of the chinchilla. IV. Discharge properties of utricular afferents. *J. Neurophysiol.* 63: 781-790.

Goldberg, J. M., Desmadryl, G., Baird, R. A. & Fernández, C. (1990b). The vestibular nerve of the chinchilla. V. Relation between afferent discharge properties and peripheral innervation patterns in the utricular macula. *J. Neurophysiol.* 63: 791-804.

Goldberg, J. M. & Fernández, C. (1975). Vestibular mechanisms. *Ann. Rev. Physiol.* 37: 129-162.

Goldberg, J. M. & Fernández, C. (1977). Conduction times and background discharge of vestibular afferents. *Brain Res.* 122: 545-550.

Goldberg, J. M. & Fernández, C. (1980). Efferent vestibular system in the squirrel monkey: anatomical location and influence on afferent activity. *J. Neurophysiol.* 43(4): 986-1025.

Guinan, J. J., Jr. & Gifford, M. L. (1988). Effects of electrical stimulation of efferent olivocochlear neurons on cat auditory-nerve fibers. I. Rate-level functions. *Hearing Res.* 33: 97-114.

Guinan, J. J., Jr. & Li, R. Y.-S. (1990). Signal processing in brainstem auditory neurons which receive giant endings (calyces of Held) in the medial nucleus of the trapezoid body of the cat. *Hearing Res.* 49: 321-334.

Guinan, J. J., Jr. & McCue, M. P. (1987). Asymmetries in the acoustic reflexes of the cat stapedius muscle. *Hearing Res.* 26: 1-10.

Guinan, J. J., Jr., Warr, W. B. & Norris, B. E. (1983). Differential olivocochlear projections from lateral versus medial zones of the superior olivary complex. *J. Comp. Neurol.* 221: 358-370.

Horikawa, K. & Armstrong, W. E. (1988). A versatile means of intracellular labeling: injection of biocytin and its detection with avidin conjugates. *J. Neurosci. Meth.* 25: 1-11.

Hwang, J. C. & Poon, W. F. (1975). An electrophysiological study of the sacculo-ocular pathways in cats. *Jap. J. Physiol.* 25: 241-251.

Igarishi, M. & Kato, Y. (1975). Effect of different vestibular lesions upon body equilibrium function in squirrel monkeys. Acta Otolaryngol. Suppl. 330: 91-99.

Johnson, D. H. (1980). The relationship between spike rate and synchrony in responses of auditory-nerve fibers to single tones. *J. Acoust. Soc. Am.* 68: 1115-1122.

Joseph, M. P., Guinan, J. J., Jr., Fullerton, B. C., Norris, B. E. & Kiang, N. Y. S. (1985). Number and distribution of stapedius motoneurons in cats. *J. Comp. Neurol.* 232: 43-54.

Kevetter, G. A. & Perachio, A. A. (1989). Projections from the sacculus to the cochlear nuclei in the Mongolian gerbil. *Brain Behav. Evol.* 34: 193-200.

Kiang, N. Y. S. & Moxon, E. C. (1972). Physiological considerations in artificial stimulation of the inner ear. *Ann Otol Rhinol Laryngol.* 81: 714-731.

Kiang, N. Y. S. & Moxon, E. C. (1974). Tails of tuning curves of auditory-nerve fibers. *J Acoust Soc Am.* 55: 620-630.

Kiang, N. Y. S., Moxon, E. C. & Levine, R. A. (1970). Auditory-nerve activity in cats with normal and abnormal cochleas. Ciba Foundation Symposium on Sensorineural Hearing Loss. Ed: Wolstenholme, G. E. W. & Knight, J., London, Churchill. pp. 241-273.

Kiang, N. Y. S., Watanabe, T., Thomas, E. C. & Clarke, L. F. (1965). Discharge patterns of single fibers in the cat's auditory nerve. M.I.T. Research Monongraphs. Cambridge, M.I.T. Press.

Kimura, R. S. & Wersäll, J. (1962). Termination of the olivocochlear bundle in relation to the outer hair cells of the organ of Corti in guinea pig. *Acta Otolaryngol.* 55: 11-32.

Klinke, R. & Galley, N. (1974). Efferent innervation of vestibular and auditory receptors. *Physiol. Rev.* 54: 316-357.

Kobler, J. B., Guinan, J. J., Jr., Vacher, S. R. & Norris, B. E. (1992). Acoustic-reflex frequency selectivity in single stapedius motoneurons of the cat. *J. Neurophysiol.* 68: 807-817.

Lenhardt, M. L., Skellett, R., Wang, P. & Clarke, A. M. (1991). Human ultrasonic speech perception. *Science.* 253: 82-85.

Lewis, E. R., Baird, R. A., Leverenz, E. L. & Koyama, H. (1982). Inner ear: dye injection reveals peripheral origins of specific sensitivities. *Science.* 215: 1641-1643.

Lewis, R. S. & Hudspeth, A. J. (1983). Voltage- and ion-dependent conductances in solitary vertebrate hair cells. *Nature.* 304: 538-541.

Liberman, M. C. (1978). Auditory-nerve response from cats raised in a low-noise chamber. *J. Acoust. Soc. Am.* 63: 442-455.

Liberman, M. C. (1990). Effects of chronic cochlear de-efferentation on auditory-nerve response. *Hearing Res.* 49: 209-224.

Liberman, M. C. & Brown, M. C. (1986). Physiology and anatomy of single olivocochlear neurons in the cat. *Hearing Res.* 24: 17-36.

Liberman, M. C. & Oliver, M. E. (1984). Morphometry of intracellularly labeled neurons of the auditory nerve: Correlations with functional properties. *J. Comp. Neurol.* 223: 163-176.

Lindeman, H. H. (1973). Anatomy of the otolith organs. *Adv. Oto-Rhino-Laryng.* 20: 405-433.

Loe, P. R., Tomko, D. L. & Werner, G. (1973). The neural signal of angular head position in primary afferent vestibular nerve axons. *J. Physiol. (London).* 230: 29-50.

Lowenstein, O. & Roberts, T. D. M. (1951). The localization and analysis of the responses to vibration from the isolated elasmobranch labyrinth. A contribution to the problem of the evolution of hearing in vertebrates. *J. Physiol. (London).* 114: 471-489.

McCue, M. P. & Guinan, J. J., Jr. (1993). Acoustic responses from primary afferent neurons of the mammalian sacculus. *Assoc. Res. Otolaryngol. Ab.* 16: 33.

Mikaelian, D. (1964). Vestibular response to sound: single unit recording from the vestibular nerve in fenestrated deaf mice (Df/Df). *Acta Otolaryngol.* 58: 409-422.

Moffat, A. J. M. & Capranica, R. R. (1976). Auditory sensitivity of the saccule in the American toad (Bufo americanus). *J. comp. Physiol.* 105: 1-8.

Pang, X. D. (1988). Effects of stapedius muscle contractions on masking of tone responses in the auditory nerve. Ph.D. Thesis. M.I.T.

Pang, X. D. & Peake, W. T. (1986). How do contractions of the stapedius muscle alter the acoustic properties of the ear? Peripheral Auditory Mechanisms. Ed: Allen, J. B., Hall, J. L., Hubbard, A., Neely, S. I. & Tubis, A., New York, Springer-Verlag. pp. 36-43.

Popper, A. N. & Fay, R. R. (1973). Sound detection and processing by teleost fishes: a critical review. *J. Acoust. Soc. Am.* 53: 1515-1529.

Rasmussen, G. L. (1960). Efferent fibers of the cochlear nerve and cochlear nucleus. Neural Mechanisms of the Auditory and Vestibular Systems. Ed: Rasmussen, G. L. & Windle, W., Springfield IL, C C Thomas. pp. 105-115.

Retzius, G. (1884). Das Gehörgan der Wirbelthiere, Morphologisch-Histologische Studien, II. Das Gehörgan der Reptilien, der Vögel, und der Säugethiere. Stockholm, Samson & Wallin.

Ribaric, K., Bleeker, J. D. & Wit, H. P. (1992). Perception of audio-frequency vibrations by profoundly deaf subjects after fenestration of the vestibular system. *Acta Otolaryngol.* 112: 45-49.

Ross, M. D., Rogers, C. M. & Donovan, K. M. (1986). Innervation patterns in rat saccular macula. *Acta Otolaryngol.* 102: 75-86.

Saidel, W. M. & Popper, A. N. (1983). The saccule may be the transducer for directional hearing of nonostariophysine teleosts. *Exp. Brain Res.* 50: 149-152.

Sewell, W. F. & Starr, P. A. (1991). Effects of calcitonin gene-related peptide and efferent nerve stimulation on afferent transmission in the lateral line organ. *J. Neurophysiol.* 65: 1158-1169.

Smith, C. A. (1961). Innervation patterns of the cochlea. The internal hair cell. *Ann. Otol. Rhinol. Laryngol.* 70: 504-527.

Smith, C. A. & Rasmussen, G. L. (1963). Recent observations on the olivocochlear bundle. *Ann. Otol. Rhinol. Laryngol.* 72: 489-497.

Spoendlin, H. (1966). Some morphofunctional and pathological aspects of the vestibular sensory epithelia. Second symposium on the role of the vestibular organs in space exploration. *NASA report* SP-115. pp. 99-116.

Spoendlin, H. (1970). Auditory, Vestibular, Olfactory and Gustatory Organs. Ultrastructure of the Peripheral Nervous System and Sense Organs. Ed: Bischoff, A., St. Louis, C. V. Mosby. pp. 173-338.

Spoendlin, H. H. & Gacek, R. R. (1963). Electron-microscopic study of the afferent and efferent innervation of the organ of Corti of the cat. *Ann. Otol. Rhinol. Laryngol.* 56: 660-686.

Townsend, G. L. & Cody, D. T. R. (1971). The averaged inion response evoked by acoustic stimulation: its relation to the saccule. *Ann. Otol. Rhinol. Laryngol.* 80: 121-131.

Ver, I. L., Brown, R. M. & Kiang, N. Y. S. (1975). Low-noise chambers for auditory research. *J. Acoust. Soc. Am.* 58: 392-398.

Walsh, B. T., Miller, J. B., Gacek, R. R. & Kiang, N. Y. S. (1972). Spontaneous activity in the eighth cranial nerve of the cat. *Intern. J. Neurosci.* 3: 221-235.

Warr, W. B. (1975). Olivocochlear and vestibular efferent neurons of the feline brain stem: their location, morphology and number determined by retrograde axonal transport and acetylcholinesterase histochemistry. *J. Comp. Neurol.* 161: 159-182.

Warr, W. B. & Guinan, J. J., Jr. (1979). Efferent innervation of the organ of Corti: two separate systems. Brain Res. 173: 152-155.

Warr, W. B., Guinan, J. J., Jr. & White, J. S. (1986). Organization of the efferent fibers: the lateral and medial olivocochlear systems. Neurobiology of Hearing: The Cochlea. New York, Raven Press.

Weiss, T. F., Peake, W. T., Ling, A., Jr. & Holton, T. (1978). Which structures determine frequency selectivity and tonotopic organization of vertebrate nerve fibers? Evidence from the alligator lizard. Evoked Electrical Activity in the Auditory Nervous System. Ed: Naunton, R. F. & Fernandez, C., New York, Academic Press. pp. 91-112.

Wersäll, J. (1956). Studies on the structure and innervation of the sensory epithelium of the cristae ampullaris in the guinea pig. A light and electron microscopic investigation. *Acta Otolaryngol. Suppl.* 126: 1-85.

Wersäll, J., Flock, Å. & Ludquist, P.-G. (1965). Structural basis for directional sensitivity in cochlear and vestibular sensory receptors. *Cold Spring Harbor Symp. Quant. Biol.* 30: 115-132.

Wever, E. G. (1974). The evolution of vertebrate hearing. Handbook of Sensory Physiology. New York, Springer-Verlag.

Wever, E. G. (1979). Middle ear muscles of the frog. *Proc. Natl. Acad. Sci. USA.* 76: 3031-3033.

Wiederhold, M. L. & Kiang, N. Y. S. (1970). Effects of electric stimulation of the crossed olivocochlear bundle on single auditory-nerve fibers in the cat. *J. Acoust. Soc. Am.* 48(4): 950-965.

Wilson, V. J., Gacek, R. R., Maeda, M. & Uchino, Y. (1977). Saccular and utricular input to cat neck motoneurons. *J. Neurophysiol.* 40: 63-73.

Wit, H. P., Bleeker, J. D. & Mulder, H. H. (1984). Response of pigeon vestibular nerve fibers to sound and vibration with audiofrequencies. *J. Acoust. Soc. Am.* 75: 202-208.

Young, E. D., Fernández, C. & Goldberg, J. M. (1977). Responses of squirrel monkey vestibular neurons to audio-frequency sound and head vibration. *Acta Otolaryngol.* 84: 352-360.